N73-13213
NASA CR-120954

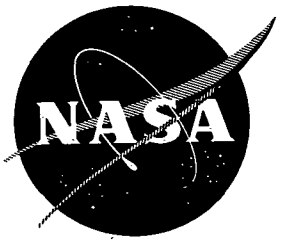

DESIGN STUDY FOR A LIQUID METAL SLIP RING SOLAR ARRAY ORIENTATION MECHANISM

by

R. B. Clark

HUGHES AIRCRAFT COMPANY

Prepared for

NATIONAL AERONAUTICS AND SPACE ADMINISTRATION

NASA Lewis Research Center

Contract NAS 3-13731

Robert R. Lovell, Project Manager

Requests for copies of this report should be referred to:

National Aeronautics and Space Administration
Scientific and Technical Information Facility
P. O. Box 33
College Park, Md. 20740

NASA CR-120954

FINAL REPORT

DESIGN STUDY FOR A LIQUID METAL SLIP RING SOLAR ARRAY ORIENTATION MECHANISM

by

R. B. Clark

HUGHES AIRCRAFT COMPANY
Technology Division
Los Angeles, California 90009

Prepared for

NATIONAL AERONAUTICS AND SPACE ADMINISTRATION

March 30, 1972

Contract NAS 3-13731

NASA Lewis Research Center
Cleveland, Ohio
Robert R. Lovell, Project Manager
Spacecraft Technology Division

FOREWORD

The work described herein was done at the Technology Division of Hughes Aircraft Company under NASA Contract No. NAS 3-13731 with Mr. Robert R. Lovell, Spacecraft Technology Division, NASA-Lewis Research Center, as Project Manager.

TABLE OF CONTENTS

TABLE OF CONTENTS (continued)

LIST OF TABLES

LIST OF FIGURES

LIST OF FIGURES (continued)

TABLE OF CONTENTS (continued)

LIST OF FIGURES (continued)

ABSTRACT

The design of a single axis orientation mechanism for solar arrays on high power synchronous satellites is studied primarily with respect to providing 116 liquid metal slip rings for reduced friction and improved electrical characteristics. Designs and tradeoff studies for the slip rings and other components are presented. An assembly containing 33 slip rings of three design approaches was designed, fabricated, and vacuum tested to 30 amperes and 30,000 volts. Containment of the liquid metal gallium in large diameter slip rings was difficult. A design approach is presented which is expected to provide improved retention of the liquid metal.

SUMMARY

Problem Statement

Liquid metal slip rings offer promise for eliminating coulomb friction and reducing power loss, electrical noise, size and weight associated with transferring signals and power between large solar arrays and the body of a spacecraft. Projected high power applications may require over 100 slip ring circuits through the array orientation mechanism, rotating at one revolution per day in the case of a geo-synchronous satellite. The use of liquid metal at these interfaces may contribute significantly to attitude stability and pointing accuracy.

Gallium has many properties which appear desirable for use in slip rings for space. Among these are a very low vapor pressure, a convenient melting point and high surface energy. However, since little is known about using gallium in the cited space application, development is needed to identify and solve the problems.

Objectives

The objective of the work herein described was to advance the technology of liquid metal slip rings for space use by designing a solar array orientation mechanism to requirements anticipated for high power technology satellites, by testing to explore problem areas in the liquid metal slip rings, and by investigating design limitations and necessary controls.

Technical Requirements

The slip ring requirement includes 14 rings to operate at potentials to 15,000 volts, 4 rings to carry 30A at up to 300 volts and a variety of signal and power leads for operation at up to 2000 volts with currents from 0.2A to 15A. Total: 116 rings minimum.

Dual brushless torquers and a brushless angular position pickoff were to be "off-the-shelf" designs. Ball bearings were to be used. The total package was not to exceed 10 inches diameter by 24 inches long by 40 pounds weight and was to have a through shaft with flanges for mounting solar panels at both ends.

Tasks and Results

Design

Following tradeoff studies a design approach for the Solar Array Orientation Mechanism was established which included space-qualified brushless torquers, brushless resolvers and 118 slip rings arranged in

ten disc-shaped subassemblies of concentric slip rings. The approach set conservative limits on the electrical stresses, provided open construction to minimize residual gases and employed the vacuum of space as the principle dielectric. Electrical breakdowns through the solid dielectric were to be avoided at all cost because of the catastrophic nature of such failures compared to a discharge through space. The calculation of electrical stresses took account of the geometrical configurations of the conductors. Stress between conductors was limited to 40,000 v/cm. Surface discharge was guarded against by providing long paths over the dielectric surfaces between conductors.

Engineering Test Unit

Three candidate slip ring configurations were selected for incorporation into an Engineering Test Unit containing a total of 33 rings. All rings employ gallium wetted to either nickel or stainless steel electrodes with retention of gallium primarily accomplished by surface tension. The ring pairs are arranged concentrically around a central shaft in 3 layers or platters. An integral electrical heater can ensure that the gallium is molten, and the rings may be driven at one revolution per hour through a shaft coupler in a vacuum chamber.

Design Evaluation Tests

Following an extensive outgassing period the test unit was rotated in an ion-pumped vacuum chamber for the equivalent of 3 years in synchronous orbit. Voltages of up to 30 kilovolts were impressed and currents of 30 amperes were transferred.

Gallium Properties Tests

Gallium was held under high vacuum at an elevated temperature for over a year with daily agitation in the presence of sensitive instrumentation to detect evaporation and condensation. Experiments were also conducted on liquid and solid gallium in vacuum and in the presence of various concentrations of gases to detect formations of surface film which could be detrimental to slip ring operation.

Plans and Procedures

A Verification Test Plan was prepared to define the tests required to verify that the liquid metal slip ring/solar array orientation mechanism meets specified requirements. A Handling Procedures Document was prepared to specify the procedures and care necessary to ensure performance from final assembly through launch.

Significant Results

The tasks described above yielded much new information on the use of gallium in electrical transfer. The tests in particular contributed

valuable information, both as a result of successes and problems encountered. The primary obvious results are listed below and are discussed in considerable detail within this report.

- The concept of using air or high vacuum as a dielectric for high voltage rings is achievable with carefully conceived and analyzed designs. High voltage rings withstood a minimum of 20 kilovolts and up to 30 kilovolts without corona.

- Slip ring resistance was on the order of 1 milliohm much of which was lead resistance.

- Gallium readily absorbs oxygen which appears to be the principle contributor to formation of film and sludge.

- Frozen gallium may be exposed to air or oxygen without noticeable formation of film.

- At normal high working temperatures ($\sim 80^{\circ}C$) and pressures ($\sim 10^{-6}$ Torr) liquid gallium does not evaporate and condense on cooler surfaces to a measureable extent.

- Operation of gallium slip rings in high vacuum for 3 year life equivalency does not produce detrimental film or sludge.

- Gallium slip rings may be assembled in air, and if not rotated till soaked in high vacuum, will function satisfactorily.

- A double-ended solar array orientation mechanism with capability for handling 15 KV, 30 amperes, and signals can be produced within the specified size and weight limitations.

- Argon atmospheres of sufficient purity can be achieved in glove boxes to maintain relatively film-free conditions on liquid gallium.

Other inferred results which may contribute to superior future designs are listed below:

- The double-ended design approach to the orientation mechanism necessarily constrains the slip rings to relatively large diameters which increase the risk of losing gallium.

- The requirement of employing high vacuum as a dielectric, although favorable from a "healing after breakdown" standpoint, requires relatively large spacings and ring sizes.

- The use of surface tension as the primary retention feature for liquid gallium requires precise dimensional control of runout, concentricity, etc.

INTRODUCTION

Background

The transfer of electrical power across rotating interfaces in spacecraft is typically accomplished with spring-loaded conductive brushes pressing against precious metal slip rings. They have proven to be very reliable when correctly designed, but the rubbing contact causes several disadvantages: starting and running friction may be detrimental to control accuracy and stability in some applications. Wear debris can be troublesome if not properly managed. Multiple brushes required to carry heavy electrical loads can require excessive space in order to hold interface losses to acceptable levels. Liquid metal slip rings appear to be capable of substantially overcoming these drawbacks but introduce new problems such as containment of the liquid metal, compatibility of materials with the liquid metal and control of surface films which may form in contact with air.

Liquid metal slip rings transfer electrical power from rotor to stator through conductive liquid metal as shown in Figure 1. There is no rubbing contact between solids so there is no Coulomb friction. The viscous friction is very low at the speeds of most spacecraft applications. There is no obvious mechanism by which wear debris is formed or by which wearout occurs. The large area of contact results in extremely low electrical resistance from rotor to stator so that electrical losses and electrical noise from the slip ring become negligible.

This combination of properties makes liquid metal slip rings attractive where mechanisms must be positioned with respect to the spacecraft with a minimum of stick-slip motion. Such an application is the solar array orientation mechanism of a synchronous satellite. The array does not require accurate pointing but it's once per day revolution must be accomplished with minimum reactions on the spacecraft which might disturb the precision pointing of the communications antennas. For projected high power satellites the number of slip rings is expected to be large and the solar arrays are flexible. Thus the control problem associated with the conventional slip rings could be significant.

An experimental project to study the use of the liquid metal gallium for this application is described in Reference 1. Gallium was used because its extremely low vapor pressure minimizes loss due to evaporation in the vacuum of space. Losses due to evaporation make mercury unattractive. Gallium melts at 303 K (30°C) so that the possibility exists of freezing the liquid metal for retention during launch. The liquid metal would be retained by surface tension in the benign acceleration regime of orbit.

The low resistance and electrical noise predicted for the liquid metal slip rings was achieved using wetted contact with the electrode materials, and suitable materials for electrodes and insulators were determined in this previous work. It was also found that gallium develops a surface film in contact with air. The film is quasi-plastic and can ball-up when the rings are rotated in air, causing sludge in the liquid gallium or the discharge of gallium debris from the rings, depending on the ring design. Further study of gallium

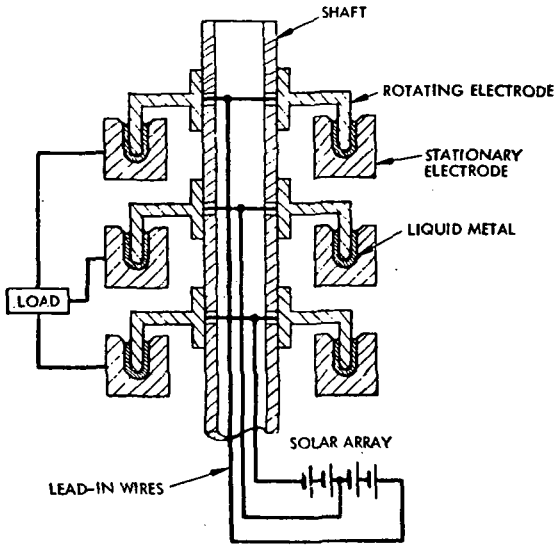

FIGURE 1. Liquid Metal Slip Rings

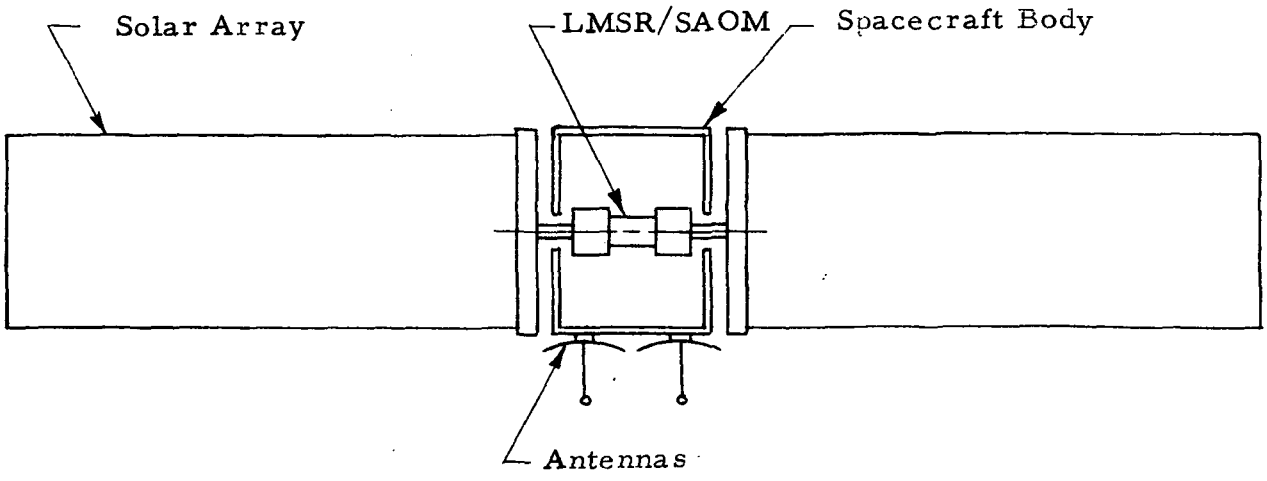

FIGURE 2. LMSR/SAOM in a Synchronous Satellite

slip rings was clearly necessary before their excellent electrical and frictional characteristics could be utilized on spacecraft.

Purpose and Scope

The present work was performed under NASA Contract NAS 3-13731 starting in November 1970. The objectives were: perform preliminary design studies on a solar array orientation mechanism utilizing liquid metal slip rings, perform preliminary design evaluation testing of certain aspects of the slip rings and their supports, provide a design of a Liquid Metal Slip Ring/Solar Array Orientation Mechanism (LMSR/SAOM) based on the above studies and testing, provide a verification test plan and a handling procedures document for the LMSR/SAOM.

Design Requirements

The LMSR/SAOM is a single axis positioning device incorporating a shaft, a housing, redundant brushless torquers, brushless angular sensor and a minimum of 116 slip rings. The shaft is to support a solar panel on each end as shown in Figure 2.

The slip ring complement is given in Table 1.

The LMSR/SAOM shall be less than 10 inches in diameter, less than 24 inches long and weigh less than 40 pounds. It shall have a minimum operating life of five years at one revolution per day. The environmental requirements are those that might be expected for an earth synchronous satellite. A cooling shroud is to be designed around the LMSR assembly. Ball bearings are to be used. The bearings, torquers and sensor are to be removable and are to be standard equipment as much as possible so that the principal effort in the program shall be expended on the liquid metal slip rings.

More detailed requirements will be presented in the text where appropriate.

Major Design Considerations

Five requirements had the major influences on the design of the LMSR/SAOM.

1. Liquid metal slip rings using gallium.
2. Operation at high voltage (HV) and very high voltage (VHV).
3. A through-shaft requirement with significant loading on both ends of the shaft.

TABLE 1. SLIP RING REQUIREMENTS

	Operating Voltage (a)	Current, dc Max.	Power Loss, watts Max. (b)	Rings Per Set	No. of Sets	Total No. of Rings
Very high voltage	0 to 15,000	0.5 A	-	7	2	14
High voltage	0 to 2,000	1 A (3 rings) 3 A (7 rings) 15 A (2 rings)	2/set	12	4	48
Signal	0 to 2,000[c] (±300V between rings in a set)	0.2 A	-	-	4	50
Power	-300 to +300	30A	2/ring	-	-	4

(a) Ring to ring and ring to ground.

(b) Connector to connector at 353K (80°C).

(c) Set to set and set to ground.

4. A large number of slip rings (116) in a confined weight and volume.

5. Open vented construction and no potting near high voltage leads.

Slip rings employing gallium require special electrode materials because of the corrosiveness of the gallium. Reliance was placed on the materials selection studies of Reference 1 to choose nickel for power slip rings and stainless steel for signal and very high voltage (VHV) slip rings. The gallium must wet the slip ring in the desired area to aid in retention and to produce the low interface resistance necessary for good electrical performance. The rate of chemical attack must be low to permit adequate life.

The slip ring design is critical to assure that the gallium is retained. A promising slip ring design evolved in the studies of Reference 1 but further effort was felt to be needed on this subject in the present project. Retention of the liquid metal becomes more difficult with large diameter rings and large clearances between rotor and stator rings.

The requirement to operate at voltages up to 15,000 had a large influence on the design studies. Small size and light weight require reliance on insulation materials subjected to high electrical stress. A breakdown in this highly stressed insulation would be likely to leave a conductive track and be catastrophic. Another approach is to rely on vacuum as the dielectric and make breakdown paths through insulation very long. This approach results in a larger but electrically conservative design.

The structural shaft extending through the slip rings requires a substantial diameter and eliminates any prospect of really small diameter slip rings sized by their electrical requirements. The large number of slip rings has the same effect in that the large number of rotor leads must be accommodated within the slip ring diameter in addition to the shaft. The long shaft will flex when loaded. The flexing determines the necessary clearance between rotor and stator rings. This clearance must be bridged by the liquid metal.

The large number of slip rings also poses the problem of how to support and arrange the slip rings for minimum weight and volume while maintaining electrical and structural integrity. Assembly is also rendered difficult by the large number of rings. Access to a ring which proves defective in test must be considered.

Open vented construction is required by the design specifications to avoid pressures in the assembly which might be in the Paschen discharge region, resulting in corona when high voltage is applied. Potting and encapsulation are not allowed because they are subject to voids and outgassing and are thus conducive to corona discharge and eventual failure of electrical insulation. These stipulations eliminate many common techniques of slip ring construction and lead to a bolt together design with many detail parts.

In summary, the design choice was between a large LMSR/SAOM with platters of concentric rings which would be structurally and electrically conservative, and a design with a small diameter shaft and axially arranged rings which might result in lower weight and improved retention of the liquid metal. The first approach was chosen for the proposal, as shown in Figure 3.

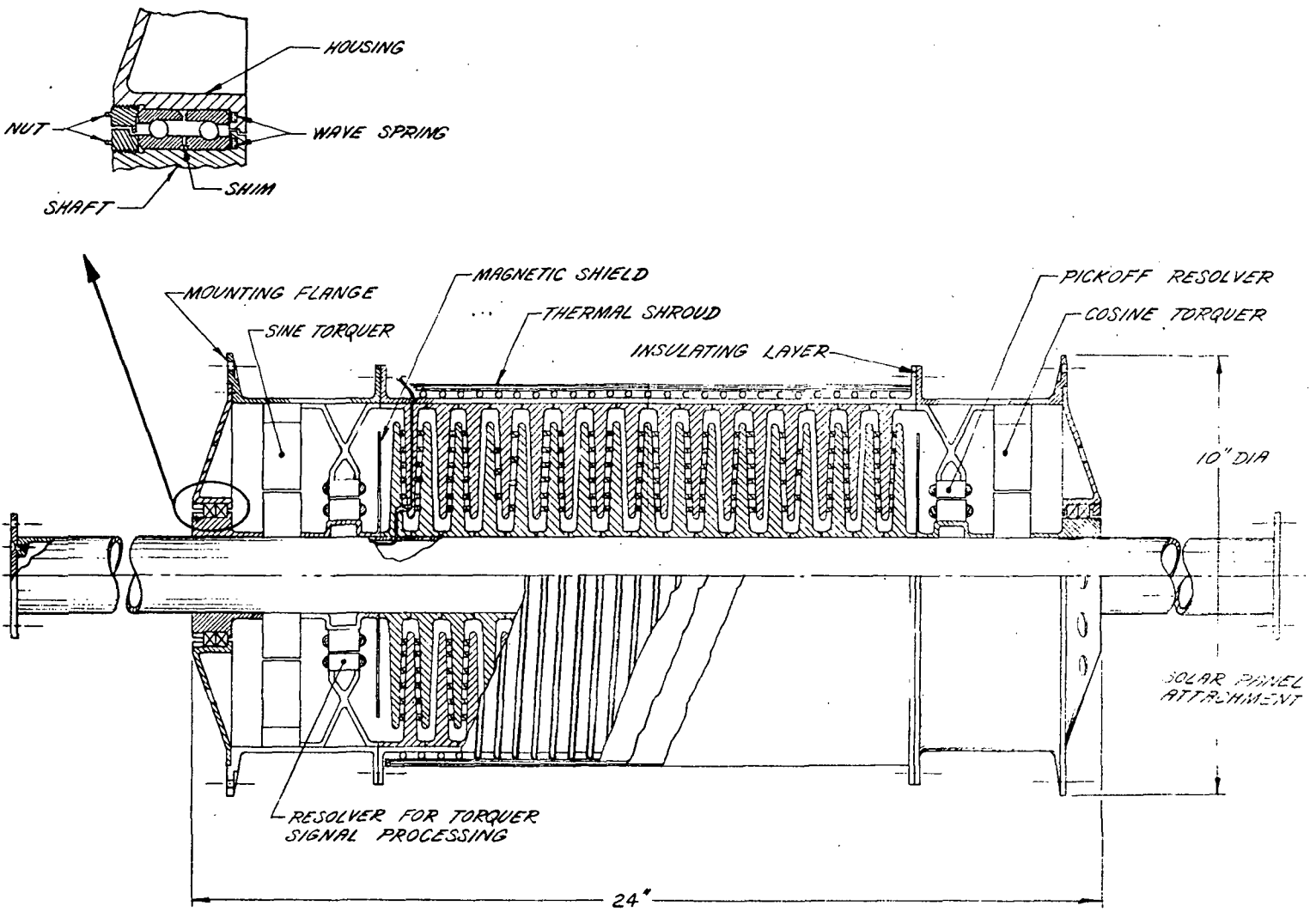

FIGURE 3. Proposal Concept for LMSR/SAOM

PRELIMINARY DESIGN STUDY

Task Objectives

This task was to investigate the characteristics of three variations of liquid metal slip ring (LMSR) designs, ending with drawings and calculations which clearly show how the design objectives are to be met. Emphasis was placed on combining innovations and sound design principles so as to maximize the advancement of LMSR technology. The effort was first directed to the conception of several distinctly different LMSR design approaches and then the approaches were screened for the three most promising.

General Arrangement Tradeoffs

Much of the design of the LMSR/SAOM revolves about the general arrangement. The requirement for a minimum of 116 liquid metal slip rings of widely varying characteristics dominates the design. There are several other major constituents which must be considered.

The LMSR/SAOM consists of the following subassemblies:

1. Housing
2. Shaft
3. Thermal Shroud (for cooling and insulating)
4. Slip Rings
   a) Power, 4 rings
   b) Signal, 50 rings minimum in 4 sets
   c) High voltage, 48 rings, in 4 sets of 12
   d) Very high voltage (15 kV), 14 rings
5. Bearings
6. Torquers, 2, brushless (with commutator resolvers)
7. Position sensor, brushless (hereinafter called "pickoff")

In addition to the above, heaters and temperature sensors are required for thermal control. The heaters are expected to be included in the thermal shroud. The temperature sensors will be located in various subassemblies.

Figure 4 shows several possible alternate general arrangements. Figure 4 a) is the configuration illustrated in the design specifications. It

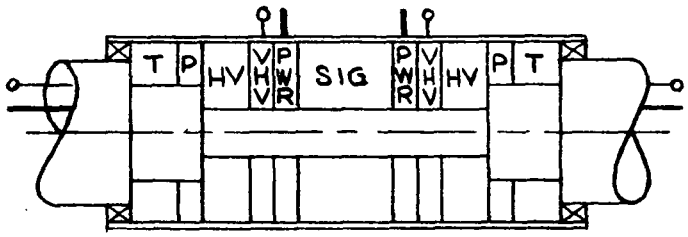

a)

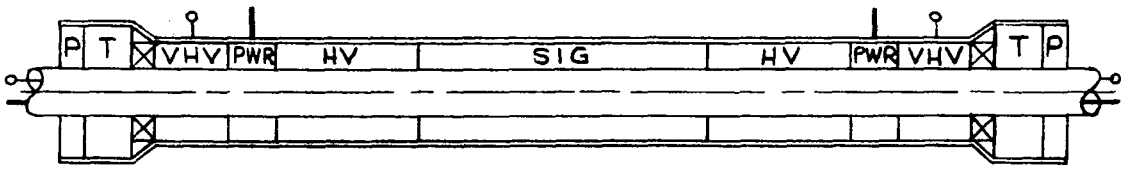

b)

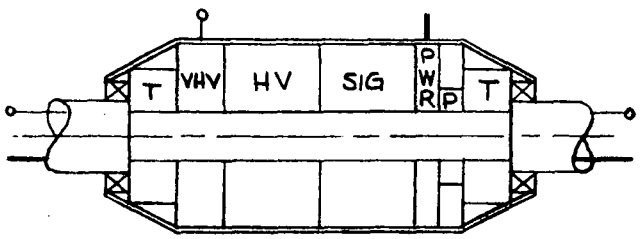

c)

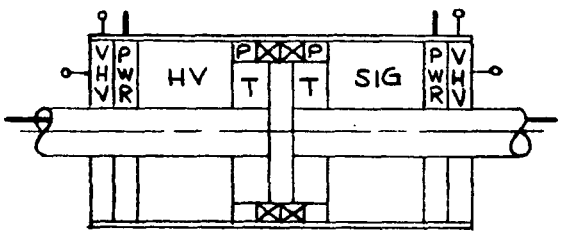

d)

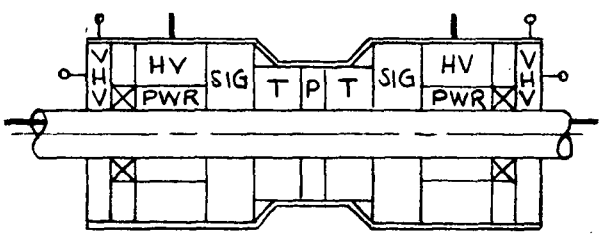

e)

KEY

═══	Housing & Shroud
	Shaft
⊠	Bearings
T	Torquer
P	Pickoff
o—	VHV Leads
—	Power Leads
	Slip Rings
PWR	Power
SIG	Signal
HV	High Voltage
VHV	Very High Voltage

FIGURE 4. General Arrangements for LMSR/SAOM

provides a good fan-out for leads coming out of a hollow shaft. The mounting flange for the solar panels is substantial. The slip rings are all in one assembly so that the torquers, pickoffs, and bearings can be readily removed. The major drawbacks of this configuration are weight and the friction torque of the large diameter bearings.

Figures 4 a), 4 c), 4 d) and 4 e) assume mounting of slip rings in concentric platters. The alternate of mounting all 116 rings in one axial stack is illustrated by Figure 4 b). This results in the smallest diameter for the rings and thus might provide the best retention of the liquid metal and the lowest weight for the slip rings. Flexure and runout of the shaft will require large working clearances in the slip rings and might cancel any advantage in retention due to smaller diameter. The long shaft would need a heavy section to attain adequate stiffness in flexure, thereby detracting from the weight decrease in the rings. This configuration would be very attractive if the axial length of the slip ring assembly could be limited to 30.5 cm (12 in.), or .263 cm (.1034 in.) for the average ring and its insulation.

Figure 4 c) shows a configuration similar to the one in the Technical Proposal. The slip rings remain in one group and the torquers and pickoff remain in separable assemblies with the bearings. The much smaller diameters permit substantial weight savings. The smaller torquer actually has a better torque to weight ratio and higher efficiency because of the reduced length of end turns. The magnetic core weight remains the same. Friction torque is reduced by smaller diameter bearings compared to Figure 4 a).

The assumption is made for all configurations that the leads from each type of slip rings are divided equally between the two solar panels. The possible advantage of combined groups of rings as in Figure 4 c) is offset by the increased conductor lengths required and by the need to intermingle the leads.

The desire to open up the assembly to provide better venting, particularly in the VHV section, suggests such as in Figure 4 d), where two ring assemblies are outboard of a central assembly of torquers, pickoffs, and bearings. This design is better suited to an "exotic" bearing such as a hydrostatic liquid metal bearing. The central flange and rigidity requirements would make the shaft heavy. Notice, however, that the VHV rings can be on the ends of the LMSR/SAOM so that the rotating VHV leads can be supported by a flange on the outside of the shaft, eliminating the need for the large VHV leads to run within the shaft. The length of the power ring leads is also minimized.

This thinking led to the arrangement of Figure 4 e). The VHV rings remain outside of conventional bearings, simplifying the lead arrangement and permitting the best possible venting. The lead length for the power rings is still quite low. The power rings are all on small diameters for minimum weight and power loss.

In Figure 4 e) the pickoff and torquers are a single assembly and the redundant pickoff can be eliminated without loss of symmetry. This arrangement was believed to have the lowest weight. A possible disadvantage is that the torquers, with their high radial forces and small radial clearances, are

relatively far from the bearing support. This could be overcome by moving the bearings to just outside of the torquers or to between the power and signal rings. Another possible disadvantage is the separation of the slip rings into four groups. This is offset by the shorter length of leads.

The general arrangement of Figure 4 e) was thus considered to be the compromise with the best chance of meeting the difficult design goals for the LMSR/SAOM.

High Voltage Considerations

Introduction

The potential problem of electrical breakdown of the insulating material used in the LMSR needed careful study to obtain reliable operation for long periods with a large number of slip rings and conductors operating at thousands of volts difference between each other and with respect to the case.

The need to conserve space and weight in the LMSR/SAOM requires that the structural support of slip rings be accomplished by the dielectric material which provides the insulation. The selection of structural dielectric materials and configuration was based on both the structural and the electrical requirements of the slip ring assembly.

The mechanisms of electrical breakdown were first considered.

Bulk Breakdown

Breakdown through the material (bulk breakdown) results from electrical stresses within the dielectric due to voltage gradients and may be characterized by any of the following processes:

- Intrinsic breakdown
- Thermal breakdown
- Inclusion induced breakdown
- Electrolytic deterioration
- Emission discharge

Of these forms of breakdown, the gas inclusion (void) induced and emission discharge processes are considered most likely in the slip ring insulation. The failures can result from the presence of separations at interfaces or voids in material for the inclusion mechanism and from stressing solids to a level at which a charge multiplication process begins within the solid as indicative of the emission discharge phenomenon. Inclusion induced stresses generally occur at much lower stresses than does the emission process and stresses as low as 20 volts per mil have been noted to cause failures when

inclusions are present. Emission discharge has been noted at 50 to 100 percent of the bulk breakdown voltage depending on the electric field conditions.

Surface Breakdown

Surface breakdown of dielectrics is a complex phenomena depending on many factors. The two basic processes are flashover and tracking. Flashover occurs when the electric field along a surface exceeds the breakdown strength of the medium or the surface. At a solid gas interface in a parallel electric field, flashover is ordinarily initiated by an ionic mechanism in the gas which has a lower dielectric strength. In such discharges, adjacent to the solid's surface, the solid can sustain damage due to the proximity of the arc. Under space conditions, in which the mean-free-path of the gas is greater than the electrode spacing, ionic breakdown is precluded, however, flashover can occur either by breakdown of the solid or field emission associated with high electric fields at the electrodes. The formation of the well-known Licktinberg figures, which have been observed in vacuum, are an example of flashover. The flashover voltage is strongly affected by:

- Surface conditions of the cathode
- Cathode material
- Dielectric surface (if it influences the cathode)
- Characteristics of the dielectric-cathode-vacuum interface

The breakdown voltage is less sensitive to similar conditions occurring at the anode. A John Hopkins study has demonstrated the importance of these factors employing:

- A smooth cathode
- A glass surface
- A gas media with mean-free-path greater than the electrode spacing

The surface flashover potential is five to ten times the values for atmospheric pressure, and corresponds to the field emission potential for the electrode material. In this same experiment comparable flashover values were observed both with and without a solid surface between the electrodes. These results indicate that the dielectric surface does not affect the flashover potential as long as it does not affect the cathode surface. Therefore, particular attention must be given to the region of the cathode-dielectric junction where methods must be used to preclude the existence of high electric fields.

Although flashover is not directly dependent upon the exposed dielectric surface, the second mode of surface breakdown is related to the characteristics

of this surface. Tracking is the formation of a conducting path on a surface as a result of:

- Electrical discharges
- Thermal degradation
- Electrolytic degradation

Electrical discharges in the form of emission discharges on or adjacent to the dielectric surface can result in deterioration of the surface and the formation of conductive paths. These discharges may be induced by:

- Gaseous inclusions at a surface
- Conductive or semi-conductive contaminants on or in the surface
- Excessive electrical stress within the dielectric

Within a slip ring mechanism, surface breakdown is most likely between rings on the same mounting surface which are operating at large voltage differences.

An additional surface consideration with a liquid metal (gallium) device is the possible surface contamination by adsorption of metal vapors on the dielectric surfaces. The presence of vapor deposited metal films could be catastrophic to the operation of a high voltage assembly.

Electrical Breakdown in Air and in Vacuum

The voltage at which a gas produces electrical discharges is determined by the electric field conditions, the type of gas and its pressure, and the conductor material.

The probable limiting design condition results from the requirement for the LMSR/SAOM to operate at full voltage in air at nominally one (1) atmosphere. Since the critical field, i. e., the electrical field at which either emission discharge (corona) or electrical breakdown occurs, for air is between 70 and 100 volts per mil, this stress becomes the design value.

Under vacuum conditions the electrical breakdown mechanism is either the field emission phenomena or impact ionization of the rarified gas. The field conditions for the latter are described by Paschen's Law and for the slip ring mechanism this mode of failure will not exist if pressures within the device are maintained below 10^{-4} mm Hg. Below this pressure, field emission will be the primary breakdown mechanism; the fields for this process range between 500 and 1000 volts per mil. A design stress of 100 volts per mil results in a five times (5X) safety margin when the mechanism is in vacuum operation.

Because of the superior electrical discharge characteristics obtainable at very low gas pressures and because of the size and weight limitation of the slip ring mechanism, the upper limit of 100 volts per mil was selected as the design value. This value leaves a minimum margin of safety when testing in air, but to reduce to a lower value would increase size and weight. If testing in air were to prove troublesome, a dielectric gas such as sulfur hexafluoride or one of the Freons could be mixed with air to provide the necessary margin without requiring design changes. Alternately, the air test could be conducted at a lower voltage and the data correlated with vacuum results.

Conductor material effects are associated with the field emission potentials for electron emission and secondary sputtering processes and are negligible when compared with the other factors since these phenomena occur at fields of 500-1000 volts per mil while the nominal design stress is 100 volts per mil.

Electric Field Determination and Control

The electric field is dependent upon the geometry of the conductors. An analysis of field conditions for several geometries in the range of interest of the LMSR/SAOM was made using the formulas of Reference 2:

For infinite parallel plates $$E = \frac{V}{a}$$

For cylinder to plate $$E = \frac{0.9\ V}{2.3\ r \log\left(\frac{r + a}{r}\right)}$$

For parallel cylinders $$E = \frac{0.9\ V/2}{2.3\ r \log\left(\frac{r + a/2}{r}\right)}$$

For sphere and plate $$E = 0.9\frac{V}{a}\left(\frac{r + a}{r}\right)$$

For sphere to sphere $$E = 0.9\frac{V}{a}\left(\frac{r + a/2}{r}\right)$$

Where E is the electrical stress, r the radius, a the separation and V the voltage between conductors.

A useful variation of these formulas is derived by setting the center-to-center or center-to-plate distance, s, as a constant and solving for the stress as a function of the ratio of the conductor radius (or diameter) to the spacing. The results are seen in Figure 5.

The lowest electrical stress between parallel cylindrical conductors for constant center-to-center distance occurs when the diameter is 0.36 times the center-to-center distance. This stress is 57 percent higher than the

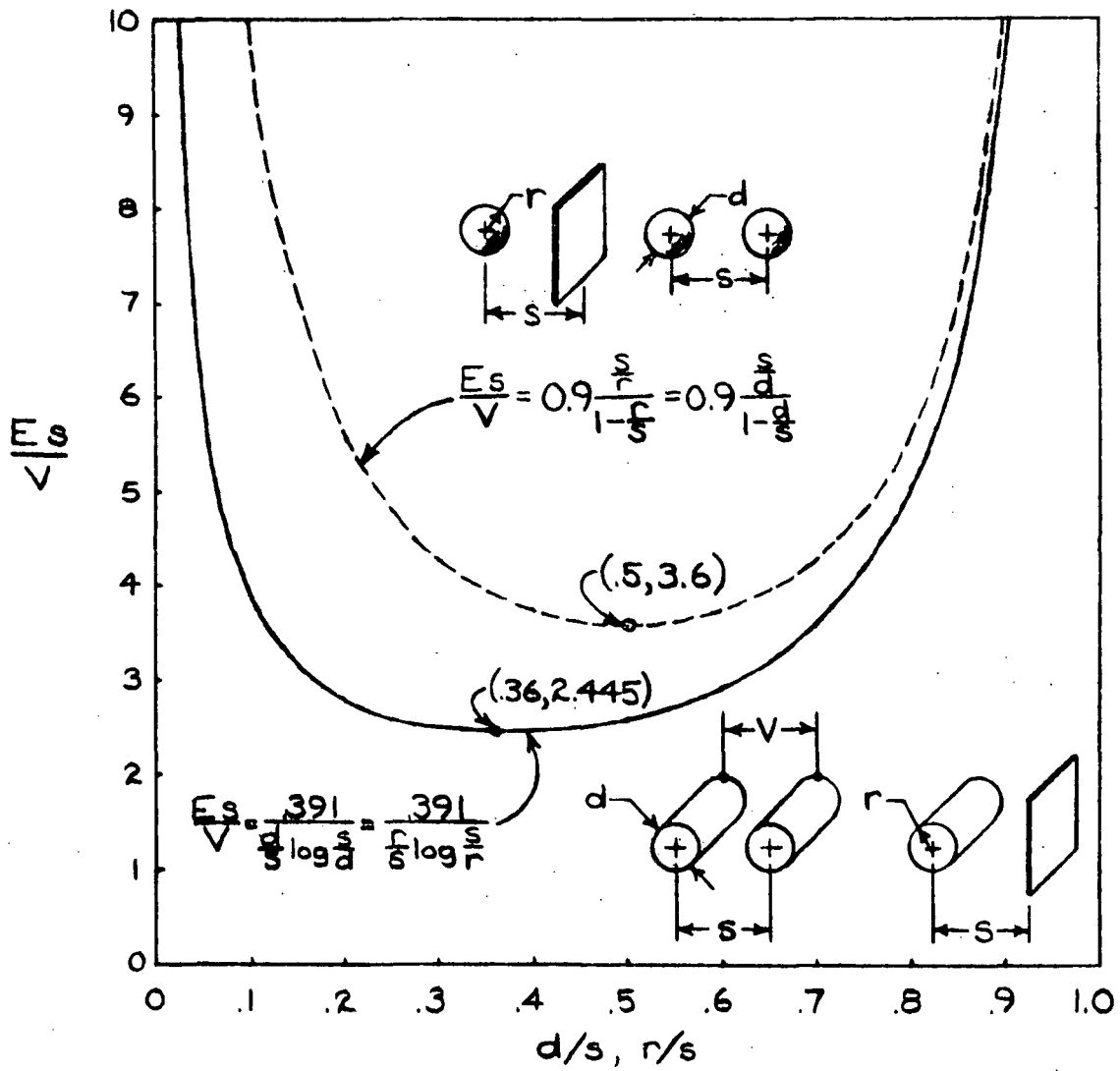

FIGURE 5. Electrical Stress vs Conductor Size for Fixed Spacing

electrical stress between infinite flat plates at the same potentials and metal-to metal spacing. For lowest electrical stress between a cylinder and a flat plate the radius of the cylinder should be 0.36 times the center-to-plate spacing.

For spherical conductors, such as corona balls, the radius should be one-half the distance to a plate or the diameter should be one-half the spacing between centers of spheres. For these conditions the stress is 80 percent higher than that for two infinite flat plates with the same metal-to-metal spacing and 47 percent higher than for the optimum cylindrical conductors on the same spacing.

One conclusion to be drawn from the above is that a change in direction of a high voltage lead in the vicinity of other leads or structure is better accomplished by a gentle bend than by a sharp change of direction capped by a corona ball.

Table 2 gives the minimum spacing for various geometries and voltages.

A conductor which is larger or smaller in diameter than that tabulated will result in increased electrical stress when used with the same center-to-center spacing. These figures must be used with caution because of the possibilities of field enhancement. The constraints on design are obvious. Conductors smaller than .132 inch diameter are to be avoided and clearances between conductors and to structure should not be less than one-quarter of an inch in the VHV sections.

Tabulations of spacing versus conductor diameters are presented in Table 3.

It should be noted that these analyses are approximations based on simple geometries and the absence of space charge conditions within the gas. Space charge which can distort the field is generally present only if ionizing conditions exist such as those resulting from electrical discharge or ionizing radiation, or if ionic gases are present. Space charge effects are not anticipated under any of the test conditions.

Because the actual geometries are more complex with the possibility of some field enhancement due to fringing effects it may be necessary to increase separations and/or diameters within the design to allow for the one atmosphere air test. Under vacuum conditions where the critical fields are significantly higher than the design value, the inaccuracies of the field determinations are of little consequence.

High Voltage Design Criteria

The following criteria were established for the design based on high voltage considerations:

- Electrical stresses through solid dielectrics such as the ring support are to be maintained at very low stresses, 50 volts

TABLE 2. MINIMUM CONDUCTOR SPACING FOR 100 VOLTS PER MIL

Conductor Shapes	Volts	Conductor Diameter, inches	Spacing, inches	
			Center-to Center*	Metal-to-Metal
Plate to plate	15,000	-	-	.150
Cylinder to cylinder	15,000	.132	.367	.235
Cylinder to plate	15,000	.264	.367	.235
Sphere to sphere	15,000	.270	.540	.270
Sphere to plate	15,000	.540	.540	.270
Plate to plate	2,000	-	-	.020
Cylinder to cylinder	2,000	.0176	.0489	.0313

*Or center-to-plate.

TABLE 3. CONDUCTOR SPACING VS DIAMETER FOR 100 VOLTS PER MIL

Diameter, inches	Potential Volts	Spacing, inches					
		Cylinder-to-Cylinder		Cyl.-to-Plate	Sphere-to-Sphere		Sphere-to-Plate
		Clearance	Centers	Clearance	Clearance	Centers	Clearance
.050	2,000	.0217	.0717	.0264	.0281	.0781	.0643
.075		.0204	.0954	.0231	.0237	.0987	.0346
.100		.0197	.1197	.0217	.0219	.1219	.0281
.125		.0194	.1444	.0209	.0210	.1460	.0253
.150		.0191	.1691	.0204	.0205	.1705	.0234
.175		.0190	.1940	.0200	.0201	.1951	.0227
.200		.0189	.2189	.0197	.0198	.2198	.0220
.250		.0187	.2687	.0194	.0194	.2694	.0210
.375		.0185	.3935	.0189	.0189	.3939	.0199
.050	15,000	.696	.746	5.544	a	a	a
.075		.380	.455	1.341	a	a	a
.100		.286	.386	.696	a	a	a
.125		.244	.369	.481	a	a	a
.150		.219	.369	.380	1.350	1.500	a
.175		.204	.379	.323	.591	.766	a
.200		.193	.393	.286	.415	.615	a
.225		.185	.410	.262	.338	.563	a
.250		.179	.429	.244	.293	.543	a
.275		.175	.450	.229	.265	.540	7.425
.300		.171	.471	.219	.245	.545	1.350
.325		.168	.493	.211	.231	.556	.798
.350		.165	.515	.204	.220	.570	.591
.375		.163	.538	.198	.210	.586	.482
.500		.155	.655	.179	.185	.685	.293
.750		.148	.898	.162	.164	.915	.211
1.000		.144	1.145	.155	.156	1.156	.185

a) For these small diameters the approximate expressions yield a negative value for spacing.

per mil or less, to virtually eliminate this failure mode because if bulk breakdown were to occur it would be catastrophic.

- Surface flashover and tracking is to be avoided by using clean, smooth, void-free surfaces on dieletrics and limiting the stresses to 30 volts per mil.

- The edges of conductive surfaces are to be radiused and conductors and terminations designed such that the electrical stresses do not exceed 100 volts per mil.

- Open construction is to be employed to eliminate voids and gas pockets so that the effective mean-free-path of the gases in vacuum test or orbital conditions will be long in relation to the separation between conductors at high voltages.

- Solid dielectric materials must be free of voids and out-gassing and must be dimensionally stable.

- Conductors in the VHV section should be of refractory materials to reduce field emission.

The above criteria result in a design in which the vacuum is relied upon as the primary dielectric. The design is electrically conservative.

Liquid Metal Slip Ring Design

Slip Ring Gap Configuration

The consideration of the shape of the solid rotor and stator portions of the slip ring in the vicinity of the liquid metal is dominated by the following factors:

1) The rings need to be wetted by the gallium because of the greatly reduced electrical interface resistance and the greatly increased adhesion compared to non-wetted.

2) The operating gap needs to be kept as small as possible to aid in the retention of the fluid against acceleration, magnetic or other forces.

3) Radial and axial clearances in the operating gap must accommodate the tolerances of rotor and stator and any shaft deflections under load without displacing the gallium from the gap.

4) The configuration must inhibit and contain any debris which comes from the gallium.

5) The conductivity of the gallium is very good and any configuration which contains the gallium between rotor and stator by capillary forces is likely to have negligible power loss. Resistance from rotor to stator is likely to be determined by the cross-section and conductivity of the rotor and stator electrode rings and the relative locations of the connections.

The study of many different gap configurations led to the selection of four basic and different design approaches which each meet the following criteria:

- The gallium wets the surfaces to which it attaches so as to provide good adhesion and low electrical contact resistance.
- The gallium is in direct contact only with metal electrode surfaces and these are metals shown to be compatible with gallium during the previous technology contracts.
- Simple axial displacement permits rotor and stator to be separated.
- The gallium is concave at the gallium-to-gas interface to inhibit residue.
- Reservoirs are provided at the gallium-to-gas interface to collect any surface residue. The reservoirs are configured to return escaping gallium liquid to the "parent" gallium pool in the operating gap between rotor and stator.
- The escape path for gallium liquid residue is through a baffle or partial labyrinth seal which is non-wetted.
- Each configuration must provide for a minimum of ±0.010 inch (0.25 mm) radial and/or axial displacement of the rotor with respect to the stator before rubbing occurs.

1. Radial Gap

The radial gap ring configuration has an internal cross-section resembling a dumbbell. See Figure 6. Surface tension must be relied upon for retention of the gallium in a one gravity field.

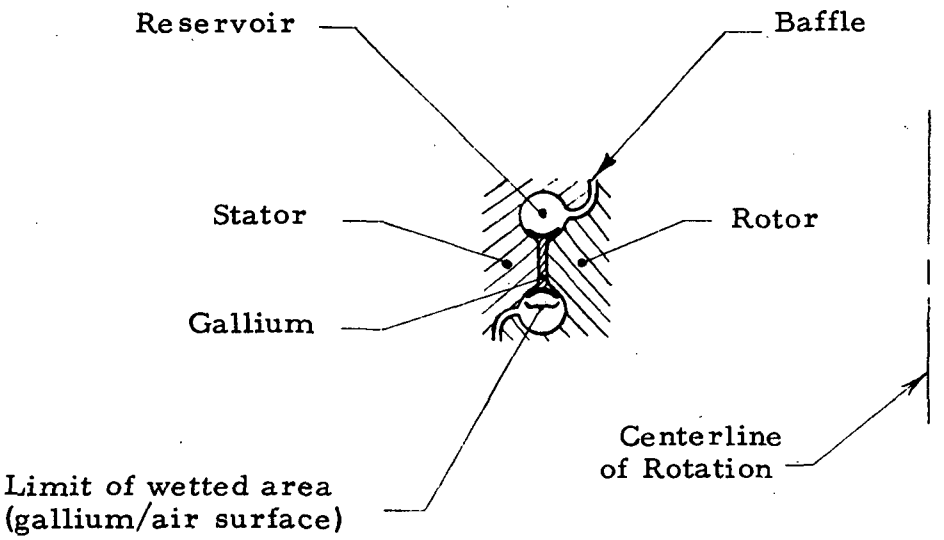

Figure 6. Radial Gap Configuration

2. Cup Gap

This design is a development of the successful cup gap rings used on the engineering test model of Contract NAS 3-11537. See Figure 7. It will be noted that a cup gap ring is likely to use more radial space and less axial space than a radial gap ring. The cup gap ring has an advantage in retention in a one gravity field. Surface tension is not called upon to retain the liquid in the gap as long as the ring is in a horizontal plane.

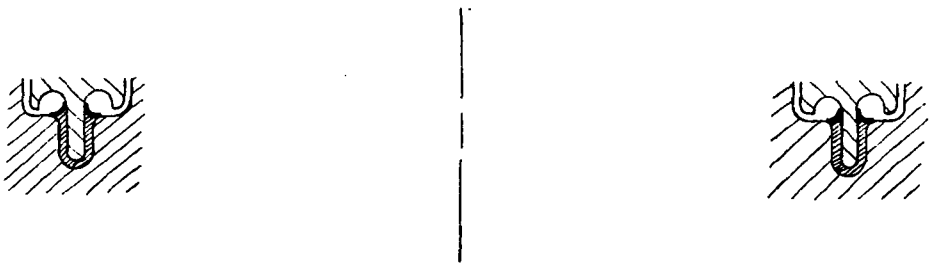

Figure 7. Cup Gap Configuration

3. Probe

The probe is a design approach distinctly different from the radial and the cup configurations in that one electrode occupies only one or more short tangential lengths rather than the complete circumference. This greatly reduces the length of the shear lines in the gallium surface film when the rotor rotates with respect to the stator. This may greatly reduce the production of gallium debris such as twirlies and sludge. See Figure 8.

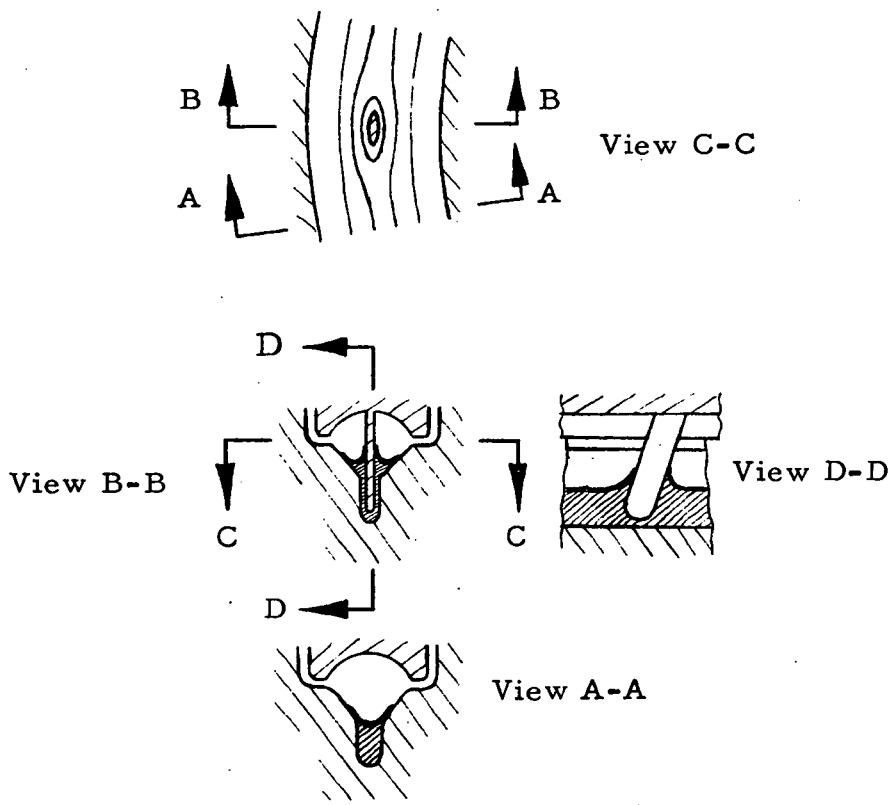

Figure 8. Probe Gap Configuration

The cross-section of the probe shown in Figure 8 is elliptical rather than circular so as to reduce the width of the groove necessary to accommodate an electrode probe of a given cross-section and wetted area. The swept-back leading edge is to reduce any tendency to collect residue. Probe designs have a gap more than twice as wide as the radial or cup gap, except where the probe is, so they do not retain gallium as well for a given required clearance between rotor and stator.

4. Brush

The "brush" design concept is similar to the familiar brush-on ring sliding contact slip ring except that a positive gap is maintained and the gap is filled with gallium. See Figure 9.

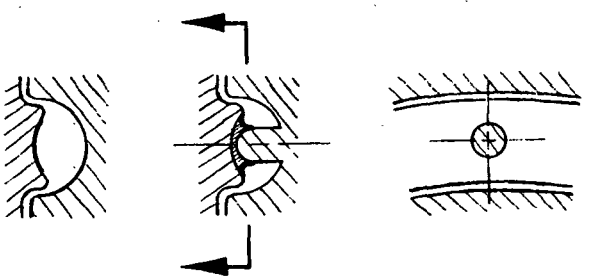

Figure 9. Brush Gap Configuration

The attempt is made in this design, as in each of the others, to retain separated gallium in the reservoir. The gallium may have originally broken free as debris from the breaking of gas bubbles in the gallium.

The brush design is well-suited to the establishment of a reservoir of gallium to make up for inadvertent losses or provide for runout tolerances as shown in Figure 10. Alternate means of providing a reservoir are wicks or brushes made of porous materials filled with liquid gallium. The ring could be operated very "dry" and would thus be quite insensitive to acceleration. Most of the gallium in the ring would be at the point(s) of contact.

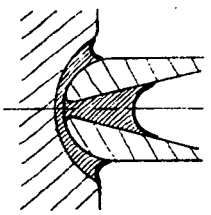

Figure 10. Brush with Gallium Reservoir

Retention of Liquid Metal in the Gap

The retention of liquid metal in an operating gap between rotor and stator can be calculated from the expression for capillary pressure.

$$\Delta P = \sigma\left(\frac{1}{R_1} + \frac{1}{R_2}\right)$$

where: ΔP = the difference in pressure across the liquid interface

σ = the surface tension

R_1 & R_2 are the principal radii of the surface at the interface

For the simple gap configuration of Figure 11, the acceleration capability can be derived to be

$A_a = 4\sigma/\rho HL$ axial

$A_r = 4\sigma/\rho HD$ radial

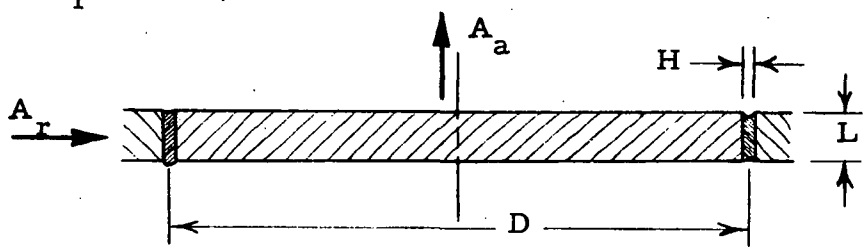

Figure 11. Basic Gap Dimensions

Where σ = 735 dyne/cm

ρ = 6.095 gram/cm^3 for gallium

The maximum acceleration capabilities are plotted in Figure 12.

In the experimental studies of Reference 1, it was found that if the gallium bulged from the gap when the rings were rotated in air that the quasi-plastic surface film caused lumps of film-covered gallium debris to roll up and separate from the main body of gallium. If the surface was concave the lumps went into the gallium and formed a kind of sludge. The sludge was preferable to the debris so the concave gallium surface was desired for all ring configurations as shown in Figures 6 through 10. This tends to result in a wetted area extending up chamfers on either side of the gap. The acceleration capability is reduced to about 1/2 that shown in Figure 12 when this is done.

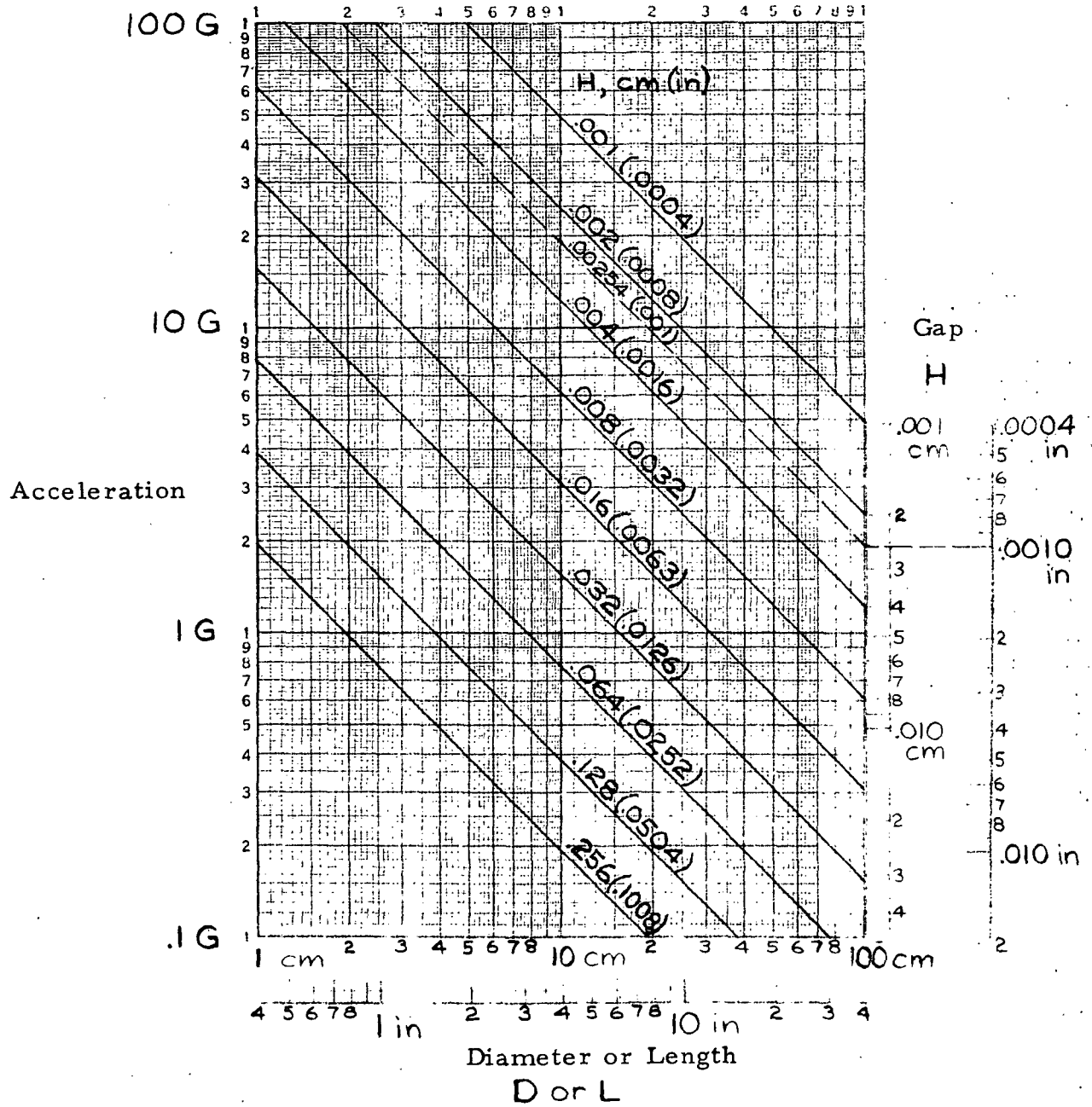

FIGURE 12. Maximum Acceleration Capability of Gallium Contained in a Gap

It was intended that the reservoirs and baffles seen in Figure 6 would avoid the escape of any debris which might separate from the gallium in the gap.

To illustrate the use of Figure 12, let us assume a ring with radial gap configuration and the following dimensions:

Diameter	D = 30 cm	(7.62 in.)
Length	L = 1 cm	(0.394 in.)
Gap	H = .064 cm	(0.025 in.)

For axial accelerations the length L is used and the intersection of L and H in Figure 12 is at 7.8 times gravity. For radial accelerations, the diameter D is used and the intersection of D and H is at 0.25 times gravity. Such a ring cannot be operated with a horizontal axis.

The maximum gap H for a 30 cm diameter ring to operate with a horizontal axis in one gravity is 0.016 cm (0.0063 in). Such small clearances would be difficult to maintain in such a large structure.

Another force which conceivably could displace gallium from the gap is that due to magnetic fields. The specified field is 0.01 tesla (100 gauss). A calculation was performed which indicated that the worst case force on a ring at 30 A would be equivalent to less than 0.03 times gravity. Magnetic fields are thus likely to be of concern only if they are modulated at a frequency which is close to a sloshing frequency of the gallium in a gap.

Electrical Power Loss

The large number of rings and the high currents specified, see Table 1, require that conductors be quite large to prevent excessive temperature build up in the LMSR/SAOM. The maximum power loss in a 30 A circuit is specified as 2 watts, connector to connector at 353K (80°C).

The two major sources of power loss considered were the resistance of the electrical leads and the resistance around the rings from the current connection (tap) on the rotor ring to the current tap on the stator ring. To limit the loss to 2 W the resistance must not exceed 2.22 milliohm.

Figure 13 a) is the sketch of a typical slip ring pair. Assume that the area of the cross-section is 0.126 cm^2 for rotor and stator combined and 0.0077 cm^2 for the gallium. The mean diameter is 8.89 cm (3.5 in.). This is a typical power ring design.

Figure 13 b) shows the resistance elements to obtain an approximation of the resistance from the current tap on the stator to the current tap on the rotor. Using a value of 6.8 $\mu\Omega$ cm for the resistivity of nickel at 20° C

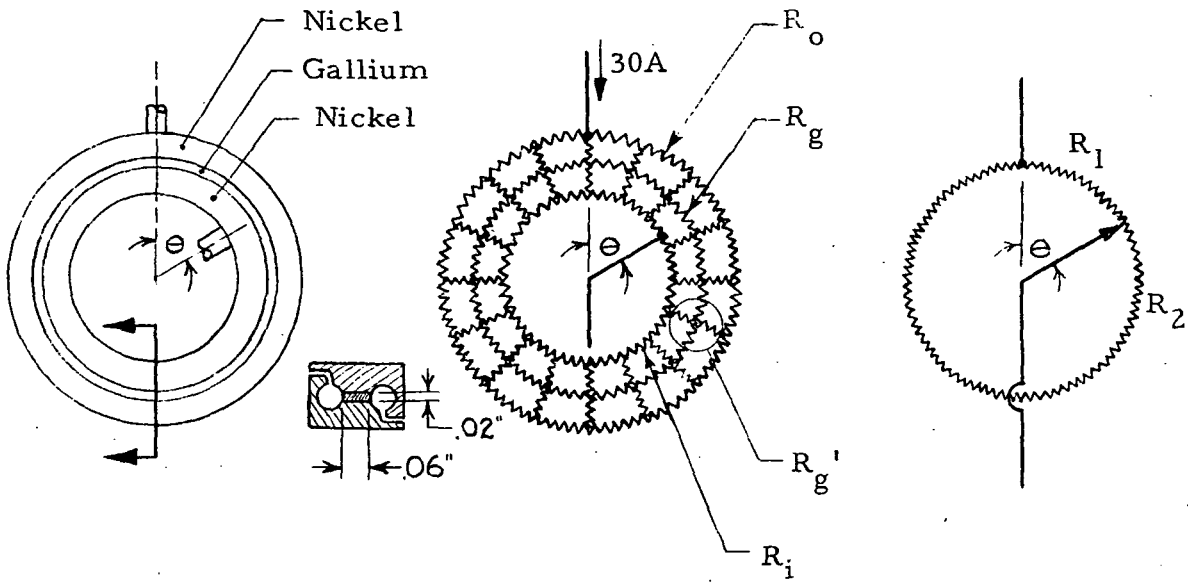

a) Physical configuration b) Electrical schematic c) Simplified schematic

Figure 13. Electrical Resistance Schematics for a Liquid Metal Slip Ring

$$R_o \cong R_i = 3.02 \text{ milliohm}$$

all the way around the ring. Using 28 $\mu\Omega$cm for gallium:

R_g = 0.101 ohm circumferential

R_g' = 0.334 microhm radial

where R_g' is the resistance through the gallium from rotor to stator. The radial resistance through the gallium can obviously be neglected and the inner and outer ring treated as one.

The highest resistance is with $\theta = 180^o$. At that point

$$R = 0.372 \text{ milliohm}$$

and the power $P = I^2R = 0.335$ W at 30 A. The power dissipated in the gallium is only 0.30 milliwatt. This leaves adequate margin for lead resistance and increase in resistance with temperature.

The 15 A high voltage rings have a somewhat larger diameter. The average diameter for the eight rings is 10.32 cm (4.0625 in.). For the simplified model of Figure 13 c) the circumferential resistance is

$$R_1 + R_2 = 1.726 \text{ milliohm}$$

Assuming that these eight rings have their taps staggered by 45°. Table 4 shows the effective resistance and power loss for the eight rings with 15 A in each.

TABLE 4. POWER DISSIPATION OF 15A HIGH VOLTAGE RINGS

θ	R_1, mΩ	R_2, mΩ	R, mΩ	I^2R
0	0	1.726	0	0 (a)
45°	.216	1.510	.189	.0425
90°	.432	1.294	.324	.0729
135°	.648	1.078	.405	.0911
180°	.863	.863	.432	.0972
225°	1.078	.648	.405	.0911
270°	1.294	.432	.324	.0729
315°	1.510	.216	.189	.0425

(a) The simplified model is inaccurate near θ = 0.

The total dissipation in all eight rings is 0.510 watts and again there is adequate margin to allow for connections, leads, and temperature.

Note that as the rings rotate the dissipation in each will vary from near zero to near a tenth of a watt.

If these rings were made of stainless steel the resistance at θ = 180° goes to 45.8 milliohms and the dissipation in one ring at 15 A is 1.03 watts. Further calculations showed that the 3 A high voltage rings also needed to be of nickel because of its higher conductivity. Thus, it was concluded that all high voltage rings should be solid nickel.

The use of nickel-plated copper rings was investigated in Reference 1. It was found that the gallium attacked the copper through the nickel plating, causing blistering of the plating.

Nickel-plated copper conductors not in direct exposure to the gallium would be suitable for leads. It was determined that the leads for the 30 A power rings and the 15 A high voltage rings would need to be AWG #8 (0.1285 inch diameter) copper wire to keep the dissipation within the specified limits.

Support Structure for Slip Rings

Three general methods of construction and support for the slip rings were considered:

1. Rigid metal slip rings attached to spokes.

2. Flexible metal slip rings attached to discs of dielectric material.

3. Plated metal on dielectric rings.

The first method of construction has excellent venting and low outgassing but may prove fragile to the launch environment. The rings may be sheet metal or machined, the cross-sectional area depending on the current carried. The spokes may be of dielectric such as epoxy-glass or of metal with dielectric spacers to the rings. In the latter case the metal spokes could be the conductors.

Rigid rings are illustrated by the power ring in Figure 14.

In the second method the rings are too thin to retain roundness or withstand the launch environment without support from the dielectric. The dielectric disc may provide a portion of the reservoir and baffle. An example is the bicycle rim ring configuration shown in Figure 14. Venting is difficult in this configuration and outgassing is increased by the increased use of dielectric, but the assembly should be more rugged compared to the spoke method.

The structural strength of the third method comes mostly from the dielectric material with only a thin layer of plated metal where the gallium is to contact. This design is illustrated by the "plated-loop" design of Figure 15. In this case the dielectric rings are mounted on spokes to reduce weight. The spokes could be metal or dielectric.

An example of a lightweight spoked support for slip rings is seen in Figure 16. The Z-section spokes give rigid support to the slip rings and the rings at the inside and outside diameter provide convenient mounting to the shaft or to the housing.

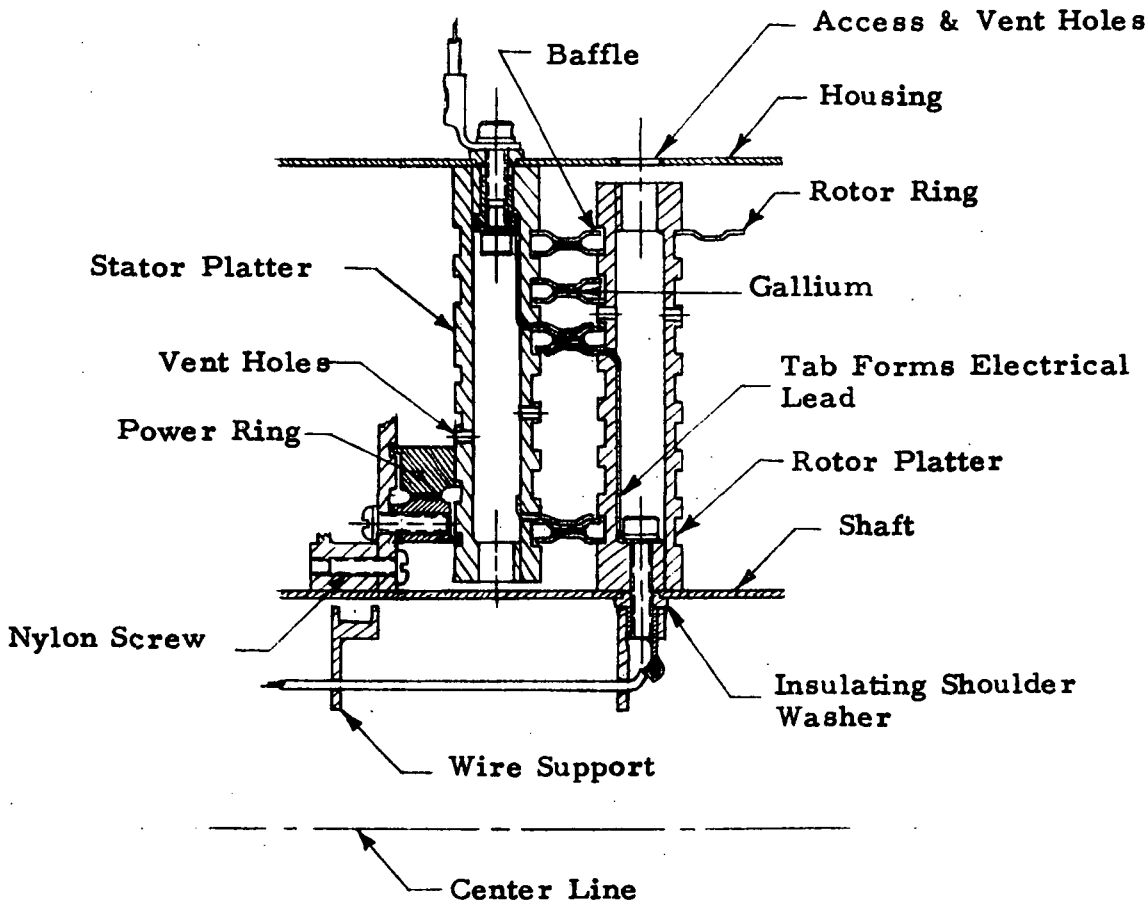

Figure 14. Bicycle Rim Ring Configuration

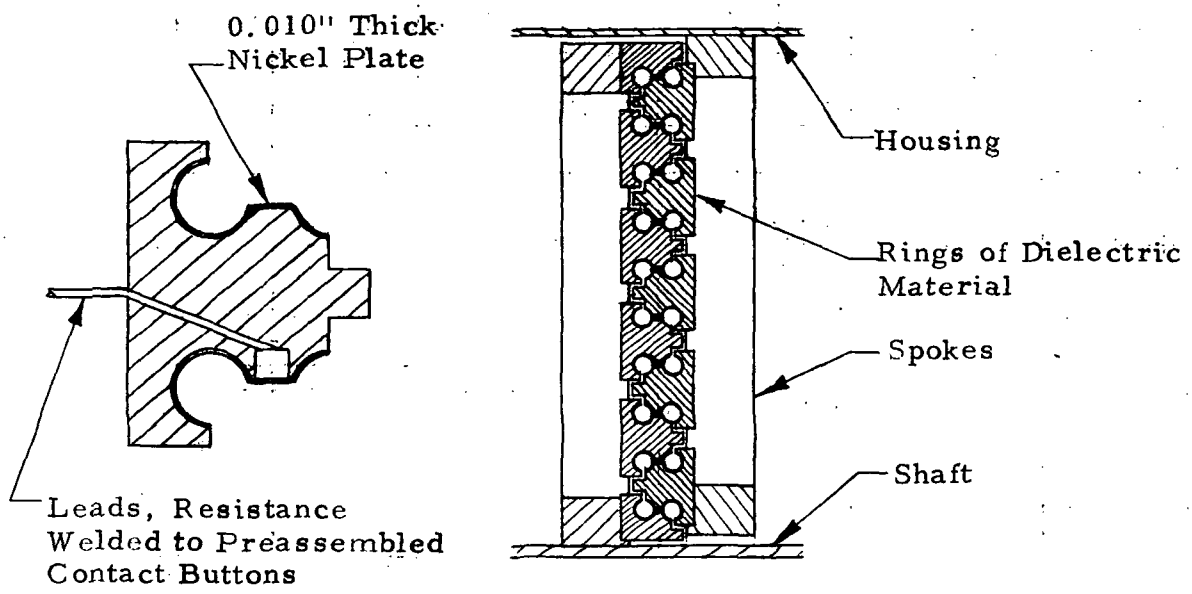

Figure 15. Plated Hoop Ring Configuration

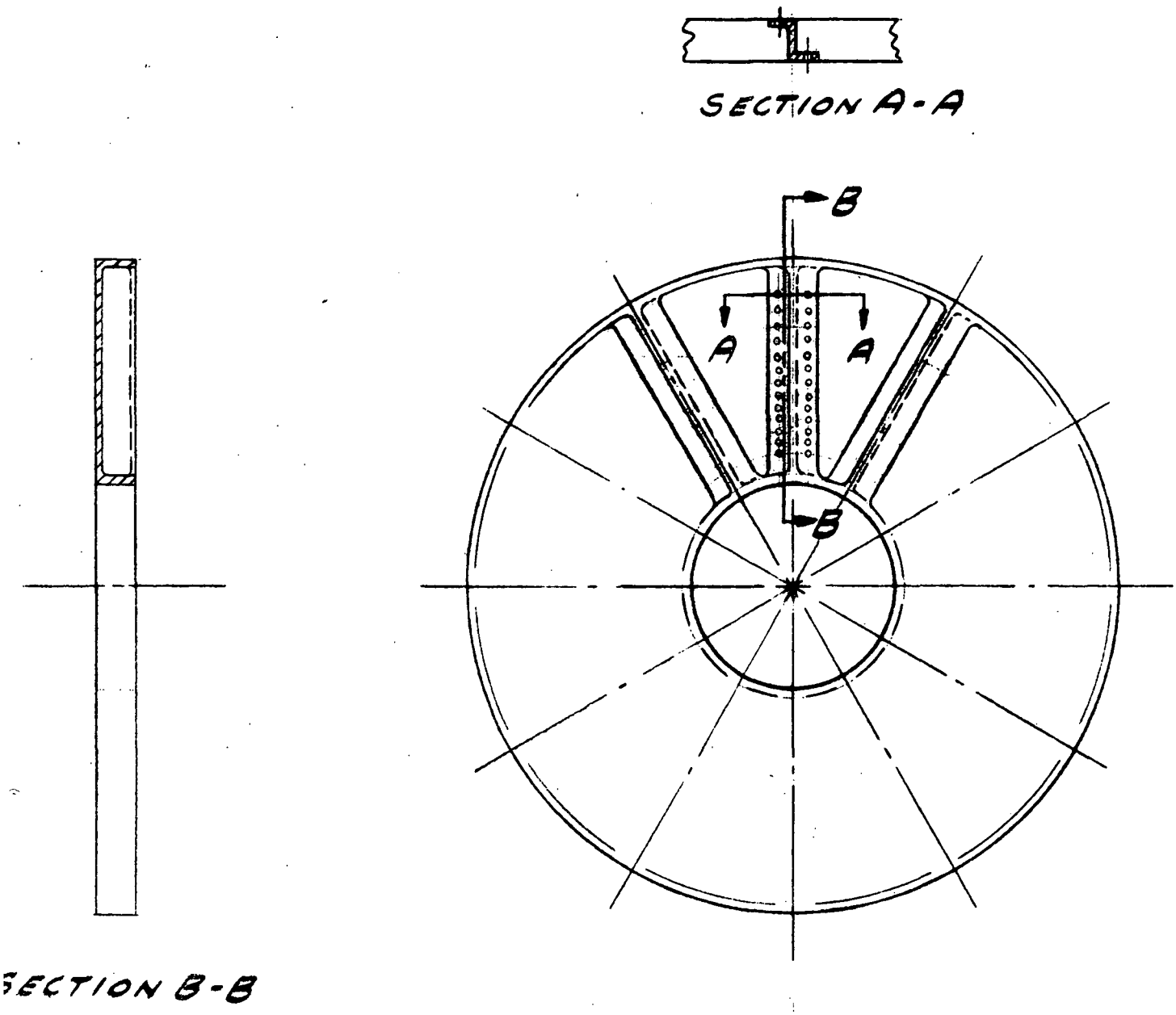

Figure 16. Spoked Insulating Slip Ring Support

Slip Ring Configuration Tradeoff Study

The objective of this study was to select the three design approaches to be pursued in the preliminary design study from among the many variations so far considered.

The design approaches are broken down into categories of Gap Configurations and Methods of Construction. Generally, any of the gap configurations could be fabricated using any of the methods of construction. The means of evaluation include:

- Gallium considerations
- Electrical considerations
- Structural (environmental) considerations
- Critical characteristics
- Cost

Numerical ratings are assigned on the point system. The points available are assigned based on the impact of an evaluation criterion to the total program based on the following guide.

Points	Relative Difficulty or Importance
1	Readily accomplished or of secondary importance
2	Important, not difficult
3	Requires extra care
4	Difficult task
5	Prime consideration

The point rating is given to a given slip ring configuration based on an estimate of the probability of meeting a given criterion with that configuration during this program. The estimates are deliberately pessimistic so as to provide a greater spread in results.

Table 5 lists the detailed criteria for evaluation.

The summary of ratings for eight configuration combinations is given in Table 6. The detailed rating for the bicycle rim construction is shown in Table 7 as an example.

TABLE 5. CRITERIA FOR EVALUATION

Gallium Considerations (Ga Liquid)

Debris Formation:

- Minimum length of shear line
- Minimum Ga surface area exposed
- Concave surface (form sludge instead of twirlies)
- Minimum eccentricity

Debris Retention: Reservoir, baffling

Sensitivity to Debris:

Minimum unevenness and discontinuities in rotor and stator. Sludge pileup causes clogging and torque. Adequate reservoir capacity. Large gaps desirable.

Acceleration Capability, Radial and Axial:

- Steady state (handling):
  - Maximum change in surface radius (small gaps, narrow wetted area)
  - Minimum "head: (small diameter rings, narrow width)
- Shock (operating and prelaunch test, 10 g peak)
  - Minimum flow path for displaced gallium
  - Avoid separation of displaced gallium
- Vibration (operating and prelaunch test)
  - Sloshing (minimum amount of gallium)
  - Folding and mixing in of surface film
- Amount of gallium: minimize to reduce damage in event of spill

Table 5. (Continued)

High Voltage Considerations

Electrical Stress: Maximum spacing, maximum radii of conductors.

Mean Free Path: Long with respect to spacing

- Maximum venting: straight-through clearances, maximum open area
- Minimum outgassing
  - Minimum volume of dielectric
  - Minimum surface area of dielectric
  - Minimum vapor pressure dielectric
  - All surfaces readily cleaned, kept clean

Location of Dielectric

- Between conductors, bulk breakdown, catastrophic
- Between conductors, surface breakdown, may be catastrophic
- Not between conductors, Paschen discharge, self-healing

Other Electrical Considerations

Power Loss: Within specification regardless of shaft rotation.

Capacitance: Within specification.

Structural Considerations

Weight: Within budget, 11.5 pounds

Size: Less than 10.0 inches diameter, 24 inches long

Launch Environment: No damage, Ga frozen, radial and axial

- Acceleration, 15 g
- Shock, 30 g peak: no interference at maximum deflections

Table 5. (Continued)

- Vibration: Locking fasteners, rigidity, damping of resonances

Temperature, good match of coefficients, no damage at -65°F to +250°F

Reliability: Margins, redundancy

Critical Characteristics

Special Materials: Minimize

Processing: Minimize plating, welding, heat treating, finishing

Cleaning: Avoid: porous materials, scales, strands

Wetting with Gallium: Avoid slots and discontinuities. Nickel preferred

Outgassing: Avoid bubble traps, assembly in vacuum if possible

Special Handling or Test Requirements: Minimize

Cost

Materials: Use stock sizes

Parts Fabrication: Minimize: Special tooling, difficult materials, parts count, use of tight tolerances

Processing: Plating, welding, heat treating, finishing, cleaning

Assembly: Minimize: Parts count, tooling, skill required

TABLE 6. SUMMARY OF CONFIGURATION RATINGS

CONFIGURATION				Gallium	Electrical	Structural	Critical Character.	Cost	Total	REMARKS
Descriptive Name	Gap	Rotor	Stator	31	20	18	23	8	100	Maximum Points
Bicycle Rim	Radial	Disc	Disc	16	9	12	15	4	56	
Plated Hoop	Radial	5 spokes	5 spokes	19	7	10	15	5	56	No radial space between rings.
Probe	Probe	Disc (probes)	Disc (rings)	26	12	10	15	6	69	Disqualified, technical direction
Tubing Rings 	Radial	8 spokes	8 spokes	10	19	9	13	2	62	These designs primarily suited for very high voltage.
Crab Section 	Axial	8 spokes	8 spokes	21	20	12	13	3	69	
G-Section 	Radial	8 spokes	8 spokes	22	19	9	17	2	69	
Cup Gap 	Cup	12 spokes (cups)	Disc	20	13	12	14	4	63	Z-section spokes
Brush (radial assembly of stator)	Brush	Disc	Disc (segments)	21	7	9	13	6	56	Needs improved baffle

TABLE 7 TYPICAL SLIP RING CONFIGURATION RATING

Description: Bicycle Rim Type

Gap: Radial Construction: Rotor: (B) Stator (B)

Evaluation Criteria	Points	Rating	Comments
Gallium Considerations			
Debris Formation	5	3	
Debris Retention	5	3	
Sensitivity to Debris	3	2	
Sloshing (Ga Liquid)	5	3	
Steady Accel. (Ga Liquid)	5	2	
Shock (Ga Liquid)	5	1	displaced gallium may escape
Amount of Gallium	3	2	
	31	16	
High Voltage Considerations			
Electrical Stress	5	2	sharp corners
Venting	5	2	small holes
Outgassing	3	1	much dielectric
Location of Dielectric	2	1	
	15	6	
Power Loss	3	2	
Capacitance	2	1	
Structural Considerations			
Weight	5	3	
Size	1	1	can be small
Launch Accel. (Ga Solid)	5	3	good damping of resonances
Temperature	2	2	
Reliability	5	3	ring support poor
	18	12	
Critical Characteristics			
Special Materials	3	2	pure Ni for HV rings
Processing	5	3	welding of rings
Cleaning	4	2	closed space between discs
Wetting with Gallium	4	3	
Outgassing at Assembly	4	3	
Handling and Testing	3	2	
	23	15	
Cost			
Mat., Fab., Processing	4	2	
Assembly	4	2	many parts and many operations
	8	4	
TOTALS	100	56	

Code for method of construction:

A. Rigid metal slip rings on spokes

B. Flexible metal slip rings on dielectric support

C. Plated metal on dielectric rings

The results of the study and search for additional slip ring design candidates was that the configurations considered early in the program were discarded in favor of new ideas. The bicycle rim, plated hoop and blade probe approaches each suffered from poor venting, high outgassing and high electrical stress and were considered unsuitable for the 15 kv rings.

The search for a well-vented design approach with low electrical stress led to the conception of the tubing, crab section and G-section rings supported on spokes. These concepts are well-suited to the very high voltage requirement but are larger, more fragile and more expensive than necessary for the 2000 volt requirement. These rings would probably be made of AISI type 304 stainless steel.

The fact that the crab section is an axial gap is mostly overcome by the rounded surfaces of the ring configuration, which are expected to control spurting of the gallium during sudden displacement of the rotor with respect to the stator.

A cup gap configuration that met the strict criteria was conceived and did well on the ratings. This cup gap configuration is well suited to the high current rings and can be spaced closely enough to meet the signal ring requirement without requiring undue volume. High currents can readily be transferred around the ring through the solid cup ring. Material would probably be solid nickel for high conductivity.

An outgrowth of the studies on probe approaches was the brush approach in which a wetted ring on the rotor moves in close proximity to a small wetted electrode at one or more places on the stator. Liquid gallium was expected to bridge the gap, which typically would be less than 0.015 inch with an electrode diameter of 0.060 inch. This concept has several virtues:

- The very small volume of gallium theoretically permits an assembly with acceleration capability exceeding 30 g's in any direction with the gallium liquid.
- The small size permits rings to be placed as close as 8 per inch, radially or axially.
- Tight tolerances and cost are minimized.

- The gap could readily be made adjustable.
- The shear length of gallium film during ring rotation is very low.

The main drawback seen for the brush configuration was the large exposed area of gallium compared to the very small volume. The gallium might thus be transformed to sludge more readily or it might drain from the wetted ring surface during periods of no rotation and thus resist rewetting by the brush during rotation. These problems can be reduced by providing a reservoir of liquid gallium in a hole or holes in the brush or by a matrix on the ring surface.

Further study of the probe approach was terminated by Technical Direction.

The weight of the plated hoop design was reduced from 17 pounds to 13.3 pounds by mounting the rings on spokes. The configuration was improved to provide for reservoirs, baffling and improved venting compared to the configuration given in the Work Plan. The plated hoop concept is considered questionable due to the possible leakage of gases from the dielectric substrate through the plating into the gallium. Effort on it was thus terminated.

The bicycle rim design was also bypassed because of the appearance of more promising configurations. The total point ratings of 56 for each of four configurations is a coincidence. The ratings were not "massaged" to obtain this uniformity.

The favored configurations for further development were:

1. The crab section rings, particularly for the very high voltage platters. This ring section is the most rugged of the spoke-supported rings.
2. The cup gap configuration was chosen as a good all-around design, particularly well-suited to the power and high voltage requirements. This design is similar to that used successfully in Reference 1.
3. The brush configuration was chosen because of its high acceleration capability, which would eliminate the need to maintain a vertical shaft position whenever the gallium is liquid and would reduce concern over the effect of the 10 g shock which is part of the specified operational environment. This design is well-suited to the signal ring requirement where inter-ring voltages are low and spacing can be close to save space and weight.

STRUCTURE

Housing

Figure 17 is a preliminary layout showing some aspects of the packaging considerations when using a general arrangement as shown in Figure 4 e). The titanium housing is one piece out to the removable bulkheads which support the ball bearings. Bulkheads are conical instead of flat so as to be as rigid as possible. The short section of housing which supports the very high voltage rings outboard of the bearings might be made of dielectric material to eliminate the feed-through insulators and reduce weight except for the need for the thermal shroud to control the temperature of the gallium in the rings.

The very high voltage rings have excellent ventilation in this design so that there should be no problem with Paschen discharge. The electrical stress has been limited to 100 volts per mil. The VHV rings illustrated are a version of the G-section rings. Each ring is supported by ball-ended posts at four places each on the rotor and stator from the spoked supports. The rings are 0.180 inch section diameter with 0.012 inch wall thickness. For launch, when the gallium is frozen, the spokes would be arranged so that the support posts would be alternated between rotor and stator every 45 degrees, resulting in support for the outside ring every 3 inches on its periphery. The crab section ring would be more rugged in this application because of its closed tubular elements.

A thermal radiation shield is shown to reduce the heat losses from the VHV rings. This may be necessary to reduce the heater requirements. Such a shield might be of dielectric material.

The power, signal and high voltage rings are illustrated only as to general location, not actual cross section. The 15A high voltage ring and the 30A power rings will have heavy sections to minimize power losses and they will be on the smallest diameters. They are indicated by broken circles. The high voltage and signal rings with currents of 3A and less are indicated by broken ellipses.

A candidate ring support for the high voltage, power and signal rings is illustrated in Figure 16. Each of the 12 spokes has a Z section permitting each ring to be attached to each spoke. The rings can be smaller because of the lower electrical stress. The closer spacing is permissible at 2000 volts. The smaller rings need more support. Freezing the gallium with spokes spaced 15 degrees apart provides support for the outermost ring every inch of periphery.

The weight for the LMSR/SAOM configuration shown in Figure 17 was estimated as shown in Table 8. The design goal of 40 pounds can be achieved if wall thicknesses as illustrated are reduced by one-third and many lightening holes are added.

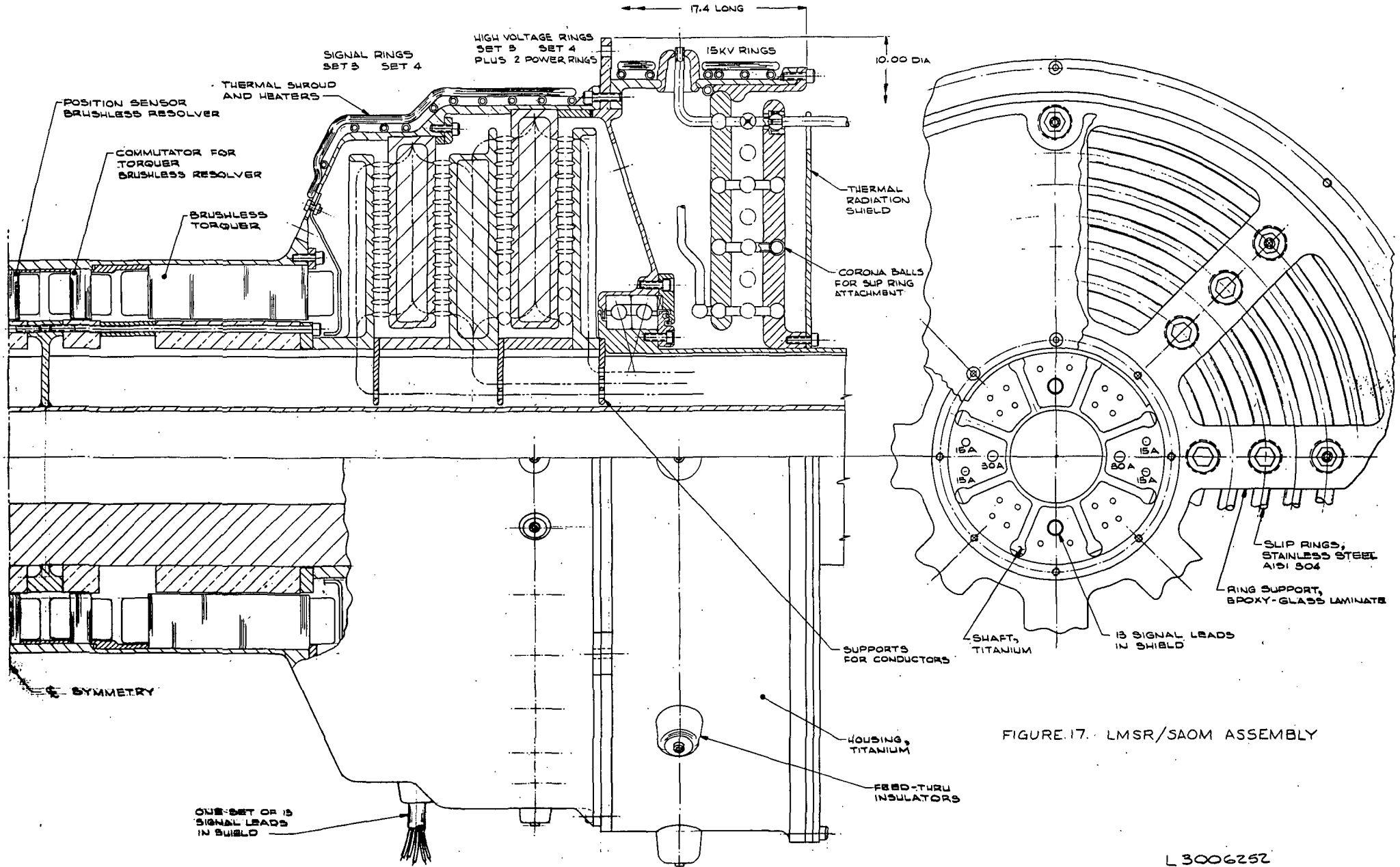

FIGURE 17. LMSR/SAOM ASSEMBLY

L3006252
LMSR/SAOM

TABLE 8. LMSR/SAOM WEIGHT ESTIMATE

Item	Weight, pounds
Shaft and flanges	3.25
Housing	3.2
Bearing subassemblies	2.75
Torquers (2) and resolvers (3)	12.0
Thermal shroud	2.2
Electrical leads (to shaft ends)	2.4
Hardware and miscellaneous	1.0
Slip ring assemblies	13.2
Total	40.0

Titanium is the favored material for the housing and shaft because of its high stiffness-to-weight ratio. Aluminum cannot be used because of the corrosiveness of gallium. Beryllium is not used because of its high cost and concern for structural integrity, particularly in the presence of gallium.

Figure 18 illustrates a structural design approach suitable to the probe or brush type rings. The housing consists of bulkheads supported on rails. The slip ring stators (except for the VHV rings) can be segmented so that by removing one rail they can be removed. The convenience of such an arrangement for assembly, adjustment, wiring and troubleshooting is obvious. The thermal shroud might be on a large diameter, thin wall tubing which would slip over the entire assembly. The question is whether adequate structural integrity can be attained within the weight requirements.

Shaft

Extensive studies were made of the shaft configuration. The finned tubing cross-section shaft as in Figures 17 and 18 is preferred to a simple tubular shaft. The simple tubular shaft of maximum diameter requires many holes to accommodate the lead wires from the slip rings. Assembling the leads and supports inside the tube and making connections to them through the holes present many problems. The finned tube provides large troughs in which the leads can be placed externally. The central tubing provides torsional

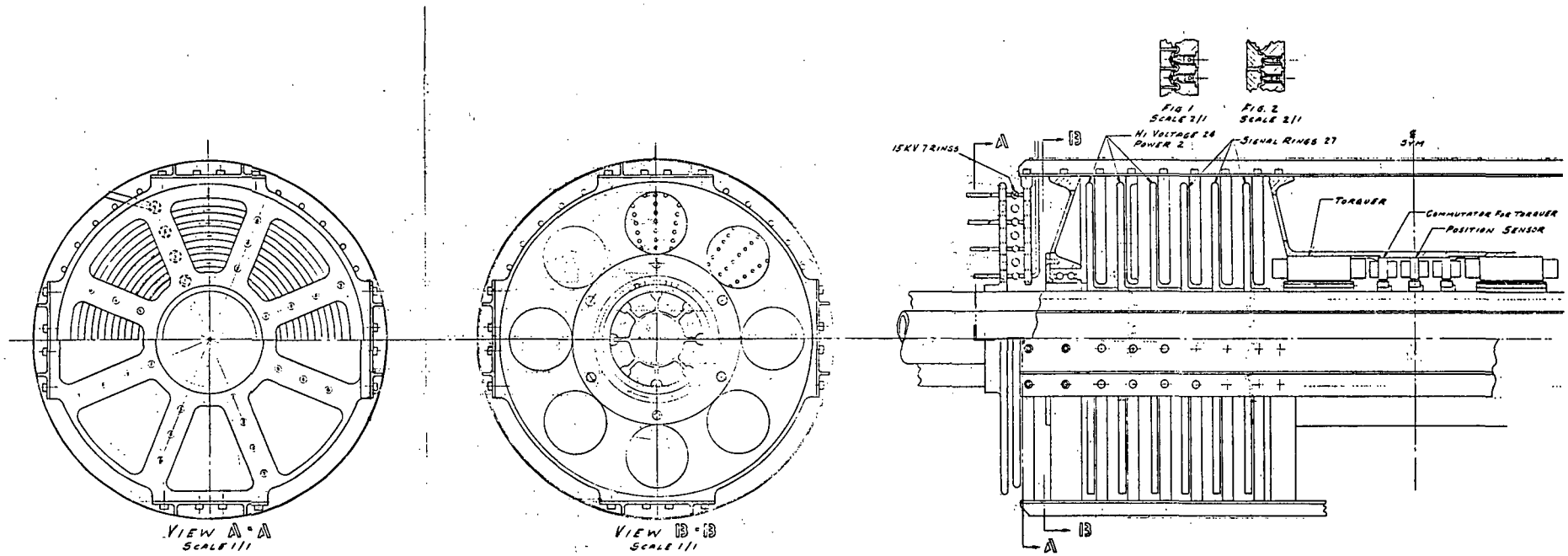

Figure 18. Rail Type Assembly with Liquid Metal Brush Slip Rings

46

rigidity and a central hole in the event that direct connections between solar panels proves necessary.

The shaft is required to support the solar panels in the operating environment of zero gravity. Launch locks of some type are expected to assist in supporting the solar panels during the launch environment.

Prelaunch operating tests represent a special environment where the full load of the solar panels may have to be supported in earth's gravity. The LMSR will need to remain in a vertical axis orientation whenever the gallium is liquid because the radial retention capability of this design is less than one gravity. This orientation avoids bending loads and deflections on the shaft which might otherwise be a design construction.

Table 9 compares structural parameters for various shaft designs which are 24 inches long. The stiffness is approximately proportional to the shaft weight as the wall thickness is increased. The advantage of titanium as a shaft material vs stainless steel and epoxy-glass laminate is demonstrated where weight is an important factor.

The moment required to produce 0.010 in deflection was used as a design criteria because the slip rings are being designed to accommodate 0.010 inch radial or axial displacement of the shaft with respect to the housing. The space between supports (bearings) is assumed to be 20 inches.

The mass properties of rolled-up solar array were used to calculate the torsional period for the shaft. This was found to be more than one second for the finned shaft, indicating the need for careful control of dynamic characteristics.

A brief investigation was made of the optimum bearing location with respect to shaft deflection. If the bearings are positioned between the high voltage ring platters and the signal ring platters the deflection of the shaft due to applied moments will be approximately equal at the resolvers and at the very high voltage slip rings.

Using the refined data on electrical stress permits reduction in the shaft cross-section required for wire routing. With a 2.6 inch torquer I.D. the shaft can be increased in size to 2.15 inches I.D. and 0.050 inch wall thickness. Fins are greatly shortened. For a fin thickness of 0.050 inch the shaft weight is 1.7165 pound compared to 1.8895 pound on the previous baseline design. The torsional stiffness is increased to 106,359 from 15,278 inch lb/rad and the bending moment to cause 0.010 inch deflection is increased to 1922 from 756 inch lb.

Bearing studies indicated that industrial class ball bearings will be marginal to meet the friction torque requirements of 10 oz-in starting and 3 oz-in running at one earth rate. Bearing preload can be only 15 to 20 pounds on bearings with pitch diameter about 3.5 inches. Control of the bearing class and grade will be necessary to assure meeting the specification.

TABLE 9. COMPARISON OF STRUCTURAL PARAMETERS OF SHAFTS

MATERIAL	O.D. Inch	Wall Inch	Number of Fins	I.D. Inch	Weight lb	Moment for 0.010"Defl in-lb	Bending Stiffness in-lb/ rad	Torsional Stiffness in-lb/ rad
Epoxy - Glass Laminate Grade G-10	3.0	0.1	-		1.42		108,095	
Titanium 6AL-4V	2.0	0.06	-		1.40		118,629	
Titanium 6AL-4V	3.0	0.04	-		1.43		280,693	
Titanium 6AL-4V	2.6	0.03	6	1.2	1.50	693	173,315	11,240
Titanium 6AL-4V	2.6	0.03	8	1.2	1.85	900	225,149	11,270
Stainless Steel AlSl 304	2.6	0.03	8	1.2	3.36	1528	382,071	8,129
Stainless Steel AlSl 304	2.6	0.02	8	1.2	2.18	910	227,389	5,255

Magnetics Package

The brushless torquer favored for the LMSR/SAOM is a space-qualified design that has accumulated several years of failure-free service in satellites. By removing the inner bushing the shaft diameter can be increased to 2.6 inches. This is reasonable because the rotor is an integrally bonded unit of laminations and permanent magnets and has axial holes to allow it to be held together as shown in Figure 17. The stack length is 1.75 inches and the O.D. is 4.63 inches.

The specification requires two brushless torquers, each capable of 10 lb-ft torque. The purpose of the 20 lb-ft torquing capability is to be able to free a stuck bearing. The use of peak torque is thus only expected to last a few milliseconds. The proposed torquer has a continuous rating of 4 lb-ft and will develop 12 lb-ft without becoming demagnetized.

A magnetics package containing two of the above torquers, two resolvers for commutation and one angular position resolver will be 7.87 inches long and weigh approximately 12 pounds. This design is considered the baseline.

An alternate package could be developed which would have a 3.5 inch I.D., 5.5 inch O.D. and be 6.5 inches long. This unit would weigh 0.8 pound more than the baseline due to the increased volume of end turns. Active material would remain at the same volume.

The angular position resolver used for performance comparison has an accuracy of ±3 arc-minutes. Its present usage is with a 2000 Hz square wave excitation. Input impedance is 2000 ohms minimum and the output provides a 0.5 transformation ratio to a 20 Kohm load with a phase shift not exceeding 10 degrees. The laminations have a 4.75 inch O.D. and a 3.150 I.D. It is expected that similar performance can be obtained from a unit using laminations of the same diameter as the laminations of the resolvers used for commutation of the brushless torquers.

THERMAL ANALYSIS

A preliminary thermal analysis of the LMSR/SAOM was performed to identify the possible thermal control design problems. It is necessary that the gallium remain frozen during launch and for at least 6 hours coast time between thruster burns. The system must be able to operate during shadow for 75 minutes. The LMSR/SAOM is adjacent to high power transmitting tubes within the spacecraft body so the normal orbital operating environment is quite hot.

The interface between the LMSR/SAOM and the spacecraft is shown in Figure 19. Table 10 lists some thermal parameters of the LMSR/SAOM and calculates the net heat loss for the condition where the slip rings are being maintained at 40°C (10°C above the melting point of gallium) and all boundaries are at 20°C. It is estimated that the heater power requirement for such a condition would be near 50 watts. The normal spacecraft temperature will be

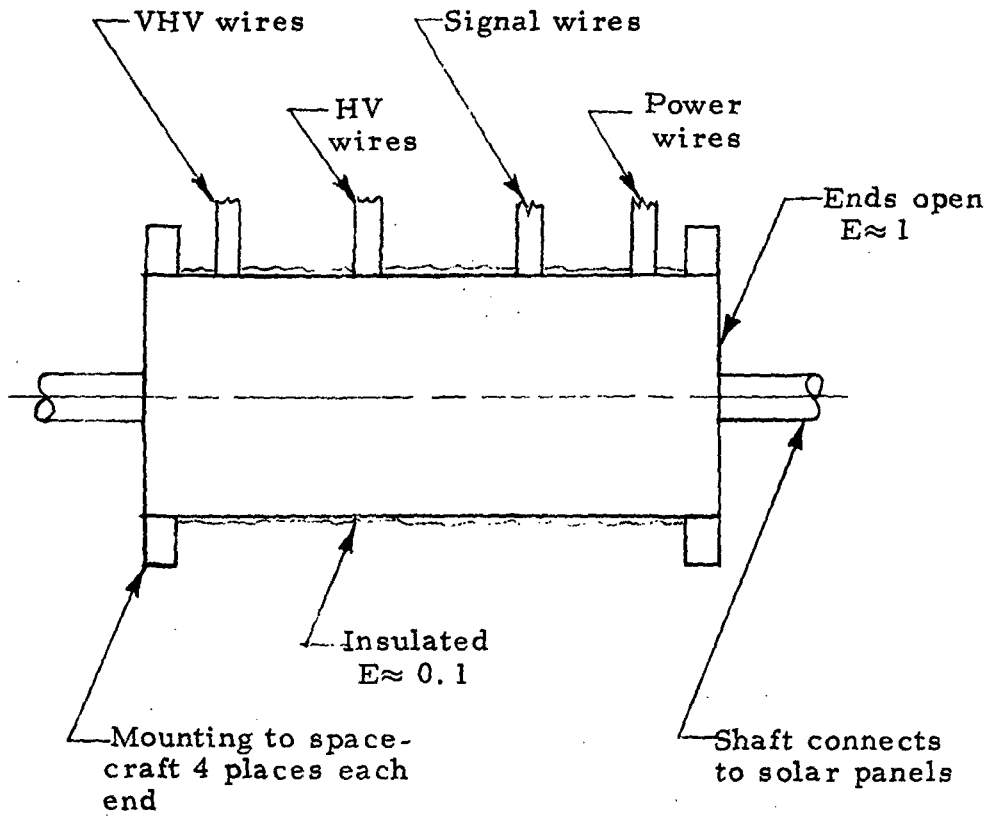

Figure 19. Thermal Interface, LMSR/SAOM to Spacecraft Hardware

TABLE 10. THERMAL PARAMETERS OF LMSR/SAOM

Nominal Heat Loss for LMSR/SAOM at 40°C, Spacecraft at 20°C

RADIATION			
Item	Area, in^2	Emissivity	Nominal Heat Loss, watts
Housing ends	157	1.0	14.4
Side (cylinder)	7500	0.1	6.9
Subtotal, Radiation			21.3

CONDUCTION		
Item	Conduction Resistance, °C/watt	Nominal Heat Loss, watts
Mounts (4 places each end)	31.8	0.6
Shaft (both ends)	12.5	1.6
Electrical conductors		
VHV (28 SS tubes)	7.0	2.9
HV (16 Cu wires 1/8" dia.)	1.7	11.8
HV (80 Cu wires 1/16" dia.)	1.4	14.3
Power (8 Cu wires 1/8" dia.)	3.5	5.7
Signal (100 Cu wires #24 gage)	10.7	1.9
Subtotal, Conduction		38.8

DISSIPATION			
Item	Quantity	Power, Each watts	Nominal Heat Gain, watts
Torquers	2	1	2
Resolvers	3	0.5	1.5
Power rings	4	1	4
HV rings (set)	4	1	4
Subtotal, Dissipation			11.5

Net Heat Loss	48.6 watts

nearer to 40°C so heater power is not expected to be required except during eclipse and when the transmitting tubes are not operating.

It will be noted in Table 10 that the uninsulated ends of the housing result in a large heat loss. For this reason radiation shields will be necessary as seen in Figure 17. The major heat loss is the unavoidable conduction through the many electrical conductors. The heat loss at the mounts for the LMSR/SAOM is kept small by employing eight insulating brackets of reinforced plastic with thermal path lengths of one inch and effective path areas of 0.25 square inch.

The thermal capacity of the LMSR/SAOM is about 0.42 watt-hr/°C. Assume that the assembly cannot be chilled below -30°C before launch, and that the maximum allowable temperature at the time of the injection into orbit 6 hours later is +20°C, 10°C below the melting point of gallium. The maximum heat flux is 21 watt-hours. This indicates that additional cooling will be required to maintain the gallium frozen between thruster burns.

PRELIMINARY DESIGN EVALUATION TESTING

Task Objectives

The objectives of the preliminary design evaluation testing were to:

- Test electrode and insulation systems designed for operation at 15,000 volts.
- Investigate critical design problems of liquid metal slip ring assemblies, including assembly procedures, electrode filling, wire routing, wire attachment, environmental testing and thermal characteristics.

Design of Evaluation Test Unit

General Description

The vehicle for the above objectives was the Evaluation Test Unit (ETU). The ETU is a liquid metal slip ring assembly consisting of a shaft supported by ball bearings in a housing and with three slip ring platter assembly pairs, each platter assembly pair being of a different design approach. The general arrangement is shown in Figure 20.

The ETU was to be tested in a vacuum. To allow the rings to be turned in a vacuum, a rotary harmonic feed through was used. The shaft drive was by a geared synchronous motor outside of the vacuum chamber. The speed of rotation was 0.977 revolutions per hour. This speed was chosen to permit adequate time for a monolayer of film to form at the expected test pressure of about 10^{-7} torr and still permit the equivalent of two years rotation in orbital operation at one revolution per day to be accumulated in 30 days of testing.

A large circumferential viewing port of high strength glass was incorporated to permit observations of the slip rings during and after operation without requiring disassembly.

Pressure seals such as O-rings and gaskets were used at all external joints. A gas port and a three-inch diameter vent valve capable of operation from outside the vacuum chamber were designed. The object was to permit the ETU to be assembled in an inert gas atmosphere (in a glove box) then sealed and placed in a high vacuum chamber. The chamber and the ETU could then be evacuated simultaneously then the vent valve opened on reaching pressures below one micron. This would permit the interior of the ETU to be subjected to high vacuum without ever having been exposed to air. In reverse, the vent valve could be closed in high vacuum, the ETU filled with argon through the port and the ETU returned to the glove box for disassembly without the interior ever having been exposed to air.

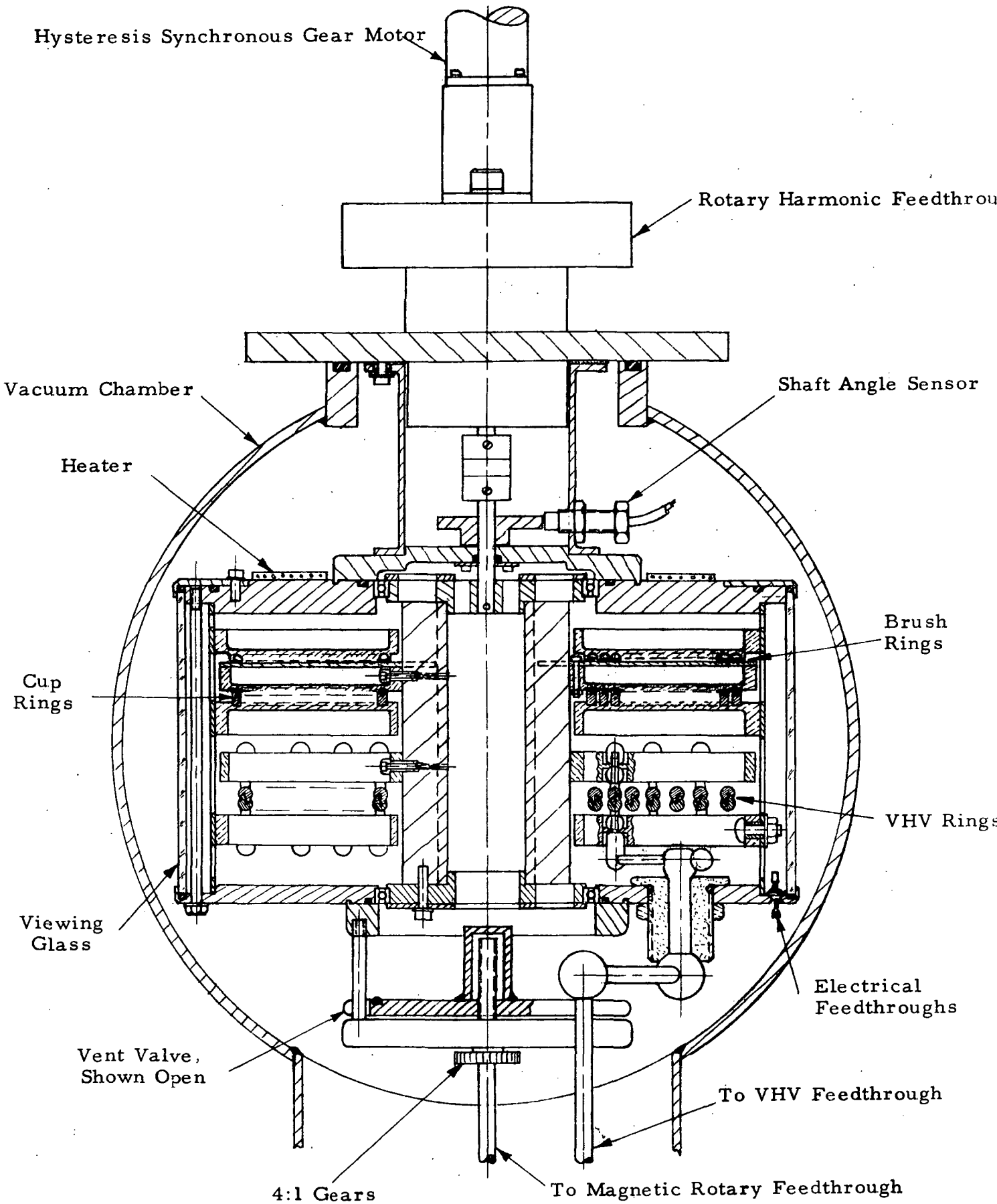

FIGURE 20. Evaluation Test Unit

A resistance wire heater was placed on the top plate. This permitted the melting of the gallium after thorough degassing in the vacuum chamber. Thermisters were used in various places in the assembly as temperature sensors.

The ETU housing and shaft were made of stainless steel to resist corrosion by the gallium. The shaft employs eight axial fins to permit wire routing along the shaft without need to penetrate the central torsion tube. Alumina ceramic insulators were designed for the four electrical feed-throughs for VHV in the bottom of the unit. Commercial high voltage feed-throughs with adequate voltage ratings were not found to be available in sizes compatible with the ETU.

Slip Ring Configurations

The slip ring complement for the ETU consists of:

- A platter pair carrying seven VHV ring-pairs
- A platter pair carrying thirteen cup-gap ring pairs suitable for power and high voltage
- A platter pair carrying thirteen signal rings of the brush type

The rotor platters for the cup-gap and brush type rings are mounted together to obtain rigidity at lower weight and space.

The support platters for all slip rings were machined from glass fiber reinforced epoxy laminate, Nema grade G-10. This material was chosen because of its excellent dielectric properties, good mechanical properties, low coefficient of thermal expansion, low outgassing and presumed dimensional stability.

The platters closest to the vent valve at the bottom of the ETU carry seven VHV ring-pairs with cross-sections as seen in Figure 21. The epoxy-glass support is an eight-spoked wheel. The rings are supported on the spokes by means of welded-on posts and spherical hardware such that no sharp edges are exposed and the 100 volts per mil electrical stress at 15 kv is maintained.

Each ring has four posts so that adjacent rings have mounting on alternate spokes. This permits the electrical path through the insulation to be quite long. The path across the surface of the insulation is made even longer by the deep counterbores in the spokes. As a final measure, vent slots are provided in the spokes to avoid trapped gas in the threaded areas which could cause virtual leaks for long periods and enhance corona discharge.

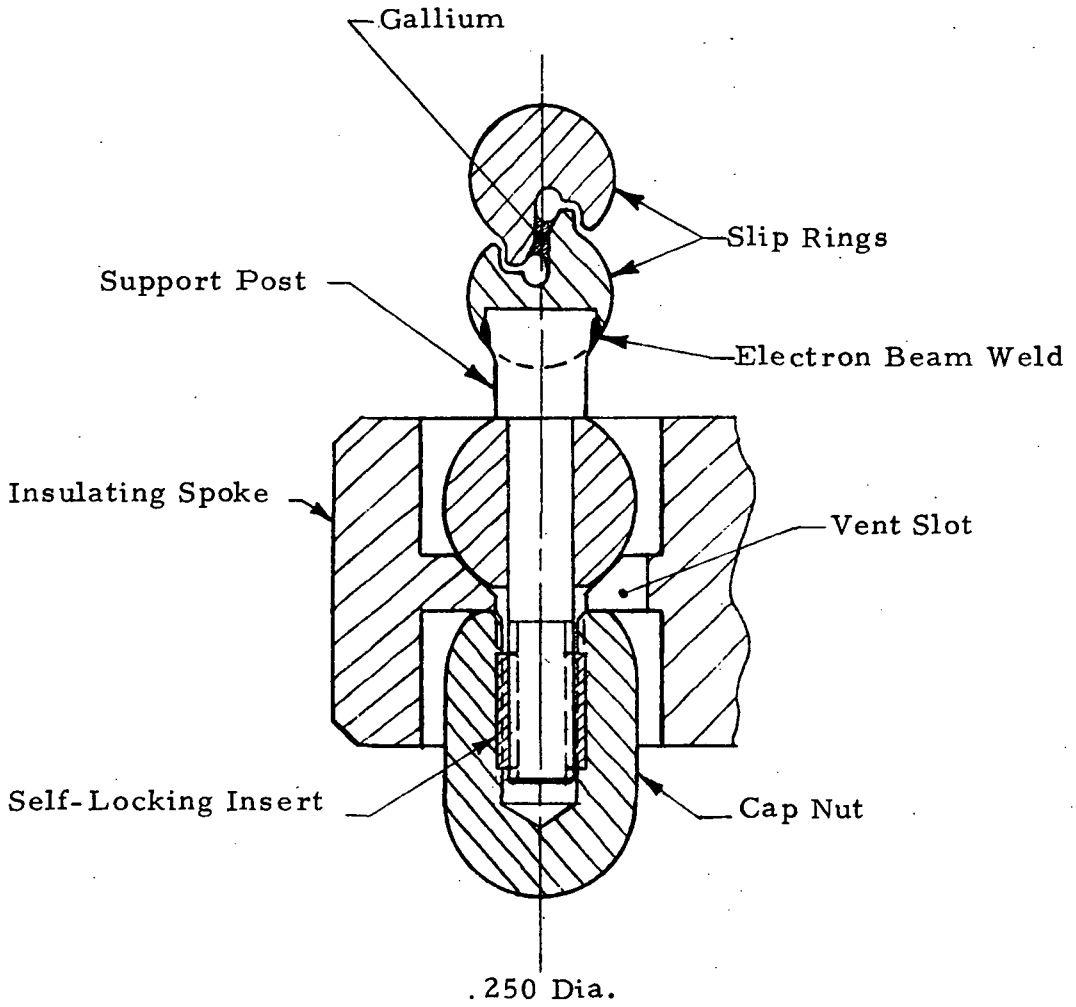

Figure 21. Very High Voltage Slip Ring Pair with Support Post

The slip ring cross-section provides for a radial gap with all the features seen in Figure 6. The lighter crab configuration seen in Table 6 was the first choice but was found to be too expensive to fabricate.

The rings are numbered from the inside to the outside. Very high voltage feed-through terminals were provided in the vacuum chamber and in the ETU to permit connections to rings 1, 3, 5, and 7. The alternate rings 2, 4, and 6 were connected by low voltage wiring to the test panel, where they were grounded through a resistor. The ETU case was electrically isolated from ground and was also grounded through a resistor at the test panel. The current through these resistors was thus a measure of leakage from the rings at high voltages to the intermediate rings and to the ETU case.

The cross-section of a ring has a diameter of 0.188 inch. Spacing between rings varies in increments of 0.025 inch from 0.125 between rings 1 and 2 to 0.250 between rings 6 and 7. The electrical stress between the rings thus varies from 140 to 85 volts per mil at 15000 volts based on the formula for parallel cylinders. The voltage drop between the rotor ring and the stator ring is so small that they can be considered to be at the same potential.

The VHV rings were made of AISI 304 stainless steel because of its proven resistance to corrosion by gallium and its resistance to field emission. The mean diameter of the rings ranged from 3.25 inches for ring 1 to 7.75 inches for ring 7.

The second platter pair contains 13 cup-gap ring pairs ranging in mean diameter from 3.375 inches to 7.875 inches and with cross-sections as shown in Figure 22. The cup rings are supported on a support wheel as in Figure 16 but with eight Z-spokes. The thin male hoops are supported on a grooved disc.

The two inner rings were to be tested as power rings at 30 amperes. The group of 13 simulate a full set of high voltage rings plus one power ring in the LMSR/SAOM configuration of Figure 17.

Each ring is held by a welded stud in eight locations. The studs for the cup rings are all 99 percent nickel alloy as are the rings and one stud on each male ring. The remaining studs on the male rings are commercially available stainless steel screws. The nickel stud serves as the current terminal on the male rings.

The third platter pair carries a set of 13 stainless steel rings on the rotor and 13 stainless steel brushes on the stator. Gallium was expected to bridge the 0.015 inch gap between the brush and the ring. The acceleration required to remove the gallium from such a gap would exceed 20G. Enough excess gallium is carried in the reservoir holes to permit the gap to go to 0.030 inch without breaking contact. See Figure 23.

The brush type rings are placed furthest from the vent valve in the ETU because the ring-to-ring voltage requirement within a set of signal rings is only ±300 volts. 2000 volts must be accommodated to ground and to other sets of rings.

The slip ring configurations adopted for the ETU as discussed above contain the basic features considered to be desirable in the Preliminary Design Study. To obtain simplicity of manufacture, the features are not always in the optimum configuration. Compare Figures 21, 22, and 23 with Figures 6, 7, and 9, respectively. The ring designs cover a broad range of electrical and mechanical characteristics so that much comparative data can be gathered.

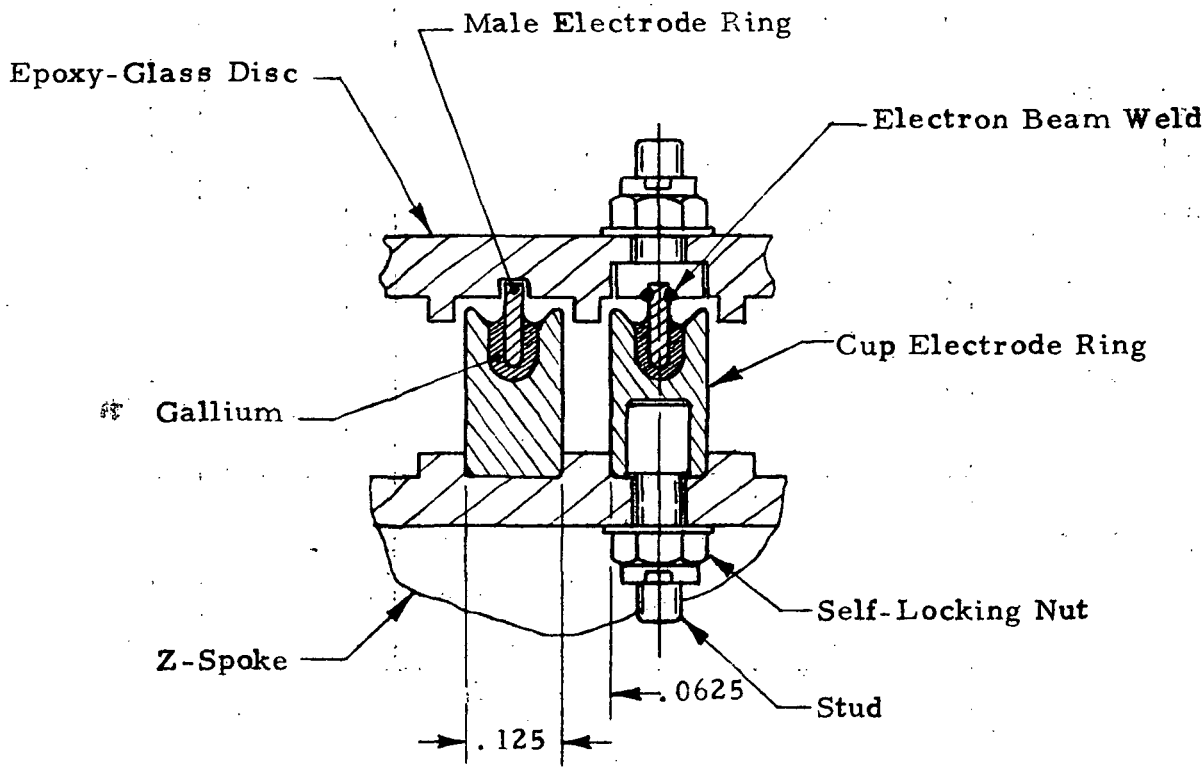

Figure 22. Cross-Section of Cup-Gap Ring

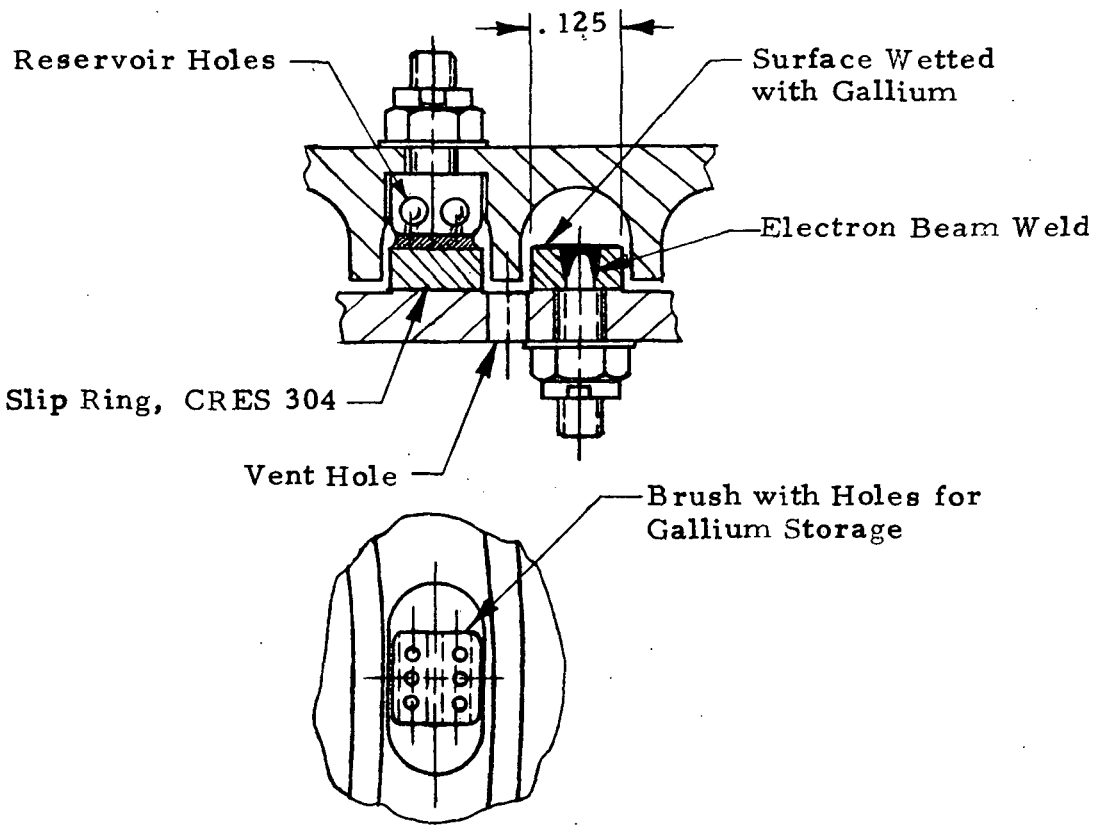

Figure 23. Brush and Slip Ring

Wiring and Instrumentation

The wiring diagram seen in Figure 24 shows the instrumentation planned for vacuum testing of the ETU. The system of jumpers and straps on the rotor rings permits all signal, high voltage and power ring-pairs to be checked for continuity. Doubling-up on wiring and feed-throughs permits currents to 30A to be routed through cup-gap power rings 1 and 2 and currents to 15A through cup-gap high voltage rings 12 and 13. Signal rings 1, 2, 12, and 13 can be supplied with up to 7.5A to permit resistance measurements. Voltage taps are provided on both rotor and stator rings where current is to be applied.

Thermisters are used for temperature instrumentation. Thermocouples were not used because electrical feed-throughs of constantan were not available for the base of the ETU.

The shaft position readout utilizes a spiral cam and a proximeter. There is no need for accuracy or linearily here because the shaft is driven at constant speed.

The ETU Test Panel consists of test points for all rings. In several cases there are current and voltage taps for the same ring. Currents and voltages are monitored by an integrating digital voltmeter with a least count of one microvolt.

Corona discharge in the VHV rings is monitored by an oscilloscope placed across resistors through which VHV rings 2, 4, and 6 and the ETU case are returned to ground. All electrical leakage from VHV rings 1, 3, 5, and 7 within the ETU case is thus measured.

Three means of instrumenting the gallium level in the slip rings to detect sloshing were tried.

1. A resistance wire in which the gallium would short various lengths of the wire as it moved.

2. A stainless steel probe in the shape of a phonograph needle touching the surface of the gallium so that the unwetted contact area would change with the level of liquid metal, thus changing the electrical resistance.

3. A resistive track on a narrow insulating film which would extend below the surface and be partially shorted out by the gallium.

These tests had very limited success. The first did not work for small gallium displacements as the gallium did not move smoothly on the unwetted probe. The second worked only as an off-on switch for first contact. The high surface tension of the gallium prevented an increase in contact area as the free gallium surface was raised. The third method

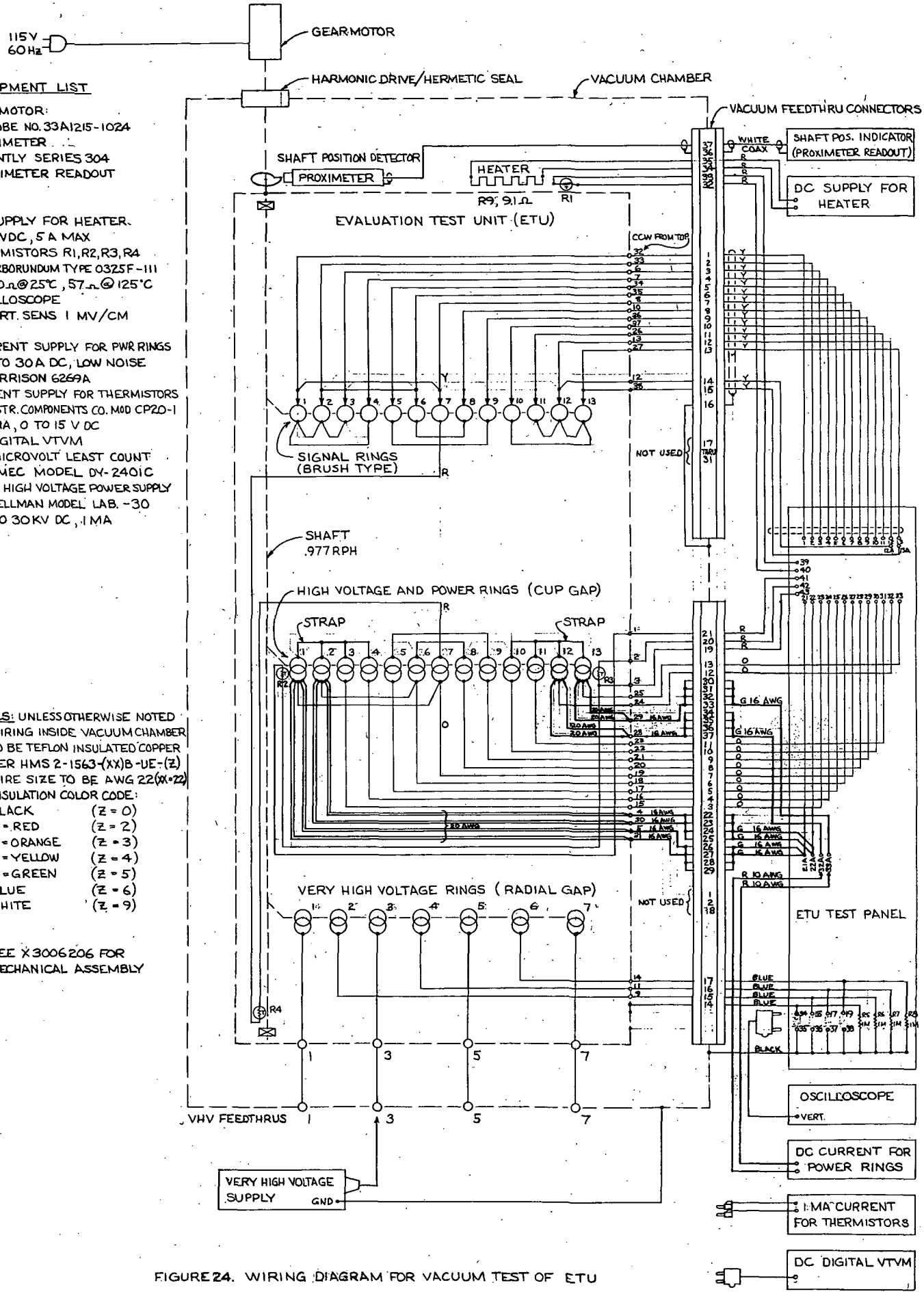

EQUIPMENT LIST

GEARMOTOR:
GLOBE NO. 33A1215-1024
PROXIMETER
BENTLY SERIES 304
PROXIMETER READOUT

DC SUPPLY FOR HEATER.
30VDC, 5 A MAX
THERMISTORS R1, R2, R3, R4
CARBORUNDUM TYPE 0325F-111
250Ω@25°C, 57Ω@125°C
OSCILLOSCOPE
VERT. SENS 1 MV/CM

CURRENT SUPPLY FOR PWR RINGS
0 TO 30A DC, LOW NOISE
HARRISON 6269A
CURRENT SUPPLY FOR THERMISTORS
INSTR. COMPONENTS CO. MOD CP20-1
1 MA, 0 TO 15 V DC
DC DIGITAL VTVM
1 MICROVOLT LEAST COUNT
DYMEC MODEL DY-2401C
VERY HIGH VOLTAGE POWER SUPPLY
SPELLMAN MODEL LAB.-30
1 TO 30KV DC, 1 MA

NOTES: UNLESS OTHERWISE NOTED
1. WIRING INSIDE VACUUM CHAMBER TO BE TEFLON INSULATED COPPER PER HMS 2-1563-(XX)B-UE-(Z)
2. WIRE SIZE TO BE AWG 22(XX=22)
3. INSULATION COLOR CODE:

BLACK	(Z = 0)
R = RED	(Z = 2)
O = ORANGE	(Z = 3)
Y = YELLOW	(Z = 4)
G = GREEN	(Z = 5)
BLUE	(Z = 6)
WHITE	(Z = 9)

4. SEE X3006206 FOR MECHANICAL ASSEMBLY

FIGURE 24. WIRING DIAGRAM FOR VACUUM TEST OF ETU

R.B. Clark
8/24/71

using the resistive track (a pencil line on a very narrow strip of mylar tape) did give a usable signal in an open breaker of gallium but could not be used in the narrow confines of a slip ring because it would interfere with the retentive action of the slip ring geometry. All three methods have this problem of interference. Actual loss of gallium from the rings remains the best way to detect sloshing.

Fabrication of the ETU

Machining of Housing

The cylindrical portion of the ETU case, AISI type 303 stainless steel tubing 8.452 inches in diameter, 4.437 inches long, has a wall thickness of only 0.060 inch. It also has several large slots to permit viewing of the slip rings. This housing positions the stator platters and the end plates which in turn support the bearings and shaft. Thus it required close tolerances and special handling.

After rough sizing of the tubing stock the material was stress relieved. The critical inside diameter was bored to size then three aluminum discs were installed to simulate the platter stators and hold the housing round while the outside diameter was machined and the viewing slots added. The inside edges of the slots in the VHV region were radiused by hand filing and emery cloth.

This machining of the housing was quite successful and the part remained within tolerance when restrained to round. The diametral clearance to the three stator platters is less than 0.003 inch and to the end plates is less than 0.001 inch but there was never a problem in assembly. The housing made a very rigid assembly despite its thin wall.

Fabrication of Slip Rings

Slip rings were machined from two materials. The VHV and signal rings which have low currents were machined from AISI type 304 stainless steel. Type 304 is used instead of type 303 because the selenium or sulfur added to type 303 to promote machinability might be attacked by the gallium.

It was hoped that a 99.98 percent pure nickel alloy be used for the cup-gap rings because of its low resistivity, 7.5 microhm-centimeters. This material was unavailable except on special order so an available alloy with the following composition was used.

Element	Nominal Percent	Limiting Percent
Nickel (plus cobalt)	99.5	99.0 min.
Carbon	0.08	0.15 max.
Manganese	0.18	0.35 max.
Iron	0.2	0.40 max.
Sulfur	0.005	0.010 max.
Silicon	0.18	0.35 max.
Copper	0.13	0.25 max.

The electrical resistivity of this alloy is 9.5 microhm-cm at 20°C.

All slip rings were cut from hot-finished plate stock except the signal rings, which were cut from cold-finished plate.

Machining of the nickel and stainless steel rings from plate was difficult. These materials would rather displace and throw up a burr than cut. High sulfur content cutting oils and sharp tungsten carbide tipped cutting tools were required.

The VHV rings were machined in the following sequence:

1. The back sides of every other ring were machined in bas-relief on a plate.
2. Mounting holes for the studs were added.
3. The four studs were electron beam welded into place on each ring.
4. The front sides including final gap dimensions were machined.
5. The rings were parted from the plate starting from the outside.
6. Burrs were removed and the rings polished with emery cloth by hand.

Figures 25, 26, and 27 show the completed VHV rings. The holes visible in the reservoir grooves near the mounting studs are vent holes for hot gases during electron beam welding. Trapped gases caused blowouts in

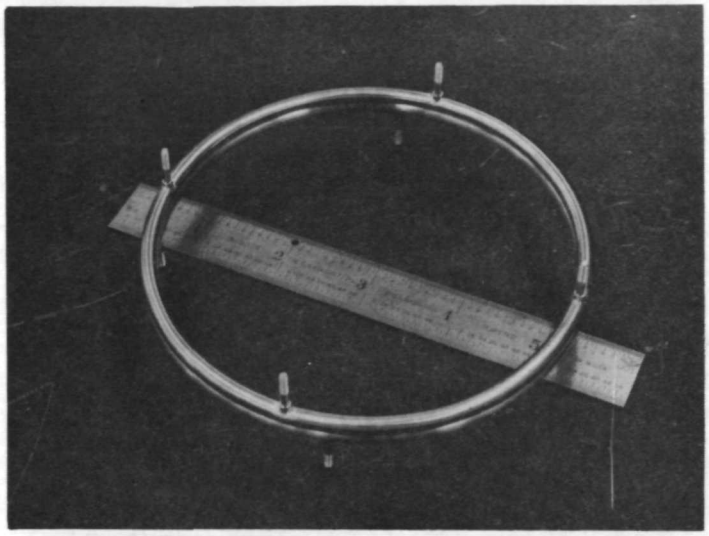

Figure 25. A Mating Pair of Very High Voltage Rings

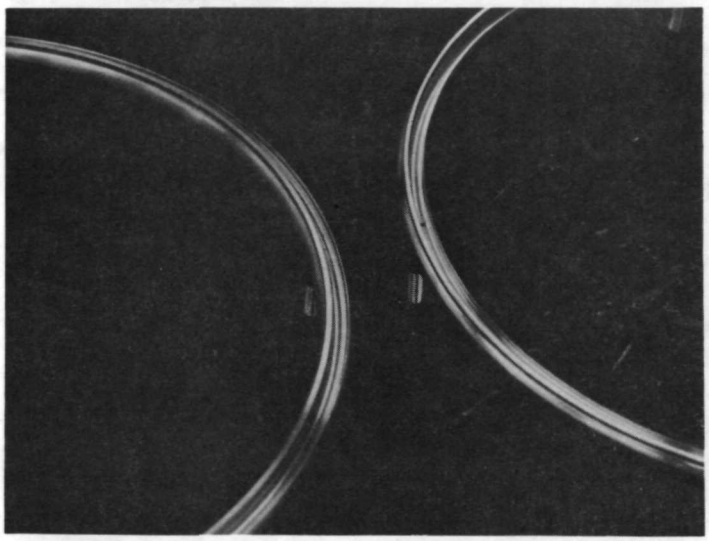

Figure 26. Interlocking Surfaces of VHV Rings

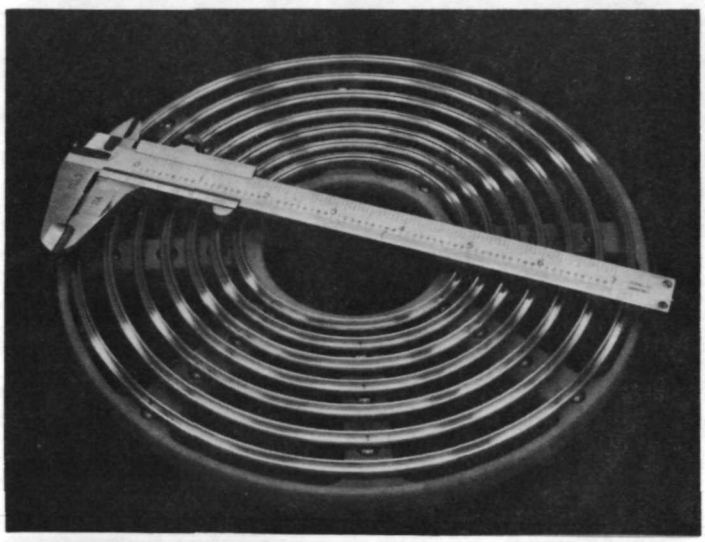

Figure 27. The Assembled Rotor Platter of VHV Rings

a few places and it was necessary to use fill wire in the resulting holes. Generally the rings were round and flat within specification as machined but some required hand adjustment.

The male electrodes for the cup gap rings are very thin hoops of nickel alloy. Their cross-section is 0.020 inch by 0.110 inch and mean diameters are from 3.375 inches to 7.875 inches. Each ring was completely machined before parting from the plate, then carefully hand deburred. Each such ring is supported at eight places on the platter by lying in the slots of the heads of eight No. 0-80 screws, one of which was machined from the nickel alloy, the remainder were commercially available stainless steel binding head screws. Grooves in the epoxy-glass platter help keep these rings round as shown in Figure 22.

The rings are attached to the screw heads by electron beam welding. The welding was done with the rings mounted in the epoxy glass platter and held in place by the fixture seen in Figure 28. The cover plate has grooves in the bottom to hold the rings concentric and round during welding; the slots provide access for the electron beam.

In Figure 29, a row of nickel studs and a row of stainless studs are shown welded to the rings. The welds are less than 0.020 inch wide and are on each side of each screw. Spattering from the electron beam charred adjacent baffle surfaces of the support platter but the direct heat on the screw did not discolor the epoxy-glass support. The char was readily removed with a stiff brush. The cleaned up rings are seen in Figure 30.

The cup electrodes were also completely machined before parting from the plate except for the holes for the studs. The holes were then added and the studs electron beam welded into place. The welding was in two places on the base of each stud and the beam came in on an angle as seen in Figure 31. The welds are along the centerline of the ring and do not show in Figure 22. This weld was the most troublefree and caused the least distortion. Figure 31 shows the support post for the VHV rings redesigned to use this type weld.

Figure 32 shows one of the completed cup rings.

The stainless steel sheet that was to be machined into the 13 signal rings was first fitted with 104 studs, No. 0-80, electron beam welded into place as seen in Figure 23. It became quite distorted and had to be annealed at 1340K (1950°F) in argon gas in a fixture to hold it flat. It was then flat within 0.003 inch and was bonded to the epoxy-glass platter with high temperature epoxy.

The platter had dams of epoxy-glass at the inside and outside diameters. They may be faintly seen in Figure 33. This was to retain the gallium while the complete surface of the plate was wetted by machining under molten gallium. The wetted surface is seen in Figure 33 with the

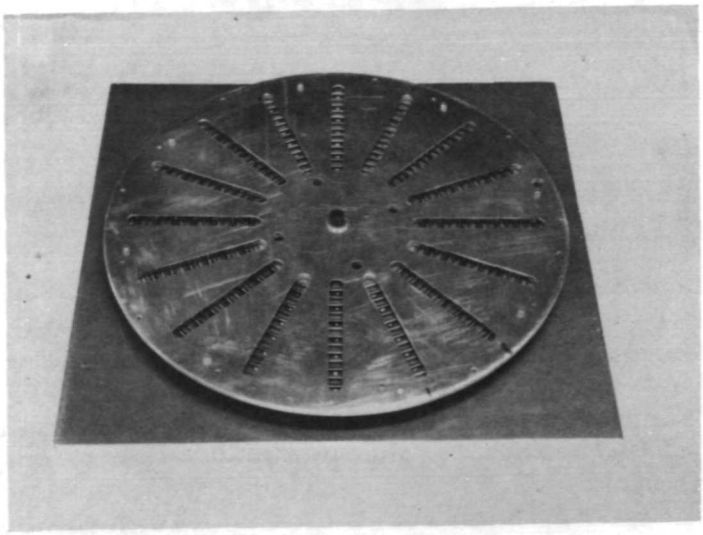

Figure 28. Welding Fixture for Narrow Rings

Figure 29. Close Up of Rings Welded Into Slots in Screw Heads

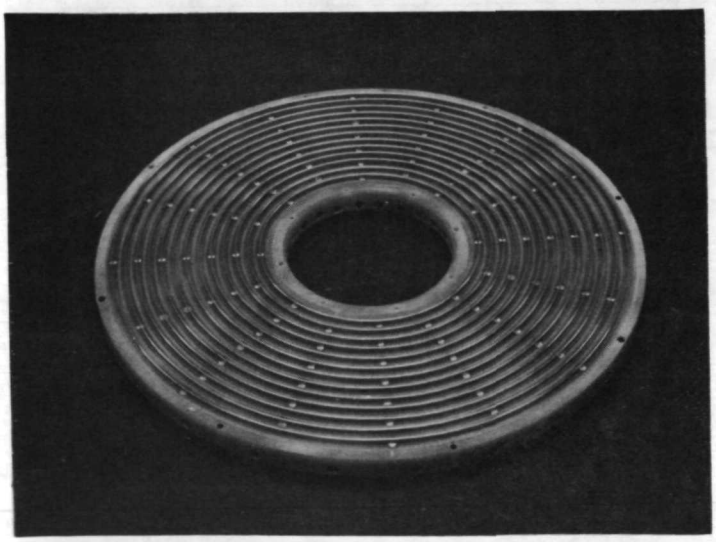

Figure 30. Welded Rings After Clean Up of Welding Debris

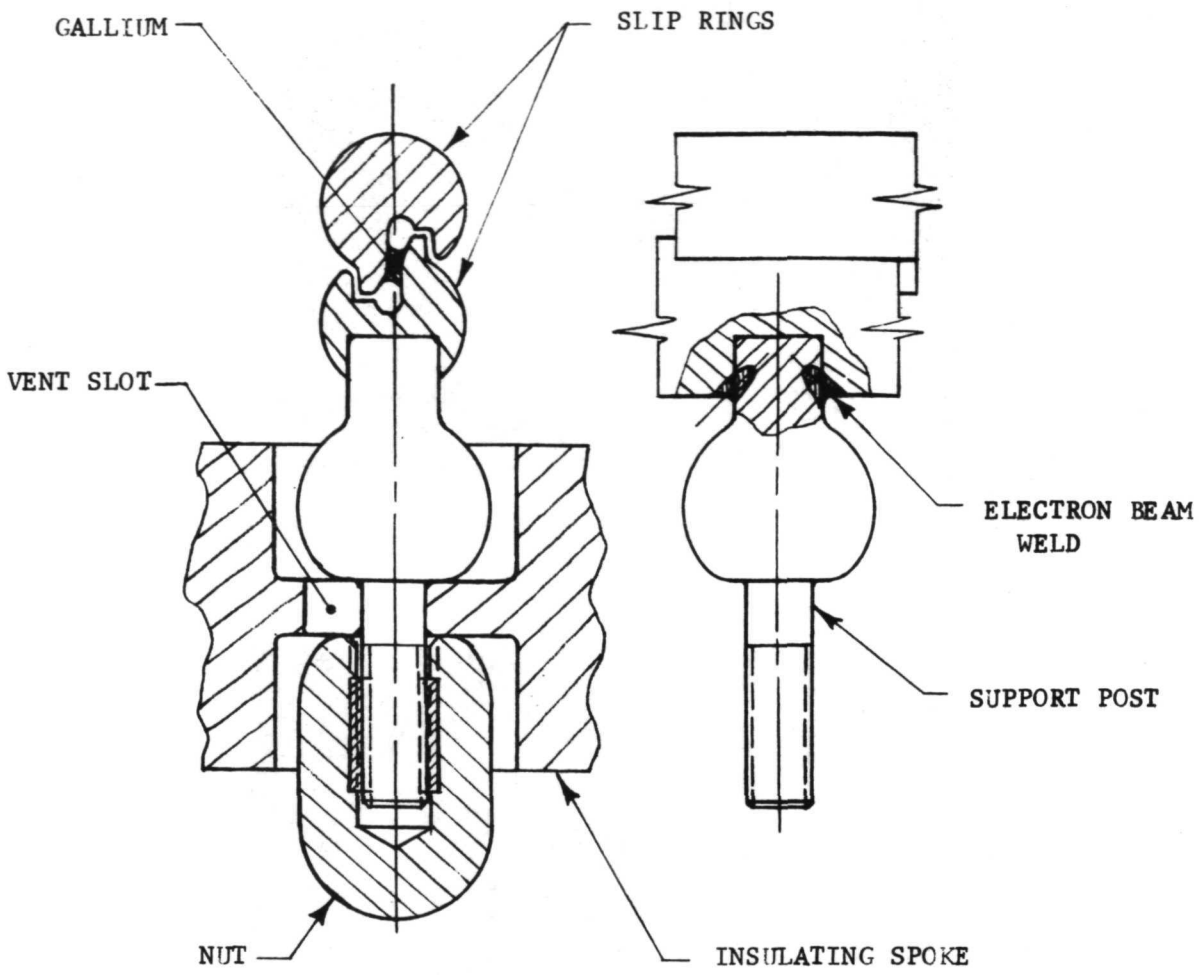

Figure 31. Improved Design Support Post for VHV Slip Rings

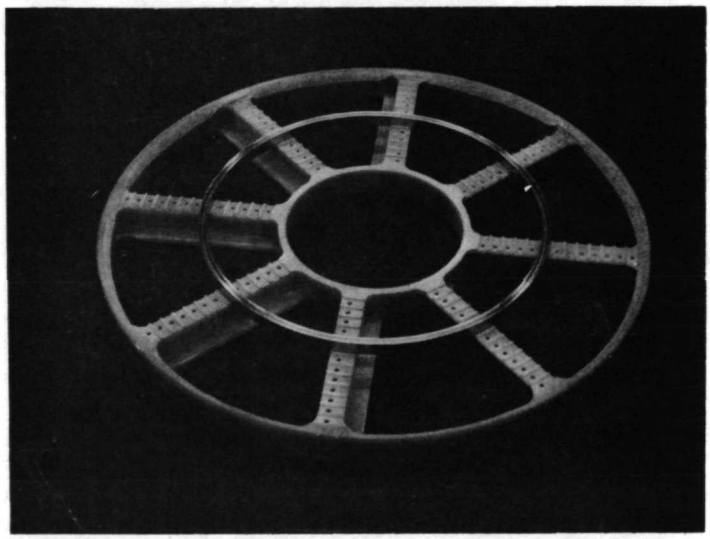

Figure 32. Cup Gap Ring on Z-Spoke Support

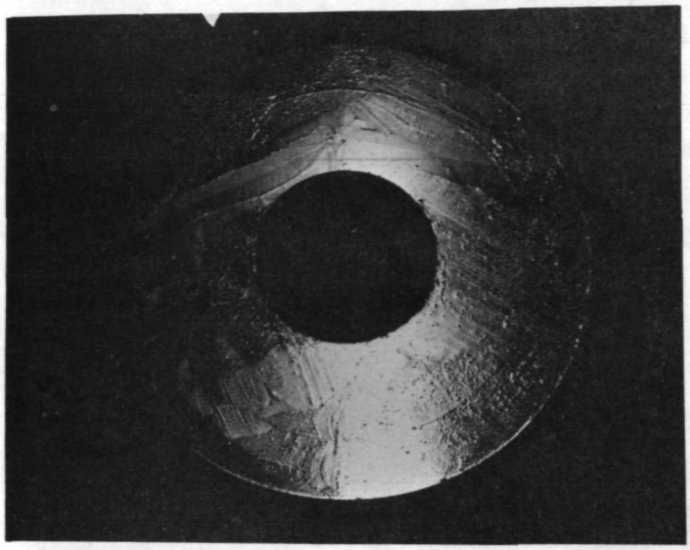

Figure 33. Stainless Steel Ring Blank Wetted with Gallium

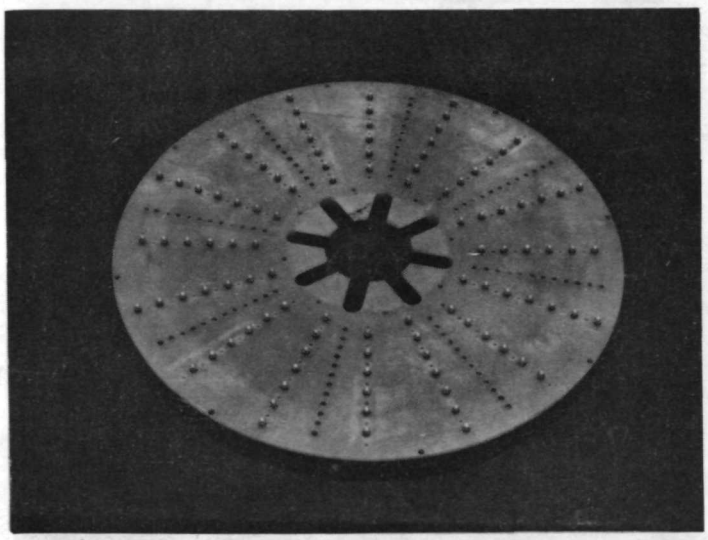

Figure 34. Epoxy-Glass Support Showing Studs from Ring Blank

Figure 35. Rings Separated from Support Between Studs

gallium frozen. Note the pattern of crystallization where the supercooled gallium was "seeded" with a flake of frozen gallium. The intentional rough machined surface, produced with a carbide-tipped flycutter, is also apparent. The plate had been annealed flat after welding but was dished 0.030 inch after wetting.

Figure 34 shows the other side of this assembly. Eight electron beam welded 0-80 studs and nuts hold each of 13 rings to a sheet of epoxy-glass laminate.

Difficulty was experienced in machining the 1/16 inch thick wetted 304 stainless steel plate into 13 separate rings while mounted on the epoxy-glass substrate. The gallium partially melted during the first cut when an aerosol can Freeze was used as coolant. Subsequent cuts utilized a spray of oil and water mist as lubricant and coolant and there was no further melting of the gallium.

The rings were distorted in the manner of a wavy washer as each was cut loose despite being bonded with high temperature epoxy to the epoxy-glass substrate. The separation from the substrate can be seen in Figure 35. The distortion was greatly relieved when the inner gallium dam was cut off.

The distortion appears to be due to a combination of stresses due to machining and burrs from the tough steel pressing against the epoxy-glass. None of the 104 0-80 studs broke under the heavy loads. The rings were straightened and deburred by hand. This fabrication technique was intended to result in reduced cost of production but it is not considered to have been successful.

The brushes to operate with the above rings are seen in Figure 36. The ridges in the epoxy-glass platter mate with the grooves between the rings

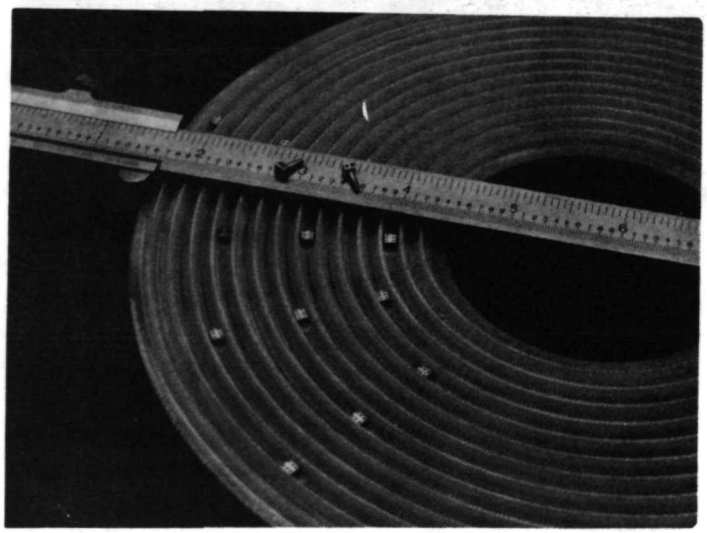

Figure 36. Brush Support Platter and Brushes

to form baffles to inhibit escape of gallium vapor and debris. The rough machining of the rings, and the reservoir holes which can be seen in the brushes, were intended to assure an ample supply of liquid gallium at minimum susceptibility to acceleration.

Dry Assembly of ETU

The housing for the ETU is shown in Figure 37, ready to receive the ring platters. From the top can be seen the shaft extension, the heater on the top plate, the external wiring harness, the glass wall, the cutaway internal housing, the ceramic VHV insulators and feed-throughs with corona balls, the large diameter, remotely-operated vent valve, and the flexible line through which the ETU was to be kept supplied with purified argon when the ETU was not at high vacuum.

The heater was installed on the top plate of the ETU. It has 55 feet of resistance wire wound non-inductively and a resistance of 7.9 ohms. A thermistor is installed in an adjacent hole.

The wiring harness internal to the ETU was made using teflon insulated stranded wire and crimp type terminals. Each wire internal to the ETU is terminated at the feed-throughs with a female connector which fits male connectors soldered to the feed-throughs with a space-rated solder. This was to permit assembly and disassembly of the ETU within the glove box with a minimum of tools and no cutting, crimping or soldering.

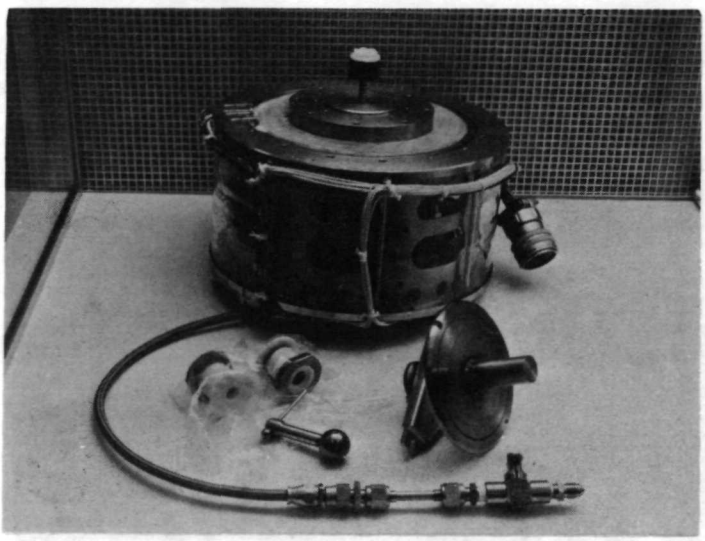

Figure 37. Housing of Evaluation Test Unit

The ETU parts seen in Figure 37 were assembled without slip rings to permit elimination of leaks. A light coating of vacuum grease was required around O-rings and gaskets to effect a seal. The use of gallium on the seals was considered as an effective means of excluding oxygen but the elastomeric materials proved resistant to wetting with gallium.

The ETU was then hung in the vacuum chamber. The linkage which operates the large vent valve in the bottom of the ETU was de-bugged and the VHV conductors were fitted.

The spacer for the ball bearings was adjusted to provide 0.0015 inch total indicated end motion of the shaft in response to an 80 pound reversing axial load on the shaft.

The rotor platters were assembled on the shaft using tubular spacers to hold them in place while holes were match-reamed to accommodate the screw-held shouldered sleeves which attach each rotor to each fin of the shaft.

The rings were assembled on the support platters and runouts were measured, radially and axially. In some cases the runouts exceeded the design tolerance of 0.005 TIR due to difficulties in machining the thin rings and epoxy-glass platters to close tolerances. Hand manipulation was employed to bring all rings within 0.008 TIR.

The rotors and stators were then assembled in the housing with the shaft and bearings. Shims 0.015 inch thick were used between rotor and stator rings to position the stators with respect to the rotor while the stators were match-reamed with the housing. The shims represented the desired axial clearance.

After complete dry assembly with all sleeves in place and the 0.015 shims removed a slight sporadic rubbing noise was heard as the shaft was rotated. Electrical continuity was used to determine that the rubbing accurred between VHV rotor and stator rings number six. On disassembly, ring 6 was found to have a burr on the inboard baffle with about 0.006 radial extension. This, combined with eccentricity, was the probable cause of the rubbing contact. The burr was removed. No other significant burrs were found.

The completed ETU was hung in the vacuum chamber. Motor-powered shaft rotation and manually operated opening-closing of the vent valve from outside the chamber were checked and found to be satisfactory.

The ETU was then disassembled and all parts cleaned and sealed in plastic bags until needed for final assembly.

Figure 38 shows a group of parts in work. In the background are the epoxy-glass support platters for the slip rings. Near center is the shaft. The flutes in the shaft provide axial passage for wires. The cup gap rings are in the foreground. The narrow male rings have been removed from the

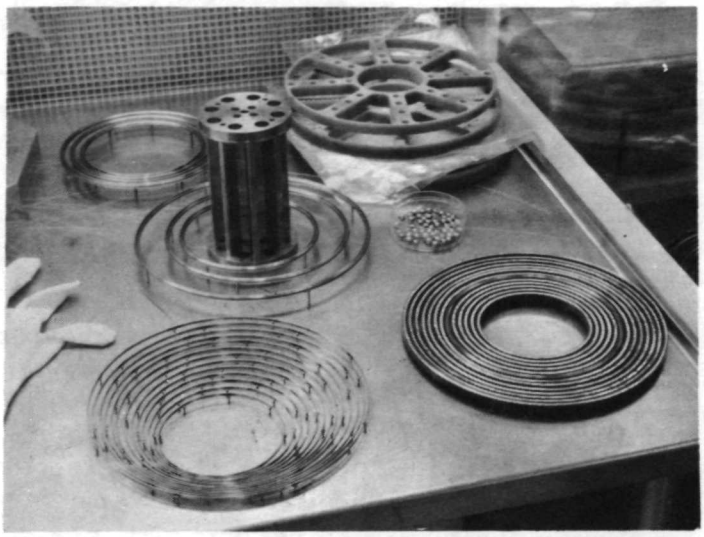

Figure 38. Assemblage of Parts for ETU

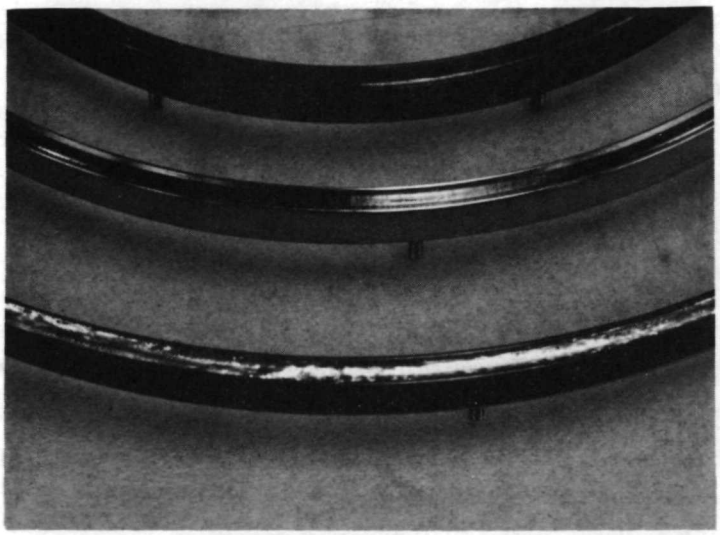

Figure 39. Cup Gap Rings Being Wetted with Gallium

epoxy-glass support for cleaning. Wetting and filling with gallium is underway on the cup rings on the right.

Filling Rings with Gallium

Each of the 66 electrodes was wetted with gallium by abrasion in the desired areas. The wetting of the 13 signal rings by machining under liquid gallium was described above. The remaining electrodes were wetted by hand.

Three nickel alloy cup rings are shown in Figure 39 in various stages of wetting. A cleaned ring is in the center. At the top is a ring which has been masked with teflon tape to limit the gallium to the desired surfaces. On the bottom a taped ring has been wetted and filled with gallium. The gallium was frozen after filling to minimize film formation and to simplify handling. The gallium was subject to sloshing in these large diameter rings.

The material used for abrasive wetting of the nickel rings was clean white stretch nylon cloth. If the nickel surface is clean and bright the application of some abrasive force in contact with gallium results in good adhesion. If the gallium layer left on the nickel is too thin, a compound soon forms which is not wet by pure gallium. Thus the nickel rings must be left with as heavy a layer of gallium as possible. This is another reason why the cup rings were filled.

The signal rings utilize small stainless steel brushes which have internal reservoirs. The first attempt to wet the brushes was in a bath of 15 percent hydrochloric acid solution which overlay a pool of molten gallium in a small glass beaker. The intent was to swish the brush in the acid to remove the surface oxide then move the brush down into the gallium without exposing it to air. The acid quickly cleaned up the surface film on the gallium but did not remove the protective layer on the 304 stainless enough to cause wetting by the gallium except in a few spots on the outside surfaces. There was no wetting in the reservoir holes or feed holes.

Abrasion was successfully used to wet the brushes with gallium. A small toolmaker's file was lightly applied on the outside surfaces in contact with liquid gallium and the gallium readily adhered wherever the surface oxide was scraped away. The test for wetting was to wipe away the gallium with a clean nylon cloth and note the areas where the gallium adheres.

The reservoir and feed holes were wetted using the size drills used to make the holes. After wetting, the brushes could be rapped sharply with the equivalent of many g's of shock before the bulk of the gallium would come out of the holes, leaving the inside surfaces wetted with gallium.

The proper surfaces of the stainless steel VHV rings were wetted by scraping with the back side of an Exacto knife blade. Dry areas on the signal rings were rewet using the same method. The gallium on wetted

surfaces was frozen by placing the ring on a chill block immediately after wetting so as to minimize surface film and sloshing of the gallium.

The wetting of the stainless steel with gallium by scraping required some skill but it appeared to produce a well-wetted surface which was readily checked and further scraping done if necessary.

All operations from this point on were to have been conducted in the glove box according to the original plan. The glove box available to the project was inconvenient to work in and was not able to maintain the oxygen content at the less than one part per million necessary to avoid film formation on the gallium. It was considered that the assembly of the gallium-wetted rings in air on the flow bench would result in less film than would form in the glove box because of the greater convenience.

The following plan was thus adopted. The gallium will be frozen as soon as possible after the stator and rotor rings are engaged, and the rings are not to be rotated until the ETU has been degassed in the vacuum chamber. A minimum of surface film will thus be enfolded in the gallium, and that remaining on the surface may evaporate before rotation. Elimination of disassembly and reassembly steps between tests will further reduce the amount of gallium debris. Debris which might escape from the rings can be detected by visual examination and by electrical tests.

Each ring pair was then heated and carefully wiped to remove all excess gallium and surface film. Fresh, pure gallium was added in the amounts given in Table 11, using a glass syringe with a stainless steel hypodermic needle. The nominal gap clearance in each ring is 0.020 inch (0.5 mm). The amount of gallium placed in the gap was calculated to be sure that the liquid surface of gallium will be concave.

The rotor portions of the cup gap rings were placed in the filled troughs of the stators with the studs on rotor and stator aligned before freezing so that the need for relative rotation at final assembly would be minimized. The filled ring pair No. 13 was tilted before freezing. An angle of about 25° was attained before the gallium began to escape. A higher angle should be obtained in a complete assembly because of the small gap ($\sim$ 0.015 inch) between the ring and the baffle through which the gallium must move to escape. This ring has a diameter of 7-7/8 inches and the gallium "head" reached before spilling was more than 3 inches.

The film due to air was clearly seen in this experiment in that the extended "bag" of gallium (where it was about to escape) fell slack when the ring was brought back to level, then refilled to its extended dimensions when the ring was tilted about 10°.

Ring-pair No. 1 has a diameter of 3-3/8 inches. It could be tilted to about 75° before the gallium escaped. Again, note that the head is about 3 inches.

The rotor of ring-pair No. 1 was moved tangentially about 0.5 inch to simulate operation in the presence of surface film. Fine diagonal wrinkles formed in the surface film from the beginning of motion due to the stretching of the film. At 0.03 inch motion there were many wrinkles forming a steep herring-bone pattern. For motions beyond 0.1 inch the wrinkles changed into a series of pockets in the surface of the gallium. The pockets were on the order of 0.03 deep and rotated like rollers in a roller bearing. These "vortexes" would certainly have broken up and formed a sludge with further rotation. With a convex surface on the gallium it is expected that the "vortexes" would have extended from the surface as was experienced with the radial gap rings of the Engineering Test Model in Reference 1. It was clear that all efforts must be made to avoid significant rotation of the rings during assembly and to allow the maximum possible outgassing period to permit the film to evaporate before permitting rotation.

Ring-pairs No. 1 and No. 13 were emptied, cleaned and refilled with fresh gallium.

Very High Voltage (VHV) ring pairs had 1/2 the calculated amount of gallium added to each ring after wiping off excess gallium. The top rings could not be inverted to mate with the bottom rings while the gallium was liquid because the gallium would run off. The gallium had to be frozen to allow inverting of the top rings.

VHV ring pair No. 1 was pulled apart after mating and adding a little heat to melt the gallium. Surface tension caused a smooth curtain of gallium to form all around between the top and bottom rings and this curtain did not rupture till it was more than 0.1 inch wide. The surface tension was almost sufficient to lift the lower ring. The ring pair was then cleaned and refilled.

The large VHV rings had to be moved very carefully after the gallium was added or the gallium would slosh and spill. Once the rings were mated the retention design eased the problem.

The gallium was frozen by placing the rings in a pan and adding a small amount of liquid nitrogen. It was necessary to chill the mated VHV rings to below $0^{\circ}C$ to freeze the gallium. This was probably because the baffling in the rings kept the cold nitrogen gas from circulating directly over the molten gallium surface.

Final Assembly

At this point all parts were weighed. Table 12 gives the weight of the ETU as summed from these measurements.

Platter assemblies for the VHV and cup gap rings were then made by mounting the rings on the lower support platters. It was necessary to melt the gallium in order to align the studs to permit assembly of the upper supports, but the motion required of any ring was very small because the rings had been frozen with the studs pre-aligned. The gallium was immediately refrozen. Wiring was then attached to the platter assemblies.

TABLE 11. AMOUNT OF GALLIUM PLACED IN SLIP RINGS

Ring No.	Cup Gap Rings		VHV Rings	
	cm^3(a)	grams(c)	cm^3 (a, b)	grams(c)
1	.52	3.2	.23	1.4
2	.58	3.5	.27	1.6
3	.63	3.8	.32	1.9
4	.69	4.2	.37	2.3
5	.74	4.5	.42	2.6
6	.80	4.9	.48	2.9
7	.86	5.2	.54	3.3
8	.92	6.0		
10	1.03	6.3		
11	1.09	6.6		
12	1.05	7.0		
13	1.21	7.4		
Total	11.20	68.2	2.63	16.0

(a) With gallium liquid.

(b) One-half of this amount was added to each ring before joining.

(c) Mass is calculated using 6.095 g/cm^3 for gallium.

TABLE 12. MEASURED WEIGHTS OF EVALUATION TEST UNIT

Qty.	Description	Grams	Pounds
7	VHV ring-pairs	766.2	
1	VHV stator support	240.8	
1	VHV rotor support	207.4	
56	VHV nuts and terminal nuts	107.8	
	VHV platter assembly	1322.2	2.92
13	Cup-gap ring pairs	868.1	
1	Cup-gap stator support	134.2	
1	Cup-gap rotor support	212.2	
104	Nuts	5.9	
	Cup-gap platter assembly	1220.4	2.66
13	Brushes, filled with Ga	2.9	
1	Brush support and hardware	202.9	
1	Ring and support assembly	302.5	
	Brush and ring platter assembly	508.3	1.12
1	Shaft	888.6	
2	Upper and lower bearing adapters	561.0	
2	Ball bearings	125.1	
16	Hardware to retain platters to shaft	34.1	
	Shaft and bearings	1608.8	3.55
1	Housing	569.5	
1	Bottom plate with VHV feed-throughs and harness	2900.0	
1	Top plate with heater	2944.0	
1	Top cap	944.3	
1	Bottom cap	443.2	
1	Vent valve assembly	640.2	
1	Top ring (holds glass)	301.5	
1	Glass cylinder	638.8	
Set	Hardware	267.5	
	Housing assembly	9699.0	21.38
1	Interior harness	80.1	
Set	VHV conductors	22.0	
1	Shaft coupling	37.2	
Set	Spacers for bearings	6.0	
1	Cam for position sensing	26.2	
1	Proximeter	24.9	
1	Mounting adapter	127.3	
	Miscellaneous	323.7	0.71
	Total	14,682.4	32.34

The VHV and cup gap platter assemblies were then installed in the housing. The rotor portions of each platter assembly were taped to the stator portions to prevent rotation or inadvertent axial separation as the gallium was melted and the shaft and bearings installed.

At this point a gallium spill occurred. It is presumed to have happened as the ETU was being moved into a chilled shroud to freeze the gallium. A few drops of gallium were found beneath the three outermost cup gap rings. The gallium was readily removed through the large openings provided in the housing for visibility. The amount of spillage was insignificant compared to the total amount in the rings so there was no need for disassembly.

The brushes on their support platter were lowered into place until the brushes touched the rings with wet gallium, then lifted 0.015 inch to their final position. Electrical contact was made on all rings.

Wiring and the remainder of assembly were completed with the gallium frozen. Thermisters were added for temperature sensing per the wiring diagram. The outer glass cylinder around the housing and the vent assembly were not added at this time because the assembly was done in air rather than inert atmosphere. Leaving out the glass was to promote outgassing of the assembly in the vacuum chamber. The completed ETU is seen in Figures 40 and 41 with the drive unit mounted on the top and the vibration test fixture supporting the ETU from below. This is a 33 ring assembly with 7 VHV rings, 11 HV rings, 2 power rings and 13 signal rings.

Figure 40. Front View of ETU

Figure 41. Rear View of ETU

Testing of the Evaluation Test Unit

Degassing

The objective of the degassing period was to evaporate the quasi-plastic surface film on the gallium so that debris would not form during rotation.

The completed ETU was mounted in the vacuum chamber supported from above by the drive unit as seen in Figure 42. The VHV connections between the ceramic feed-throughs in the ETU and those in the vacuum chamber were added and can be seen in Figure 42. The vacuum chamber was then closed, electrical continuity checked, and pump-down accomplished. Figure 43 shows the vacuum chamber during pump-down with the test cables attached to the test panel in the electronics rack.

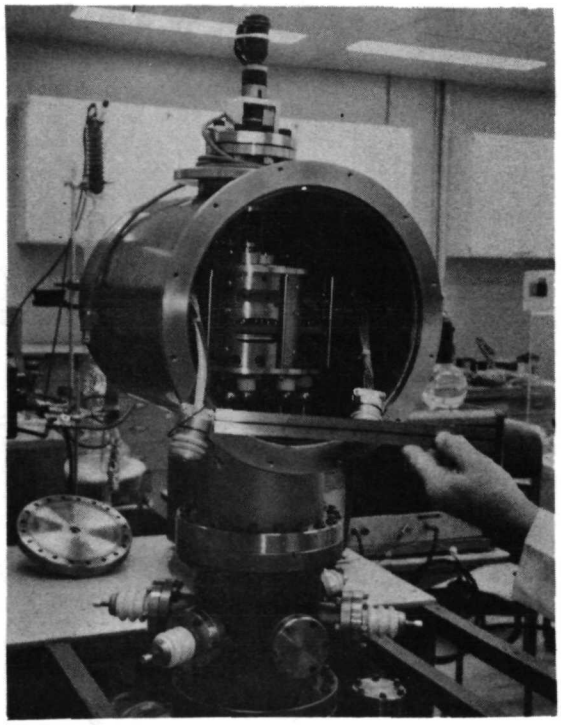

Figure 42. ETU Installed in Chamber

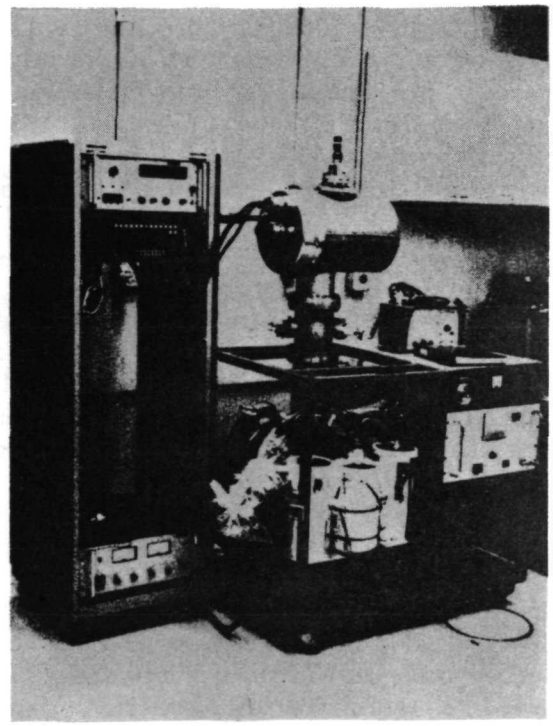

Figure 43. Vacuum Chamber During Pump-Down

During the majority of the degassing period the pressure in the vacuum chamber was near 1×10^{-5} Torr. The titanium sublimation pump (TSP) filaments used in the initial few days were soon used up and the ion pump was losing ground, so after 5 days the chamber was back-filled with dry nitrogen gas and the three TSP filaments were replaced. After these filaments were mostly exhausted the ion pump was able to hold near 10^{-5} Torr without the TSP.

On the 23rd day the ion pump was gaining ground and the heater in the ETU was turned on. It was desired that the remaining pumping capacity in the TSP would absorb the gas evolved on heating the ETU so that the slip rings would be at a temperature of 40°C to 50°C. This was not achieved and so the chamber was again back-filled with dry nitrogen gas and the TSP filaments again replaced.

During the pump-down on the 23rd day, heat was applied to the ETU while still on the sorb pumps as soon as the pressure was below 1×10^{-4} Torr. During the following week the pressure was kept below this value and typically 2×10^{-5} Torr while the temperature at the top plate was kept near 85°C and the rings about 60°C as sensed by the thermistors.

On the 30th day the heat was reduced to 10 watts, which maintains the rings between 40°C and 50°C, adequate to assure that the gallium remains liquid. The pressure then reduced to below 6×10^{-6} Torr for performance testing of the ETU.

Electrical Testing Prior to Shaft Rotation

A. Circuit Resistances

Resistance and continuity measurements were made that assured that all circuits were correct per the wiring diagram given in Figure 24. A typical circuit starts at a test point on the Test Panel, runs through a six-foot external cable to the vacuum chamber, passes through a hermetic seal electrical feed-through into the chamber, through an 18-inch cable to the ETU, through glass-sealed feed-through terminals into the ETU and then a short length of wire to the terminal stud on a slip ring. The current runs through the slip ring to the rotor side where a jumper takes it to another ring from which it returns to another test point by a parallel route. The total length of wire is about 200 inches. Special purpose jumpers permit voltage taps on rings intended for voltage drop measurements at high current. Multiple conductors are used for high currents. Typical data is given in Tables 13 and 14 for the period after the gallium was melted and with the ETU at separating temperature (40°C to 50°C).

The circuit resistance was measured with a resolution of one milliohm using a unique scheme of instrumentation. A one-milliamp constant current power supply provided a voltage drop across the circuit that was measured with an integrating digital voltmeter. The voltmeter has excellent noise rejection and readings were easily obtained to the nearest microvolt. This system

TABLE 13. CIRCUIT RESISTANCES OF SIGNAL RINGS, BRUSH TYPE, STAINLESS STEEL

Test Points	Resistance	Rings No.	Circuit Description
1 to 2	0.322 ohm	1, 2	5A current
2 to 3	.344	2, 3	ring 3 is voltage tap for ring 2 rotor
3 to 4	.339	3, 4	ring 4 is voltage tap for ring 1 rotor
5 to 9	.435	5, 9	continuity check
6 to 8	.378	6, 8	continuity check
10 to 11	.902	10, 11	ring 10 is voltage tap for ring 13 rotor
11 to 12	.377	11, 12	ring 11 is voltage tap for ring 12 rotor
12 to 13	.377	12, 13	5A current
1 to 7	.291	none	jumper on stator
2 to 6	.294	none	jumper on stator
12 to 12A	.328	none	voltage & current taps, ring 12
13 to 13A	.314	none	voltage & current taps, ring 13
1 to 8	.403	1, 2, 6, 8	note four rings in series

TABLE 14. CIRCUIT RESISTANCES OF HIGH VOLTAGE AND POWER RINGS, CUP-GAP TYPE, NICKEL

Test Points	Resistance	Rings No.	Circuit Description
21A to 22A	0.051 ohm	1, 2	30A current (power rings)
23 to 24	.324	3, 4	rotor voltage taps for rings 1 & 2
25 to 29	.343	5, 9	continuity check
26 to 28	.313	6, 8	continuity check
30 to 31	.289	10, 11	rotor voltage taps for rings 12 & 13
32 to 33	.304	12, 13	stator voltage taps for rings 12 & 13
32A to 33A	.101	12, 13	15A current
21A to 27	.128	none	current & voltage taps, ring 1 stator
22A to 27	.174	1, 2	current tap ring 2, voltage tap ring 1
22A to 26	.186	none	current & voltage taps, ring 2 stator
21A to 26	.190	1, 2	current tap ring 1, voltage tap ring 2
32A to 32	.176	none	current & voltage taps, ring 12 stator
32A to 30	.180	10, 12	12 stator current, 12 rotor voltage
33A to 33	.152	none	current & voltage taps, ring 13 stator
33A to 31	.151	11, 13	13 stator current, 13 rotor voltage

proved more accurate and easy to use than an impedance bridge. Repeatability was better than ten milliohms.

Comparing the data in Table 13 for signal ring circuits including two rings, four rings and no rings it is found that resistance through a ring varies from 16 milliohms for ring 1 (3.4 inch diameter) to 32 milliohms for ring 13 (8-inch diameter). The resistance for a signal ring includes the stainless steel brush, the resistance through the gallium (calculated to be 21 microhms), the resistance through the stainless steel ring (and its gallium-wetted face) from the brush to the terminal stud; also the resistance of the connections to the brush and to the therminal stud. These connections have stainless steel self-locking nuts and crimp lugs on the ends of the wire. A major part of the resistance is in the arc of the ring itself. Note in Table 13 that ring 10 has the largest resistance. Comparing this to the data on the day of initial pump-down (0.55 ohm) the resistance of ring 10 has increased significantly and remains the highest resistance measured. A poor connection is suspected.

The data in Table 14 for the cup-gap type rings shows the low resistance attained by multiple circuits to the 30A power rings 1 and 2 and 15A high voltage rings 12 and 13. The latter half of the table shows pairs of resistances where the differences are primarily due to the absence or presence of rings. The resistance for rings 1 and 2 and the jumper strap between their rotors is seen to be 46 milliohms and also 4 milliohms. For rings 10 and 12 and 11 and 13 the values are 4 milliohms and negative one milliohm. This predicts that the resistance of one ring is about 2 milliohms and was the first evidence of trouble in the connections to the power rings.

The resistance of the very high voltage (VHV) rings could not be measured because jumpers were not installed between rotor rings. This was done to provide more flexibility in high voltage testing. VHV rings 1, 3, 5, and 7 are connected with the outside by 0.25 inch diameter conductors with large corona balls at each joint. Vacuum is used as the dielectric inside the vacuum chamber with support for the conductors only at the ceramic feed-throughs through the walls of the vacuum chamber and the ETU. See Figure 42.

Rings 2, 4, and 6 are connected to the system electrical ground through one megohm resistors at the test panel. The case of the ETU is also isolated and brought to system ground through a one-megohm resistor at the test panel. These circuits were checked out with a multimeter.

B. Insulation Resistance

Insulation resistance was measured between VHV rings, between interconnected groups of signal and cup-gap rings and between rings and ground. The range of readings for the VHV rings was 2.5×10^{11} to 6×10^{11} ohms. For signal and high voltage rings the readings were typically 8×10^{12} ohms except interconnected signal rings 10, 11, 12 and 13 were 3×10^{12} ohms and the rings connected across the output of the high current power supply read 1.35×10^{9} ohms.

It is interesting that the insulated wires showed higher insulation resistance than the VHV rings with vacuum dielectric. It was noted when testing the VHV rings that the megohmmeter output varied with the pressure in the vacuum chamber so as to indicate that the ion current was measurable at 500 volts dc. As the vacuum improved it was expected that the insulation resistance would increase.

It was thus determined that continuity and insulation resistance were generally satisfactory before rotation and after 30 days in vacuum.

C. Current in Non-Rotating Rings

Thirty (30) amps was then circulated through cup-gap power rings 1 and 2. At this current the resistance of ring 1 was 0.8 milliohms and ring 2 was 13 milliohms. The current was maintained for only five minutes as it was apparent that the vacuum pump could not handle the outgassing from the heating of the conductors and insulation.

Five (5) amps was then circulated through cup-gap rings 12 and 13. The resistance of ring 12 was 1.1 milliohms and ring 13 was 1.0 milliohm. The heating at 5A was not a problem. Testing at 15A was not attempted because the heating of the conductors would be comparable to that in the 30A test because there are half as many conductors in the 15A circuit.

The following rings were then connected in series: Power rings (cup-gap 1 and 2), signal rings 12 and 13, high voltage rings (cup gap) 12 and 13. Power ring 2 was found to have become a high resistance (83 kilohms) so cup-gap ring 3 was substituted. A current of 5A was circulated through these rings.

Initial Rotation of Slip Rings

Two hours were allowed to elapse to obtain temperature equilibrium with current in the rings as described above, then rotation was begun at one revolution in 1 hour:1 minute: 30 seconds or 0.976 rph. The voltage drops across each type of ring are given versus time in Table 15. The voltage drop of cup-gap ring 3 could not be obtained because it does not have a voltage tap on the stator.

The pressure reading in the vacuum chamber varied from 7.4×10^{-6} Torr to 1.5×10^{-5} Torr, the high reading is a peak when the titanium sublimation pump (TSP) cycled on. The TSP was on a 30 percent duty cycle with a five minute period.

As rotation started the voltage drop across the signal rings began to drop, presumably because the brush moved from the hot spot on the ring caused by the concentrated dissipation from the brush. At about one-third revolution the voltage drop began to increase. At two-thirds revolution the signal ring circuits were opening and those with current had to be shunted.

TABLE 15. SLIP RING VOLTAGE DROPS DURING INITIAL ROTATION

Time hr:min	Event	MILLIVOLTS DROP ACROSS RING				
		Sig 12	Sig 13	Pwr 1	HV 12	HV 13
-1:56	5A current on	109.5	151.7	7.80	5.65	5.35
-1:30		114.0	155.9	7.70	5.95	5.56
- :10		114.4	156.2	7.64	5.98	5.58
0	Start rotation .976 rph					
+ :02		90.8	137.9	7.50	5.43	5.29
:06		61.9	117.1	7.53	4.80	4.90
:19		136.6	84.9	7.47	2.96	2.57
:22		156.8	112.8	7.37	9.99?	2.76
:25		168.8	132.1	7.22	3.52	2.81
:28	Circuit to R4 opens					
:31		184.3	0	6.84	4.85	3.10
:41	Current stops					
:53	Current on at 5A	shunted		7.07	6.30	5.54
:57				7.22	6.06	5.61
1:01.5	First revolution complete					
1:11.5				7.24	3.86	4.20
1:17.5				7.32	2.80	3.28
1:23.5	Contact briefly reestablished on signal rings					

At one and one-third revolution contact was briefly reestablished on some rings. All 13 signal rings thereafter remained open whenever monitored.

Evidently the gallium could not continue to bridge the gap between the brush and ring as the ring revolved.

The cup-gap rings show a cyclic variation in resistance due to the locations of the current and voltage tap studs on the rotor and stator.

Figure 44 shows this cyclic variation after 12 rotations. Ring 1 has a more constant drop because of the greater number of current taps on the stator. The higher resistance may be due to the 30A test. Rings 12 and 13 have an average reading close to the 0.8 milliohms measured for ring 1 at the beginning of the 30A test. The average resistance for ring 1 at this time was 1.3 milliohms.

Also shown in Figure 44 are the resistances of thermistors strapped against the stators of rings 1 and 13. The resistance is an inverse function of temperature. The peak-to-peak variation of ring 13 is less than 0.32°C and that of ring 1 is 0.125°C. The peak temperature reached at 50 minutes is probably when the current tap on the rotor goes by the thermistor.

Figure 45 shows these same outputs on the 44th day, after 1030 revolutions. The resistance of cup gap ring 1 has reduced to 1.1 milliohms average and the temperature variation has increased and is more uncertain.

The vacuum chamber is equipped with a small glass window which permits a view of a portion of the edge of each type of ring. No debris was seen.

Very High Voltage Testing

Within 48 hours of the start of rotation the VHV rings 1, 3, 5, and 7 were individually excited with +20,000 volts dc, approaching this level in steps of 5 kv for a few minutes at each voltage. The ion gage reading during these tests was 4 to 6 times 10^{-6} Torr. Some discharges were noted during the final stages of increasing the voltage. Rings 1 and 7 were raised in voltage until breakdown occurred at 23 kv for each.

Leakage current was monitored by measuring the voltage across a 10 kilohm resistor placed between system ground and the ETU ground. Voltages induced in rings 2, 4, and 6 were also measured while connected to ground with 10k resistor and with the ETU case grounded. The voltages were measured with an oscilloscope and an integrating digital voltmeter and are given in chronological sequence in Table 16. The sum of leakage to the ETU case and to rings 2, 4, and 6 is the total leakage in the ETU.

The AC millivolts noted on the scope consist primarily of a 2×10^5 Hz modulation from the VHV power supply. It generally increased in proportion to the applied voltage. Corona discharge is seen as a spike superimposed on this AC signal.

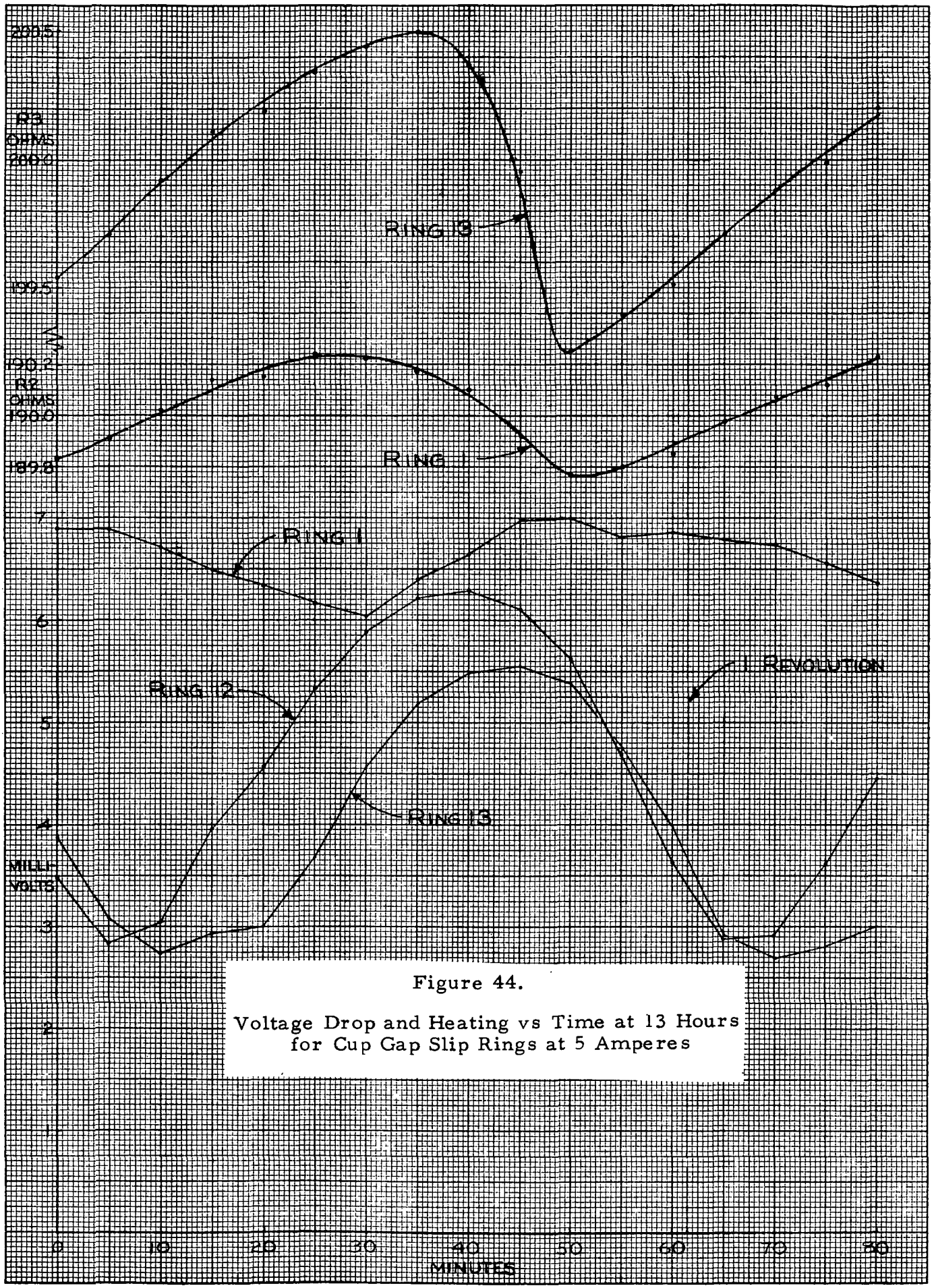

Figure 44.

Voltage Drop and Heating vs Time at 13 Hours for Cup Gap Slip Rings at 5 Amperes

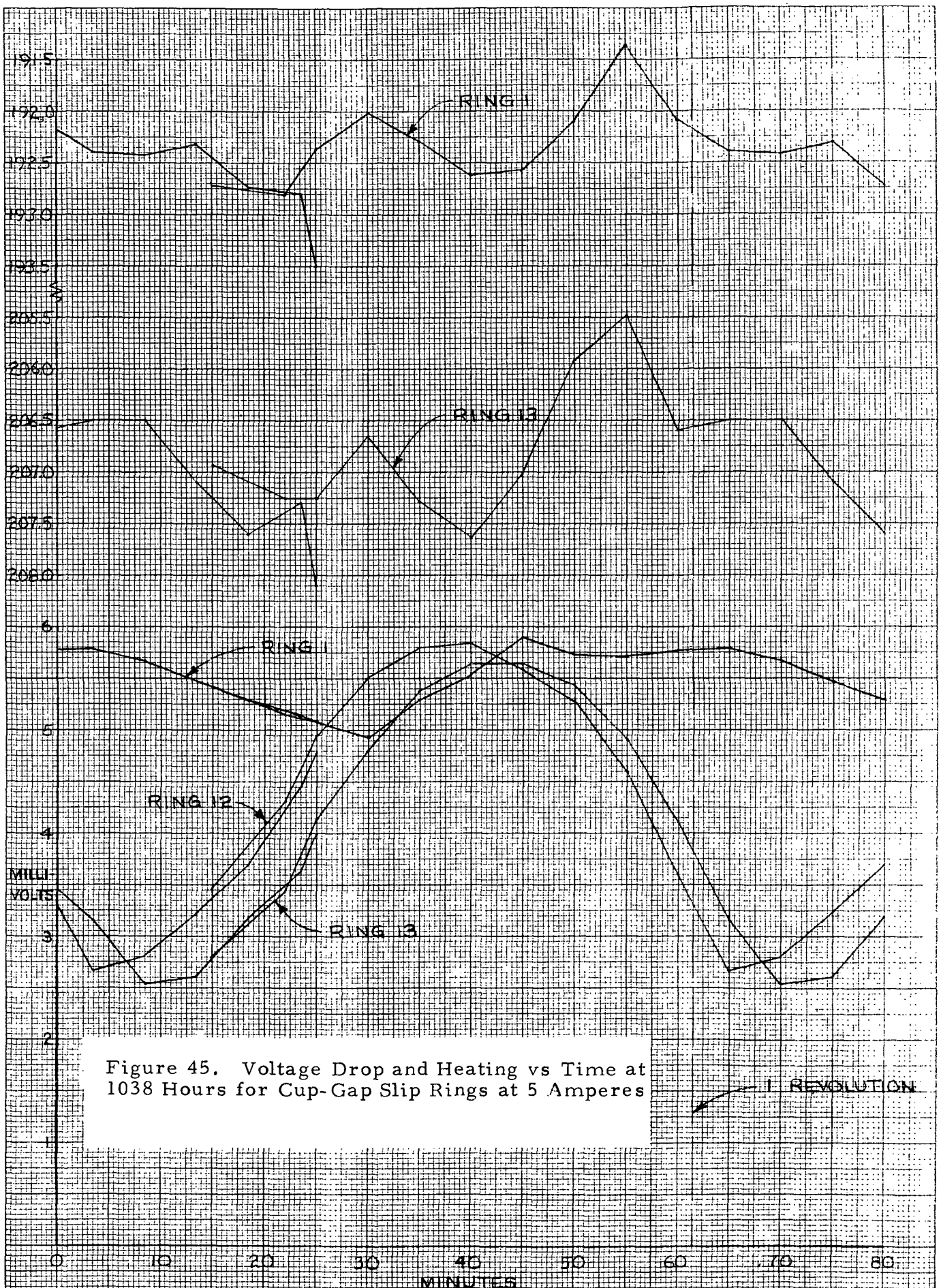

Figure 45. Voltage Drop and Heating vs Time at 1038 Hours for Cup-Gap Slip Rings at 5 Amperes

TABLE 16. PICKUP AND LEAKAGE MEASUREMENTS AT VERY HIGH VOLTAGE

Ring No.	kV	AC Millivolts, peak to peak				DC Microvolts			
			Ring No.				Ring No.		
		Case	2	4	6	Case	2	4	6
1	0					250	0-3	0-3	0-3
	5					250	0-1	0-1	0-1
	10					250	0-1	0-1	0-1
	15					250	0-1	0-1	0-1
	19	Discharge internal							
	15					175	1-3	1-3	1-3
3	0					185	1-3	1-3	1-3
	5	13	20	16	18	175	1-3	1-3	1-3
	10	25	30	10	30	175	1-2	2	2
	15	34	45	14	45	170	2	2	2-3
	20	48	63	20	63	170	2-3	2-3	2-4
5	0	10	21	7	7	4	1-3	0-2	0-21
	5	20	9	26	26	15	26	2	23
	10	32	14	40	40	12	1	2	23
	15	44	40	60	60	13	2	2	0-2
	19	Discharge external							
	20	60	28	86	84	14	2	27/55	2
7	0	18	2	7	2	4-8	2-4	1-4	1-3
	5	18	5	23	6	12-15	2-4	1-5	2-3
	10	50	8	36	10	15-18	3-4	3-4	3-5
	15	68	13	56	16	14-16	2-4	2-4	3-4
	20	100	18	80	22	12-18	3-5	3	2
	23	Discharge internal							
1	23	Discharge internal							
none	30^{+}	Power supply check							

A discharge within the vacuum chamber was evidenced by a cracking noise and a sudden increase in reading on the ion gage. An external discharge was noticed while testing ring 5. The cracking noise was not accompanied by an increase in pressure. The high voltage lead from the power supply was then repositioned and the external discharge did not reoccur.

The voltage was manually reduced immediately when a discharge occurred except for two slight pops heard at 20 kv on ring 5. Peak readings of 27 and 55 microvolts were noted on the integrating digital voltmeter on ring 4 which was being sampled at the time. These were the only meaningful corona current measurements obtained during the initial VHV tests. The other dc readings are believed to be mostly noise. The dc microvolt readings in excess of 20 for voltages less than 20 kv on ring 5 were due to a poor connection on the 10k resistor which was then corrected.

The ETU was being observed through the small window during each of the breakdowns. No lighting was used. No arcing, corona or light of any kind was seen in the ETU when the breakdowns occurred. It is considered most likely that the breakdowns occurred at the ceramic-insulated feedthroughs into the vacuum chamber.

The spacing between rings 1 and 2 is 0.125 inch, varying in 0.025 increments to 0.250 inch between rings 6 and 7. Since breakdown occurred at 23 kv for ring 1 and also ring 7 it is almost certain that there was no breakdown between rings.

On the 44th day of continuous rotation 5 kv was applied to VHV ring 7 and resulted in a series of discharges of 50 to 200 microamps with durations of 10 to 20 milliseconds. No discharges resulted when the 5 kv was applied to VHV ring 1. At 10 kv and 15 kv on VHV ring 1 there were randomly recurrent discharges of 20 to 100 nanoamps with durations of about 1 millisecond. At 30 kv there were several audible discharges, now believed to be primarily in the power supply, but no overloads. The vacuum during the above testing was near 1×10^{-6} Torr.

On the 45 th day of testing the titanium sublimation pump was used. to bring the pressure to 2×10^{-8} Torr for insulation resistance measurements. VHV rings 1, 3, 5, and 7 read from 9 to 10×10^{12} ohms. This considerably higher resistance compared to the readings of 2.5 to 6×10^{11} ohms at the start of testing corresponds to the improvement in vacuum and the degassing of the insulation material.

On this last day of vacuum testing, VHV ring 1 withstood 30 kv without evidence of discharge with a measurement sensitivity of 10 nanoamps or lower. VHV rings 3 and 5 withstood 28 kv before substantial discharges took place. VHV ring 7 caused the circuit breaker on the VHV power supply to open when voltage was applied. This ring was then found to be shorted to ground with a resistance of 11,000 ohms.

Findings at Disassembly

1. Gallium Debris

Upon opening the vacuum chamber it was immediately evident what had shorted VHV ring 7. Drops of gallium were resting on the VHV stator support and touching both the case and ring 7 stator as can be seen in Figure 46. Drops of gallium were also found on the lower plate

By turning the shaft a small amount and observing that the rings moved, it was determined that the gallium was supercooled and not frozen. Liquid nitrogen was introduced into the chamber to thermally shock and freeze the gallium. The ETU was then removed from the vacuum chamber and disassembled in a laminar flow bench.

The total amount of gallium that had spilled from the rings is pictured in Figure 47. This was 2.4 grams, or 2.7 percent of the 87 grams with which the rings had been filled at assembly.

The tops of the VHV feed-throughs in the bottom plate of the ETU are seen in Figure 48. The dark spots on the alumina ceramic insulators are drops of gallium or residue from such drops. From left to right the feed-throughs supplied VHV rings 7, 5, 3, and 1. Note that 5 and 3 have a significant amount of debris on them while No. 1 is relatively clean.

The gallium appeared mostly near the outer periphery of the ETU and on one side indicating that it came mostly from the large diameter rings and from a spill towards the front of the unit. The debris did not lodge where it could be seen through the small window in the vacuum chamber.

The spillage is believed to have come mostly from the cup gap rings. This conclusion is based on the accumulation seen near ring 7 in Figure 46. These drops are too large to have come through the baffle in ring-pair 7, particularly since they would have had to go over the barrier on the outer ring to escape. The spillage must have occurred between the initial and final VHV tests because ring 7 could never have withstood 23 kv with that group of metallic drops between it and the case. The spillage probably occurred before the chamber was placed on blocks to minimize the disturbance if someone should accidentally bump into it.

The size, shiny surface and roundness of most of the drops indicate that the gallium debris was due to spillage, such as sloshing during handling, rather than the escape of debris resulting from rotation. Gallium debris resulting from rotation typically has a shriveled gray surface, irregular shape and a spongy consistency due to many rolled up layers of surface film. (Reference 1.)

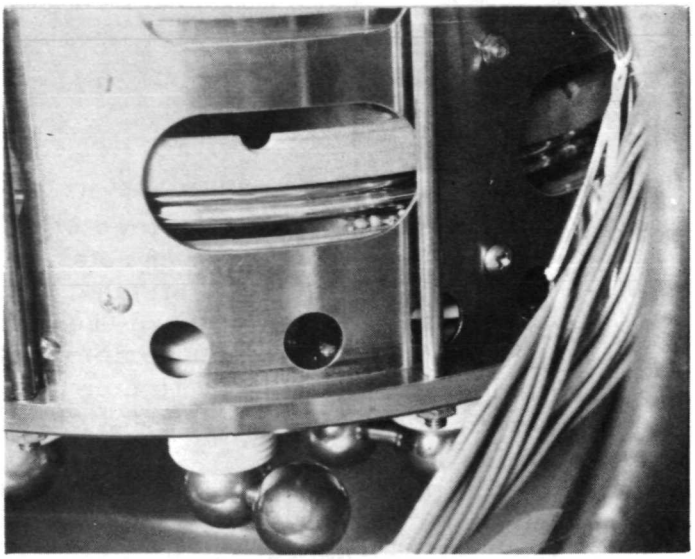

Figure 46. Gallium Drops Near VHV Ring 7 and on Lower Plate of ETU

Figure 47. Gallium Debris Collected from ETU

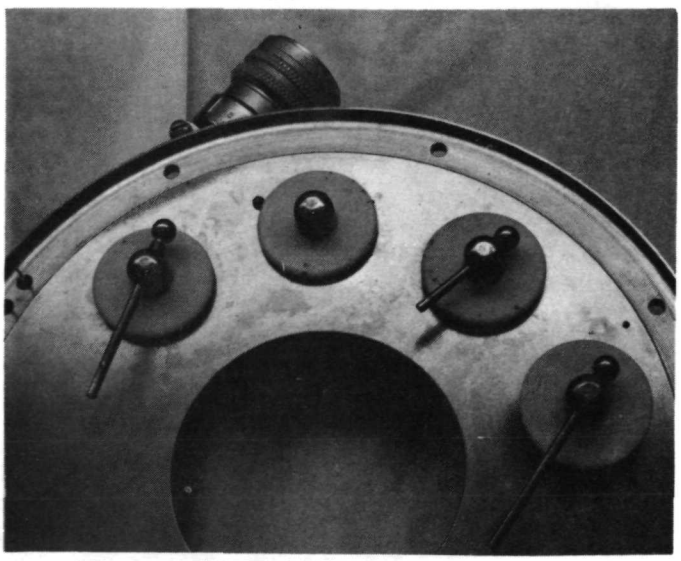

Figure 48. Gallium Debris on VHV Feed-Through Insulators

Signal Rings

The 13 signal rings of the brush type remained open whenever their resistance was measured throughout the 45 days of rotation. At disassembly it was confirmed that the gallium that had been intended to bridge the gap between rotor and stator had instead all transferred from the brushes to the rings within the first revolution. The subsequent brief reestablishment of contact was rubbing of the brush on the ring due to non-perpendicularity of the brush and ring platters with the shaft axis of rotation.

Figure 49 shows the complete array of brushes. Figure 50 shows some outer brushes and the evidence of rubbing, particularly on the outside brush. Figure 51 shows the inside brushes which did not rub. Included in Figure 51 is a spare brush showing the amount of excess gallium originally applied to all the brushes.

Figure 52 shows the marks on the rings where each brush was before rotation. The gallium from the brushes was found in the first 2/3 revolution from these marks. Figure 53 shows the rubbing marks on rings 12 and 13.

Large amounts of gallium on the rings and better control of runout may have permitted continuous operation. The excess gallium would have negated a major advantage of the brush type ring, high radial acceleration capacity. The runout is believed to be due to four factors:

1) Errors in initial setup and pinning of the platters to the shaft and housing

2) Errors in returning to the pinned position

3) Dimensional instability in the epoxy-glass laminate supports

4) Stresses caused by unequal temperature coefficients of expansion of the epoxy-glass compared to the stainless steel housing, shaft and rings

Item 2) above was aggravated by difficulties of alignment and pin insertion at final assembly. Burrs were seen at the entrances to two holes into which pins were forced before the support and shaft were adequately aligned. This problem could be reduced by improved procedures.

Cup Gap Rings

The stator platter of the cup gap rings is seen after disassembly in Figure 54 with the male rotor rings embedded in the gallium as they were when frozen before removal from the vacuum chamber. Figure 55 is a close up of the rings showing an area where the gallium level is correct. In Figure 56 is an area where the gallium level is low. This low area was on the same side of several rings, indicating that this side was the high side

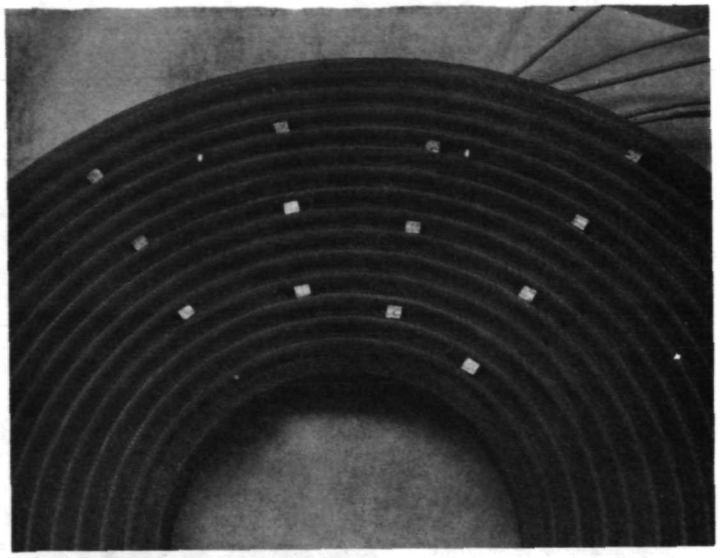

Figure 49. Complete Array of Signal Brushes After Disassembly

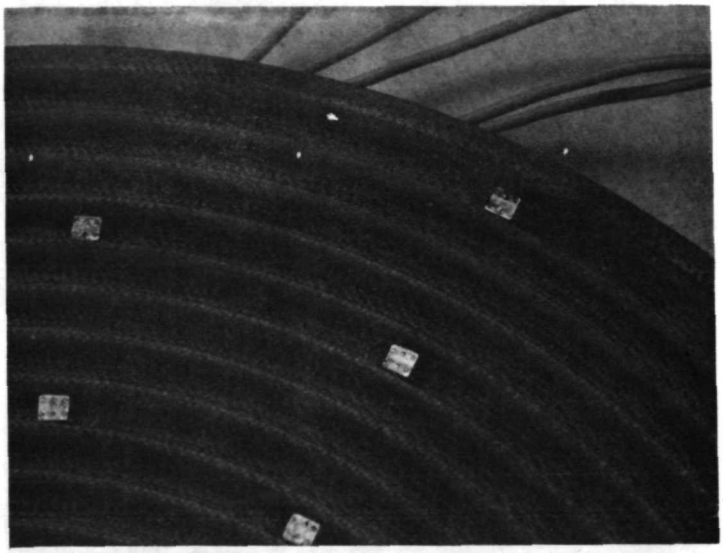

Figure 50. Brushes Showing Evidence of Rubbing. Note the Black Deposit to the Right of the Outer Brush.

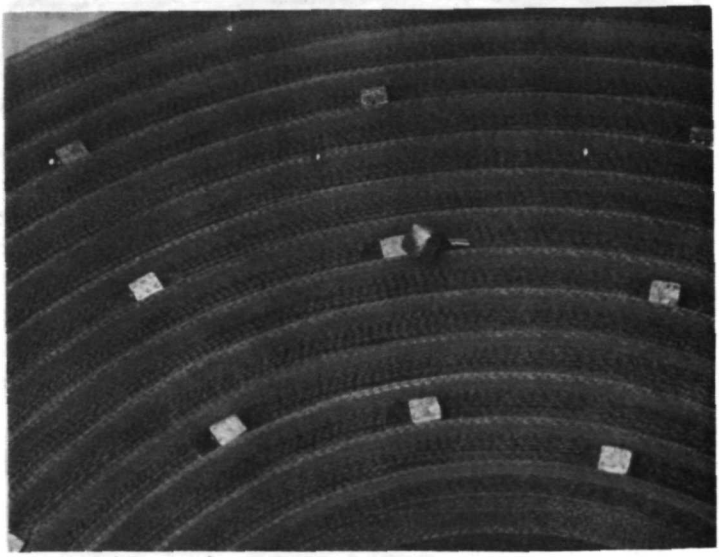

Figure 51. Brushes Which Did Not Rub, Foreground; A Brush as Originally Filled with Gallium, Near Center

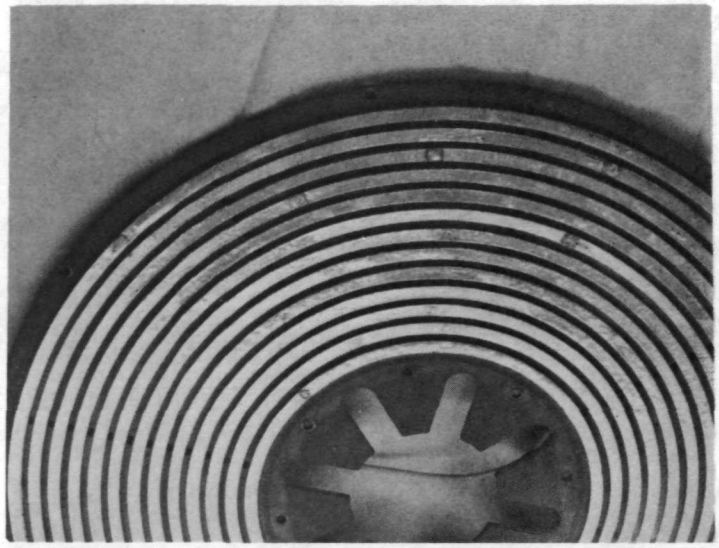

Figure 52. Signal Rings Showing Marks Where Brushes Were Before Rotation

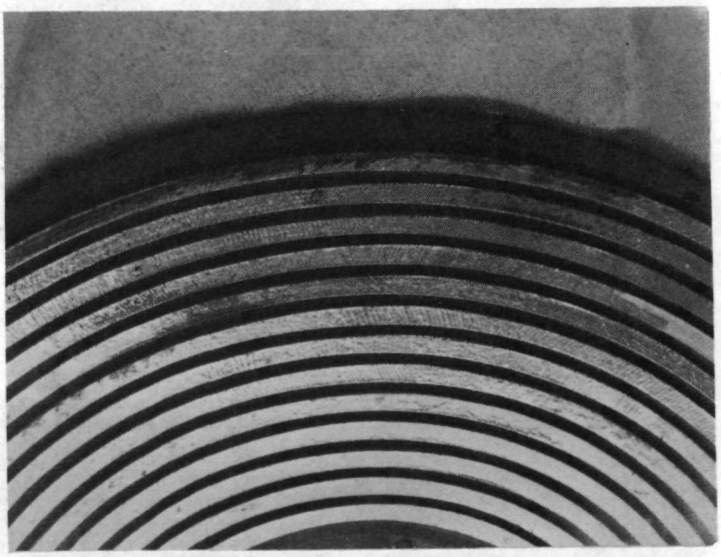

Figure 53. Signal Rings Where Brushes Rubbed

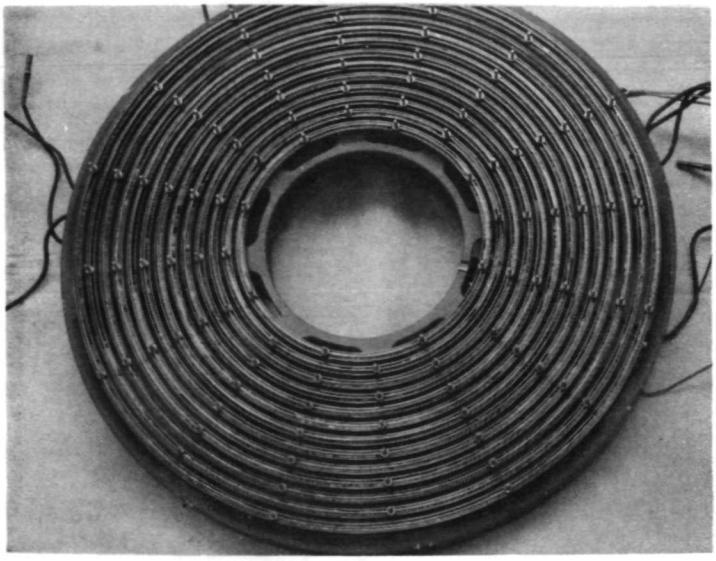

Figure 54. Stator Platter of Cup Gap Rings After Disassembly

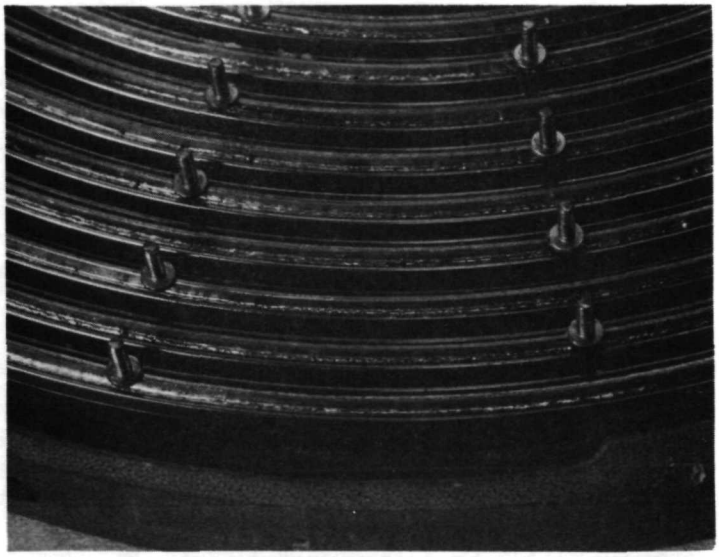

Figure 55. Cup Gap Rings Showing Normal Level of Gallium

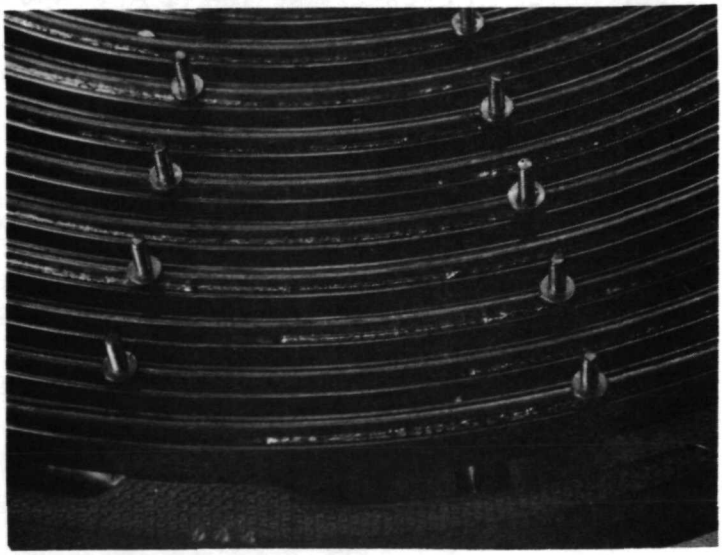

Figure 56. Cup Gap Rings Where Gallium Level Was Low

of the ETU as mounted in the vacuum chamber. The missing gallium was that which sloshed out at an unknown time and was found around the VHV rings below.

Associated with the low gallium were unwetted areas on the stator rings and powdery black deposits. The powdery black deposits have been previously seen, Reference 1, where the gallium surface is continuously being sheared and folded in a vacuum.

The support for the male rings is seen in Figure 58. Each groove has its pattern of black deposits on the epoxy-glass. These deposits correspond to uneven wetting of the rotor rings as characterized by the lower ring in Figure 59. Also seen in Figure 58 in the reservoir groove for ring 6 is a trail of gallium where a protrusion of gallium from between the rings must have rubbed on the epoxy-glass above it. The rotor rings mostly remained wetted where they were immersed.

The unwet areas of the stator rings amounted to about 20 percent of the originally wetted areas. The initial coat of gallium continued to adhere to the nickel in the unwet areas but the composition of this layer has changed and the liquid gallium no longer adheres to it.

An important finding was made when the gallium was melted and the rotor rings lifted out. The gallium was almost entirely free of the sludge that accumulates in rings that are rotated in air.

The mechanism of formation of the sludge can be explained by reference to Figure 60. Rotor rings 12 and 13 have been lifted out and are seen in Figure 59. Note the smooth surface on the remaining gallium. Rotor ring 9 has been rotated (moved tangentially) a few thousandths of an inch with respect to the stator. Fine diagonal wrinkles in the gallium surface appear as the surface film is stretched. Rotor ring 11 has been rotated 45° with respect to the stator. This is a tangential distance of a few inches. Note how the small wrinkles have developed into deep rolling pockets resembling vortices. The quasi-plastic surface film on the gallium is rolled into the liquid gallium to form sludge. When the gallium surface is convex instead of concave, the ring rotation causes a series of lumps which may roll into tiny cylinders between the non-wetted walls of the baffle (see Figure 6), and escape from the ring. These tiny cylinders of rolled-up surface film are called twirlies. Twirlies have the same gelatinous consistency as the sludge. No definite twirlies were identified in the debris from the ETU but the track of gallium in ring 6, Figure 58, suggests this may have happened.

The slight depressions in the gallium surface of ring 10 are due to unwetted areas on the rotor ring. This condition causes the black deposit during rotation in vacuum. Rotation in vacuum causes very little sludge or twirlies because the oxide film on the gallium is very thin.

Figure 61 shows the location of the thermistor used to monitor temperature variations of ring 1. A similar mounting is used on ring 13. Rotor ring 1 has been removed and is seen in Figure 59.

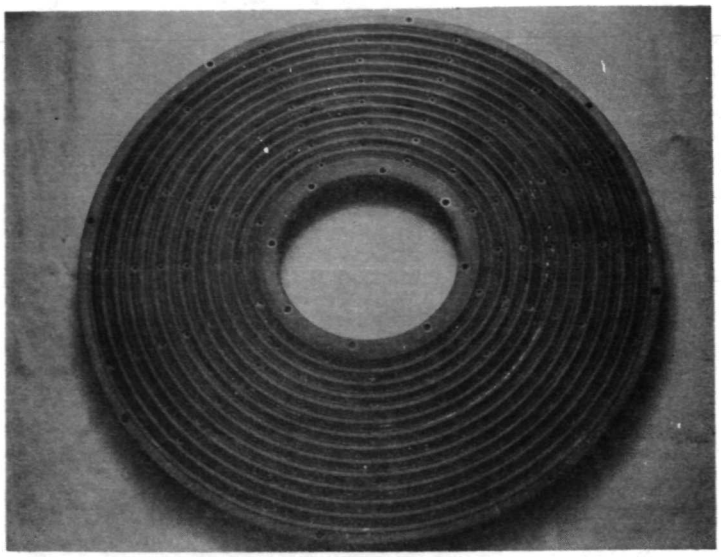

Figure 58. Support for Male Cup Gap Rotor Rings

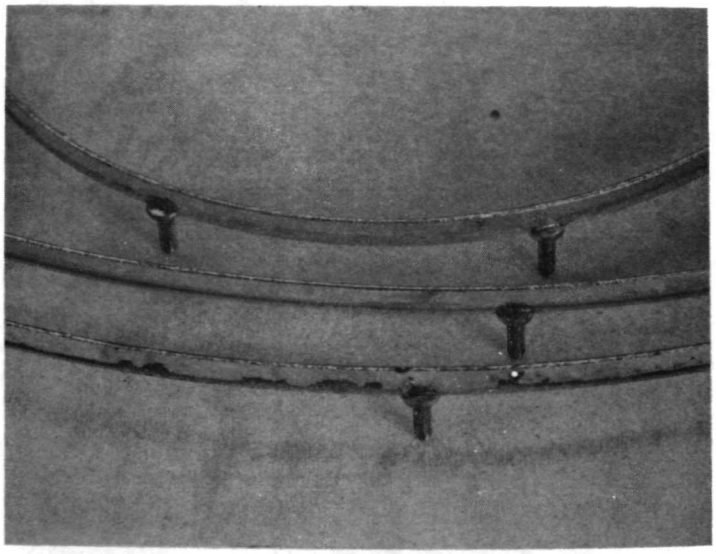

Figure 59. Male Cup Gap Rotor Rings

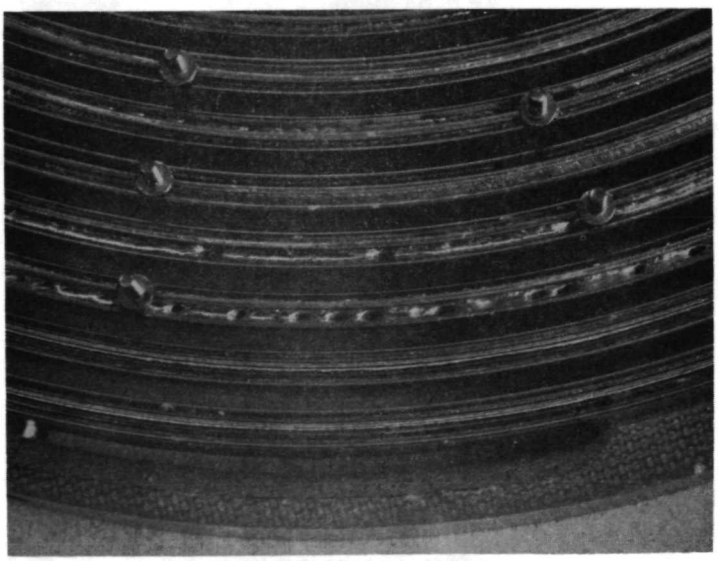

Figure 60. Cup Gap Rings After Melting of Gallium And Rotation of One Ring in Air

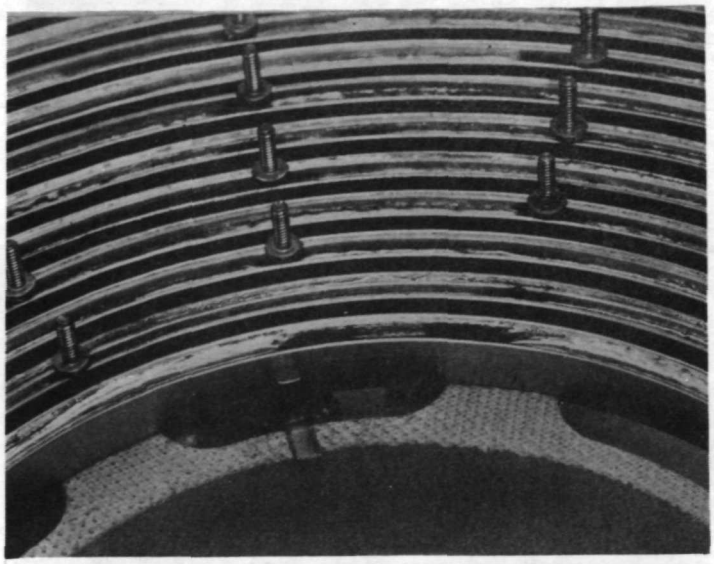

Figure 61. Thermistor Location for Power Ring No. 1

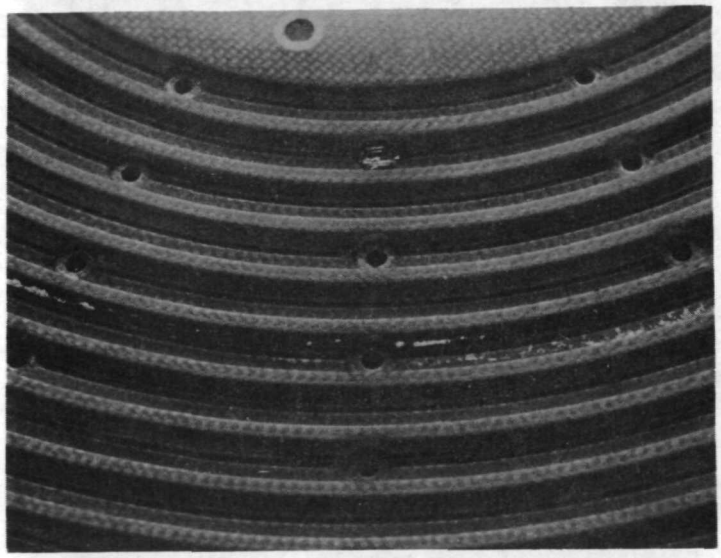

Figure 62. Broken Current Tap of Power Ring No. 2

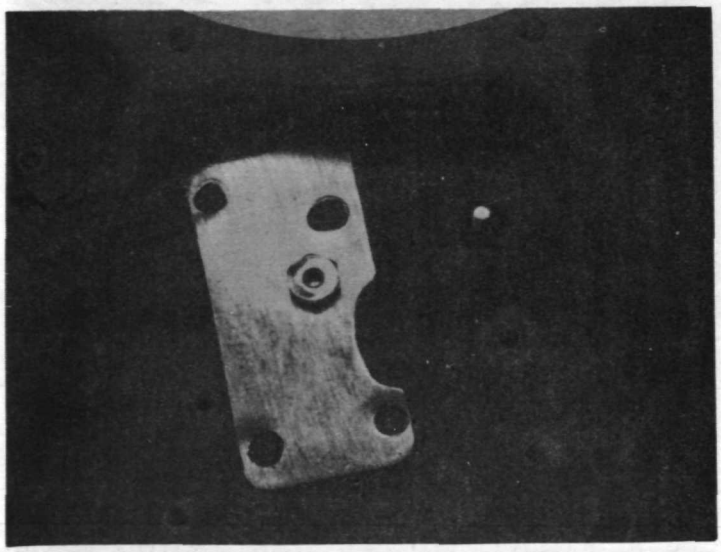

Figure 63. Discolored Insulation Around the Current Tap to Power Ring No. 2

The cause of the poor connection to power ring 2 is seen in Figure 62. The welded-on No. 0-80 nickel screw that forms the current tap had broken off. The heat of the 30A current through a very small weld area was undoubtedly responsible. The effect of this heat on the epoxy-glass support is seen in Figure 63. The copper strap that joined rotor rings 1, 2, 3, and 4 is also shown. The area around the ring 1 current tap was not discolored. Apparently the weld to the ring can handle the 30A current if it is not faulty or damaged.

Very High Voltage Rings

The complete VHV platter assembly is shown in Figures 64 and 65. The frozen gallium holds the rotor and stator together. The terminal nuts into which the VHV conductors fitted can be seen in Figure 65. The terminal nuts project above the other nuts and have a radial hole. Note the complete absence of sharp exterior corners on the metal parts, and the variable ring spacing.

The gallium in the VHV rings also proved to be free of sludge as can be seen in Figure 66.

Several areas of the VHV rings were not wet with gallium where they had originally been wetted. The gallium had peeled from these areas, in contrast to the nickel rings where the original gallium layer remained but had become hardened to the liquid gallium. The leading and trailing edges of the wet areas apparently were a source of the black powdery deposit as shown in Figures 67 and 68.

The lower reservoirs of most VHV rings contained some small lumps of gallium debris. The debris can be seen in Figure 68. Non-wetting in one portion of a ring would cause the gallium fill in another portion to be above optimum. Excess fill would cause a convex surface to develop on the gallium, particularly on the lower surface, with consequent formation of debris as the rings rotate.

The film of gallium extended the majority of the circumference of each ring pair as the rotor and stator rings were separated. This clearly demonstrated that there was little likelihood of loss of electrical contact in the radial gap VHV rings after rotations in vacuum equivalent to three years in synchronous orbit.

Figure 64. Top View of VHV Platter Assembly

Figure 65. VHV Platter Assembly Showing Terminal Nuts

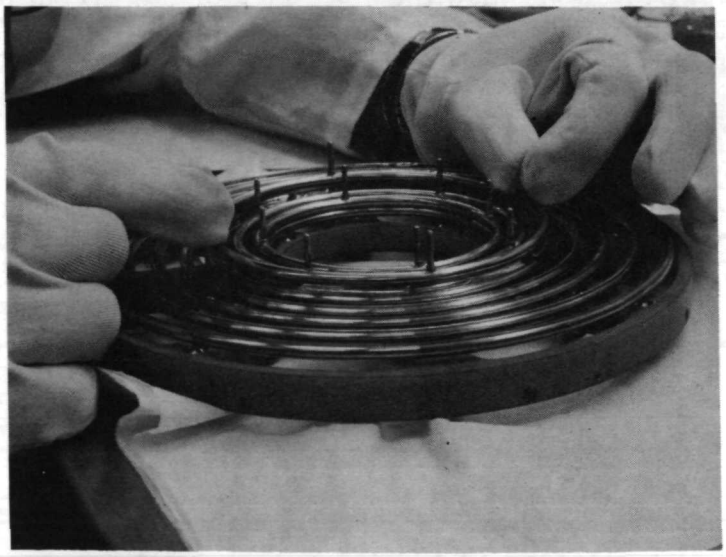

Figure 66. Separation of Rotor and Stator of Ring 3. Note Smooth Gallium Film, Free of Sludge

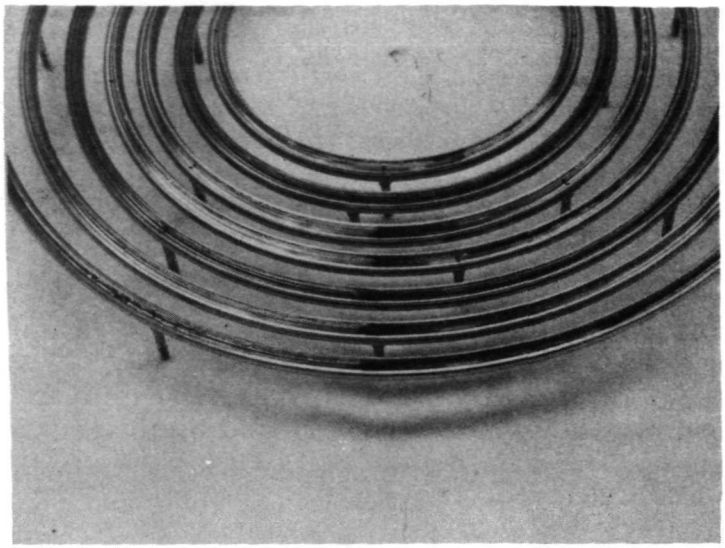

Figure 67. Black Deposits in VHV Rotor Rings

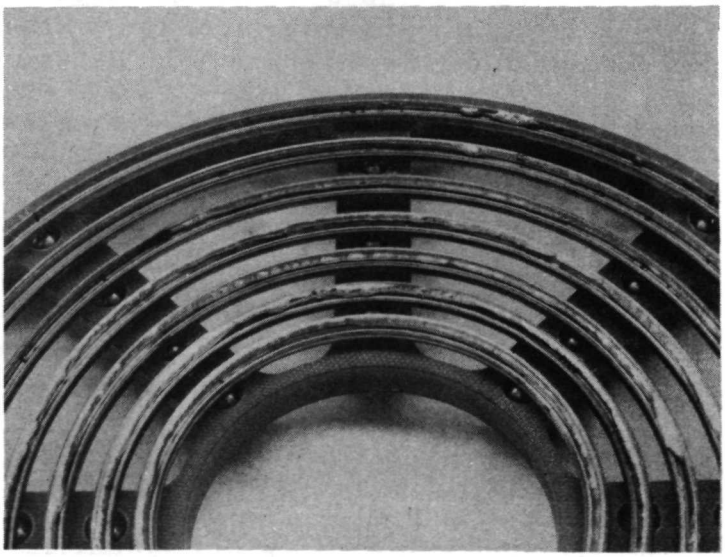

Figure 68. Gallium Debris in Lower Reservoirs of VHV Rings

Experiments with Gallium

Inert Atmosphere

Experiments were performed to determine if a suitable atmosphere could be maintained in a glove box to permit handling of liquid gallium without the formation of the troublesome quasi-plastic surface film. It was found that gallium could be exposed for reasonable working periods in a glove box with an argon gas atmosphere from which oxygen, water vapor and nitrogen have been removed such that residual amounts are less than one part per million (ppm) of oxygen, 3 ppm of water vapor and a few ppm of nitrogen.

Two trials were made in demonstration glove boxes at a supplier of such equipment. For the first trial the oxygen and water vapor were reduced to the level of about 20 ppm and nitrogen was not removed. The surface film formed quickly on freshly exposed surfaces of liquid gallium. The film wet the glass container. The film could easily be picked up with a small stainless steel spatula and exhibited the same gross characteristics as noted in air.

The second trial was successful. The glove box was then equipped with a 30 CFM purification system for oxygen and water vapor removal plus a 5 CFM nitrogen removal system employing heated titanium sponge. The gallium was melted before being passed into the chamber and a careful pass-through procedure was used involving two evacuations with a mechanical pump and an intermediate back-fill with pure argon. The box was equipped with 0.030 inch thick butyl rubber gloves. Instrumentation was an aluminum oxide hyrometer and a bare light bulb filament. A more sensitive oxygen detector was not operative. The hygrometer showed water vapor to be 3 ppm and the 40 watt light bulb filament continued to glow throughout the experiment.

In the glove box about 20 grams of liquid gallium was poured from the polyethelene bag (in which it had been heated) into a clean glass dish. A single round drop formed which stood surprisingly high from the bottom of the dish. This height was due to the gallium not wetting the glass and probably to a higher surface tension than we were used to seeing in the presence of the film. The gallium rolled freely on the glass without leaving residue. The small stainless steel spatula was also not wetted by the gallium. Small samples of the liquid gallium were separated only with difficulty from the main drop using the spatula. When allowed to touch the main drop the small drop was immediately absorbed and the drop remained round and free of wrinkles. The gallium acted as a pure non-wetting fluid would be expected to act.

The sample was manipulated for about 20 minutes without sign of film formation. The remainder of the 50 gram sample in the polyethylene bag was then added to the glass dish. This sample included film from previous air exposure. This film left some deposit on the glass as the sample was rolled about. The film could be removed a little at a time by the spatula. It adhered to the stainless steel but was easily wiped off on the back of the stretch nylon

gloves worn over the butyl gloves. This film exhibited the quasi-plastic characteristics and did not appear to be disintegrating in the argon atmosphere.

It was thus concluded that liquid gallium can be handled in an argon atmosphere. The question remained as to just how good the purification system needs to be.

A third trial was conducted to attempt to establish the need for the nitrogen removal equipment. Gallium was exposed in a glove box available to the project which does not have nitrogen removal equipment. The film formed, slowly, but it would not be possible to assemble film-free slip rings with this rate of film formation. There was, however, no instrumentation for oxygen or water vapor, and the film may have been due to the condition of the purification system. It had been running for several weeks without regeneration. The gloves were thin and there are six in the one chamber. This would permit a good deal of leakage. Thus, we had an indication but not a firm conclusion that the nitrogen removal is necessary.

It was not possible to obtain a new glove box so the available glove box was reconditioned with the intention of using it for the assembly of the ETU.

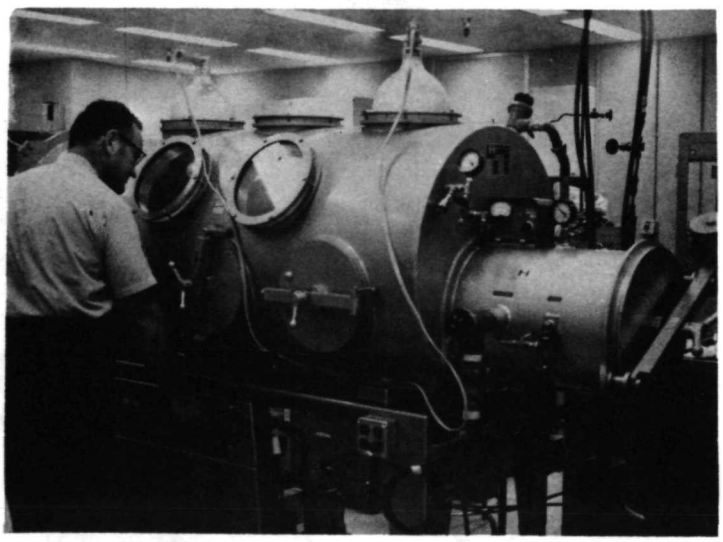

Figure 69. Glove Box with Glove Ports Closed for Vacuum Operation

The glove box is shown in Figure 69. The purification unit is below, the pass-through chamber is on the right. The purification unit handles 20 cubic feet per minute (CFM) of gas through the molecular sieve dryer. The oxygen remover circulates 5 CFM. The box is operated at atmospheric pressure with a mixture of 94 percent argon with 6 percent hydrogen so that the oxygen remover is continuously regenerated, resulting in the lowest possible oxygen content, well under one part per million.

The inside of the box was thoroughly scrubbed clean by processes used for high vacuum chambers. A chill plate cooled by coolant circulated from outside the chamber was installed. Sockets were installed for four light bulbs to be used as oxygen detectors with their glass envelopes removed.

After correction of numerous leaks the chamber could be pumped to less than one micron on the mechanical pump. Several regenerations of the molecular sieve in the purifier finally resulted in dew point readings of below -100°F for the argon in the glove box. This corresponds to water vapor below 1.5 parts per million.

Analysis of a gas sample was made using an evacuated glass flask sealed with a vacuum stop-cock and opened in the glove box. This gas was found by an outside laboratory to have the following composition:

Argon	99.841%
Water vapor	0.019%
Nitrogen	0.120%
Oxygen	0.020%

The indicated amount of oxygen is much too high to prevent film formation. Gallium exposed in the glove box formed film in a short time and the film-covered gallium wetted glass. The absence of hydrogen was evidence of an air leak that was consuming the hydrogen to form water. The water was being removed by the molecular sieve but it could keep up only if constant regeneration was employed.

The problem was eventually found to be a crack developing in the metal bellows of the evacuation valve of the antechamber. In the meantime the decision was made to go ahead with the assembly of the ETU in air, using care to avoid rotation of the rings so as to minimize formation of sludge and debris.

After correction of the leak and regeneration of the purifier the glove box has proven to have a consistently low oxygen content. At this writing, three sixty watt and one 100 watt filaments have each operated continuously for four weeks with their filaments exposed inside the glove box and work being performed in the glove box. The oxygen content is believed to be well below one ppm. Only a slight film forms on gallium. The gallium does not readily wet glass. Residual nitrogen may be responsible for the film.

Gallium Evaporation Experiment

Gallium is used in the liquid metal slip rings in preference to other liquid metals primarily because of its very low vapor pressure. Data is unavailable at room temperature but data from 600°C and above extrapolates to 10^{-44} Torr at room temperature. Still there was concern that gallium would evaporate from the rings and recondense on insulation surfaces to form a conductive film that would contribute to surface breakdown at high voltage. The black powdery deposit on surfaces opposite gallium had been previously noted in Reference 1 and by others who worked with gallium in a vacuum. A simple experiment was performed with the intent of measuring the surface conductivity of the film that condenses on insulation from the vapors of heated gallium in a vacuum.

Figure 70 shows the two layers of surface resistance patterns to be inverted above the pool of gallium in the beaker. Each pattern has 550 squares with 0.050 inch spacing between conductors. The substrate is epoxy-glass cloth laminate, NEMA grade C-10. The pattern closest to the gallium is well within the mean free path in the vacuum and represents the interior of a reservoir in a slip ring. The round substrate fits in the beaker with 0.020 inch radial spacing. The next pattern is intended to represent insulation between slip rings.

The stainless steel ball in the beaker was intended to stir the gallium when the vacuum chamber was rocked, once each day. Sludge quickly formed during testing in air and the ball would not roll freely in the beaker. The solution, after some experimentation, was a tungsten roller 1/2 inch in diameter and almost as long as the inside diameter of the beaker. The roller rolls on a hoop of stainless steel wire which rests on the bottom of the beaker. The roller is free to roll only about 1/2 inch. Shorter rollers were found to break the beaker after accumulating momentum, even in the gallium. The large roller produces a film-free surface of gallium with an area of about one square inch at each roll. It is gently arrested by angular contact at the side of the beaker at the end of the roll.

Figure 71 shows the experiment assembled. The insulation block in which the beaker is supported has two ten watt resistors and a thermocouple embedded very close to the bottom of the beaker. The white spots on the side of the block show their location. Thermocouples are also mounted on the back of each test pattern.

Subsequent to the pictures being taken, the wiring was revised so that the plus and minus leads from each pattern leave the vacuum chamber through separate feed-through connectors. This greatly improved the insulation resistance. The insulation resistance for both the upper and lower test patterns was approximately 10^{13} ohms as measured at 500 volts dc after stray leakage paths were eliminated.

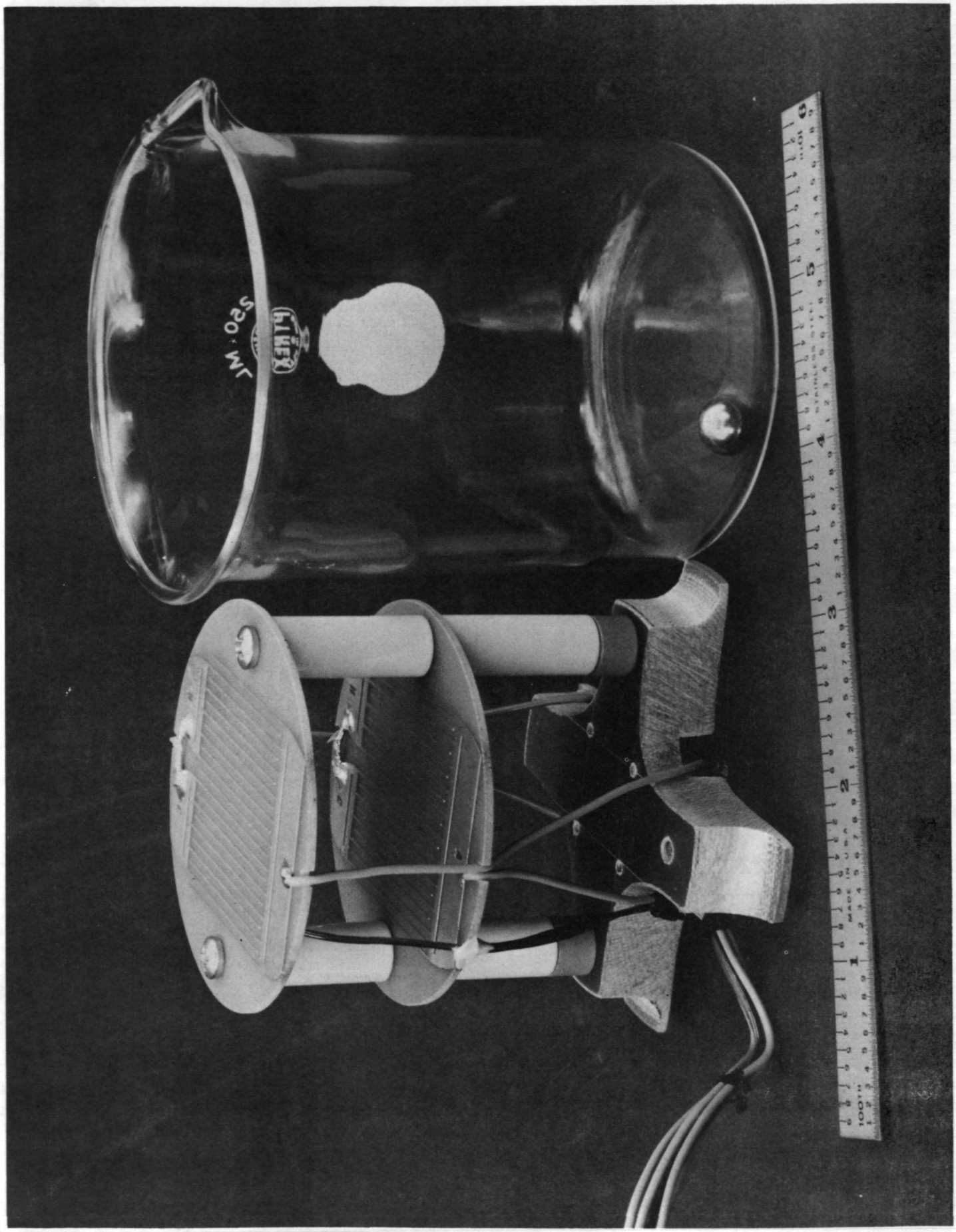

Figure 70. Surface Resistance Test Pattern

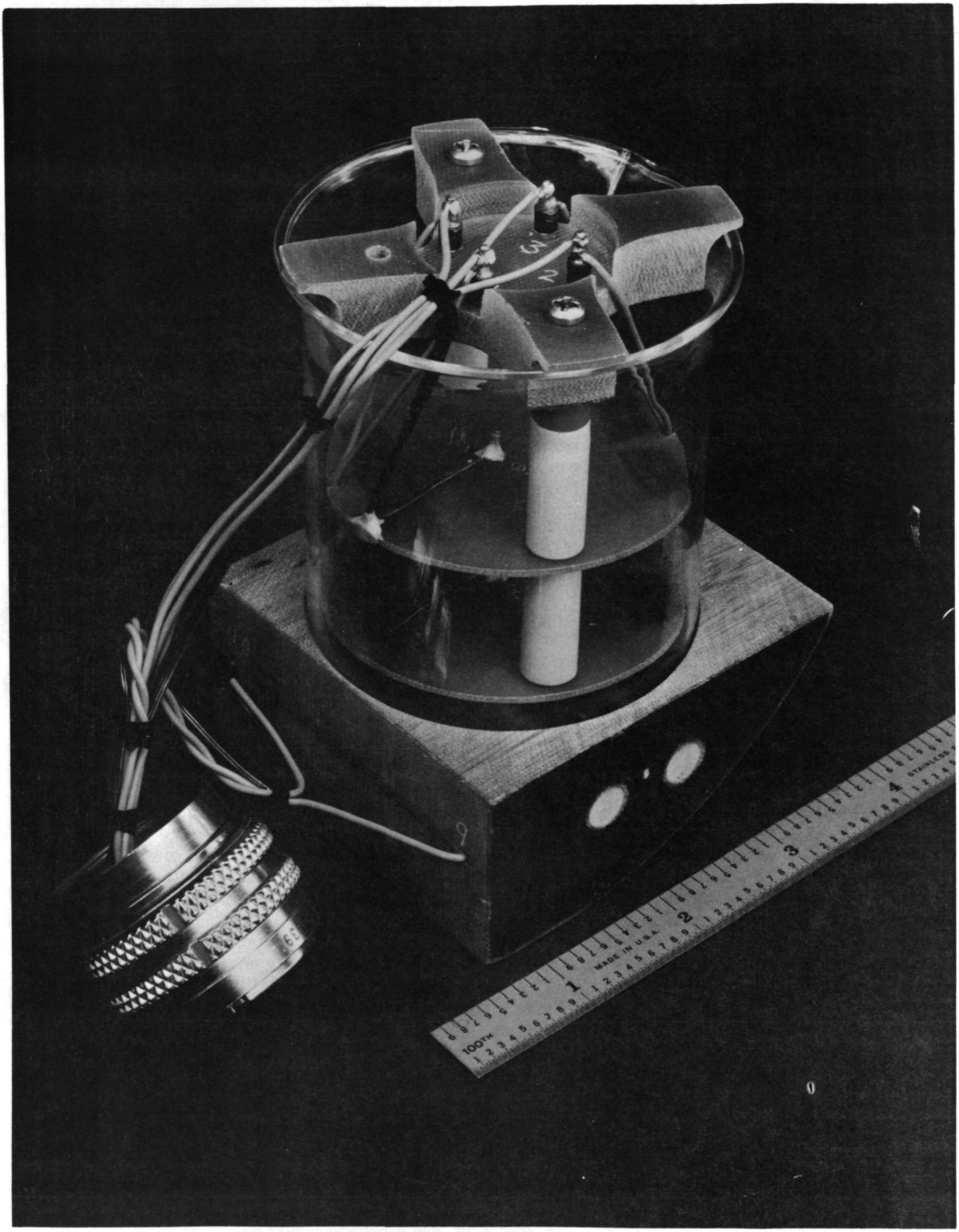

Figure 71. Gallium Evaporation Experiment Assembled

The experiment was placed in a small ion-pumped vacuum chamber. The heaters were operated to heat the gallium and the following temperatures were maintained within a few degrees for more than a year.

Bottom of beaker	93°C	200°F
Back of lower pattern	49°C	120°F
Back of upper pattern	43°C	100°F

It is considered that the gallium temperature is above 80°C. The vapor from the heated gallium should thus readily condense on the test patterns. A fresh gallium surface was exposed each day by tilting the vacuum chamber. The "clunk" of the tungsten roller was clearly audible.

The pressure in the vacuum chamber was below 10^{-5} Torr on the seventh day and below 10^{-6} Torr after 36 days. Over the last several months the pressure was 1.4×10^{-7} Torr as measured by the current to the ion pumps. The mean free path at this pressure is several hundred feet.

Insulation resistance remained near 10^{13} ohms for both patterns throughout the test. During a period of high humidity the resistance decreased to a low of 6×10^{12} ohms on the lower pattern. The return of dry weather returned the readings to their earlier values to indicate that the decrease was due to the instrumentation. Thus, any electrically conductive film that may have formed was so slight as to be undetectable at this sensitivity.

The vacuum chamber was opened after 390 days. The hardware at that time is shown in Figures 72, 73 and 74.

The patterns were found to be free of any visible film or black powder deposit. One tiny lump of black debris was found on the copper using a microscope. This may have been splashed there by the tungsten roller. There was no noticeable discoloration of the copper or the epoxy-glass laminate. The walls of the glass beaker were also free of film and powder. There was a small amount of black residue on the stainless steel wire which supports the tungsten roller.

It can be concluded that the formation on insulating surfaces of conductive films due to evaporation and recondensation of gallium is not a serious problem at the temperatures and pressures expected to prevail in the LMSR/SAOM under orbital conditions.

Gallium Surface Film Versus Gases

One objective of this experiment was to determine which of the gases or combinations of gases present in the atmosphere is responsible for the quasi-plastic film which forms on liquid gallium surfaces when exposed to air, and at what level of concentration of such gases does the film form.

Figure 72. Gallium Evaporation Experiment After 390 Days in Vacuum

Figure 73. Tungsten Roller to Expose Fresh Gallium Surface

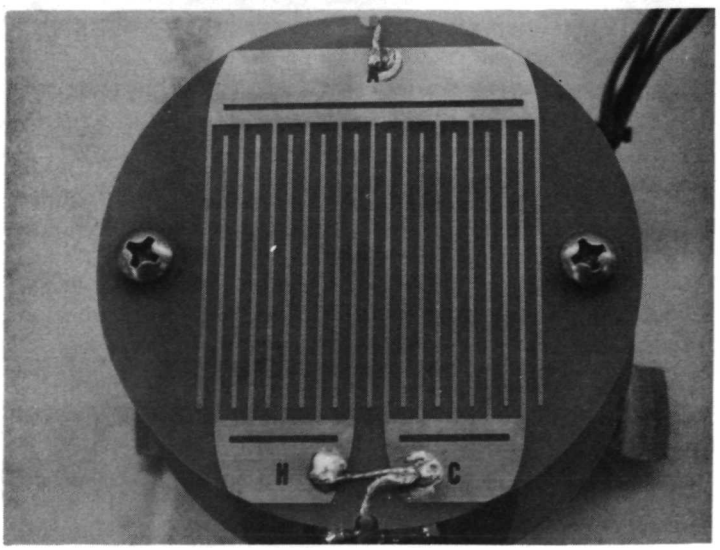

Figure 74. Surface Resistance Pattern After 390 Days Exposure to Heated Gallium

Another objective was to determine if the film is inhibited from forming by freezing the gallium.

The apparatus for the experiments is shown in Figure 75. For the first experiments the antechamber had not been added. A clean sample of gallium was provided in an evacuated glass chamber in the following manner. A glass tube was connected to the chamber from above. In the tube is a constriction to about one mm diameter. A frozen sample of gallium was placed in the tube above the constriction and the tube sealed with flame before the chamber was evacuated. After evacuation to 5×10^{-6} Torr, overnight, the tube was heated by flame and the gallium melted and ran through the hole, leaving its surface film on the walls of the tube.

The chamber has a cupped bottom to hold the gallium. A stainless steel spatula manually operated by a metal bellows extends into the cup. The chamber was heated by a heat lamp to about $40^{\circ}C$ to keep the gallium liquid.

A clean sample of gallium was examined in the vacuum with the spatula and found to not have a detectable surface film. It did not wet the glass. The surface of the three gram sample was taut and shiny and it was difficult to separate a drop from the main sample using the spatula.

Mass spectrographs were obtained of the background gas in the mass spectrometer and then a portion of the gas over the gallium sample was leaked into the mass spectrometer and a spectrograph obtained. These data are shown in Table 17. The relative absence of water vapor and oxygen over the gallium sample are to be noted. Nitrogen and hydrogen are the largest residuals.

The sample chamber was then isolated from the ion pump and the ion gage was shut down to minimize pumping. Aviators oxygen was leaked into the sample chamber with the intent to provide 7.6 microns pressure, or 10 ppm of 0_2 compared to 100 percent 0_2 at atmospheric pressure. This pressure was sampled with a thermocouple gage. It was apparent to the operator of the leak valve that gas was being used so the valve was shut with a peak reading of 5 microns. It is believed that the total dose was less than 7.6 microns. This amount of oxygen formed a slight, but noticeable, film on the gallium. Larger drops could be separated with the spatula and lumps could be formed on the previously taut surface. No significant wetting of the glass occurred. The pressure on the thermocouple gage quickly dropped below one micron and was unreadable.

The mass spectrograph obtained within 10 minutes of the admission of the oxygen to the gallium sample shows only 0.2 percent oxygen in the residual gases. Aviators oxygen is not free of nitrogen, water vapor and other gases and the method of leaking may have permitted traces of other gases to enter. Thus, no definite calibration can be placed on the mass spectrometer data of Table 17 after admission of the oxygen. Certainly the oxygen constituted 90 percent or more of the gas admitted. It was clear that the gallium was effectively scavenging the oxygen and perhaps the water vapor.

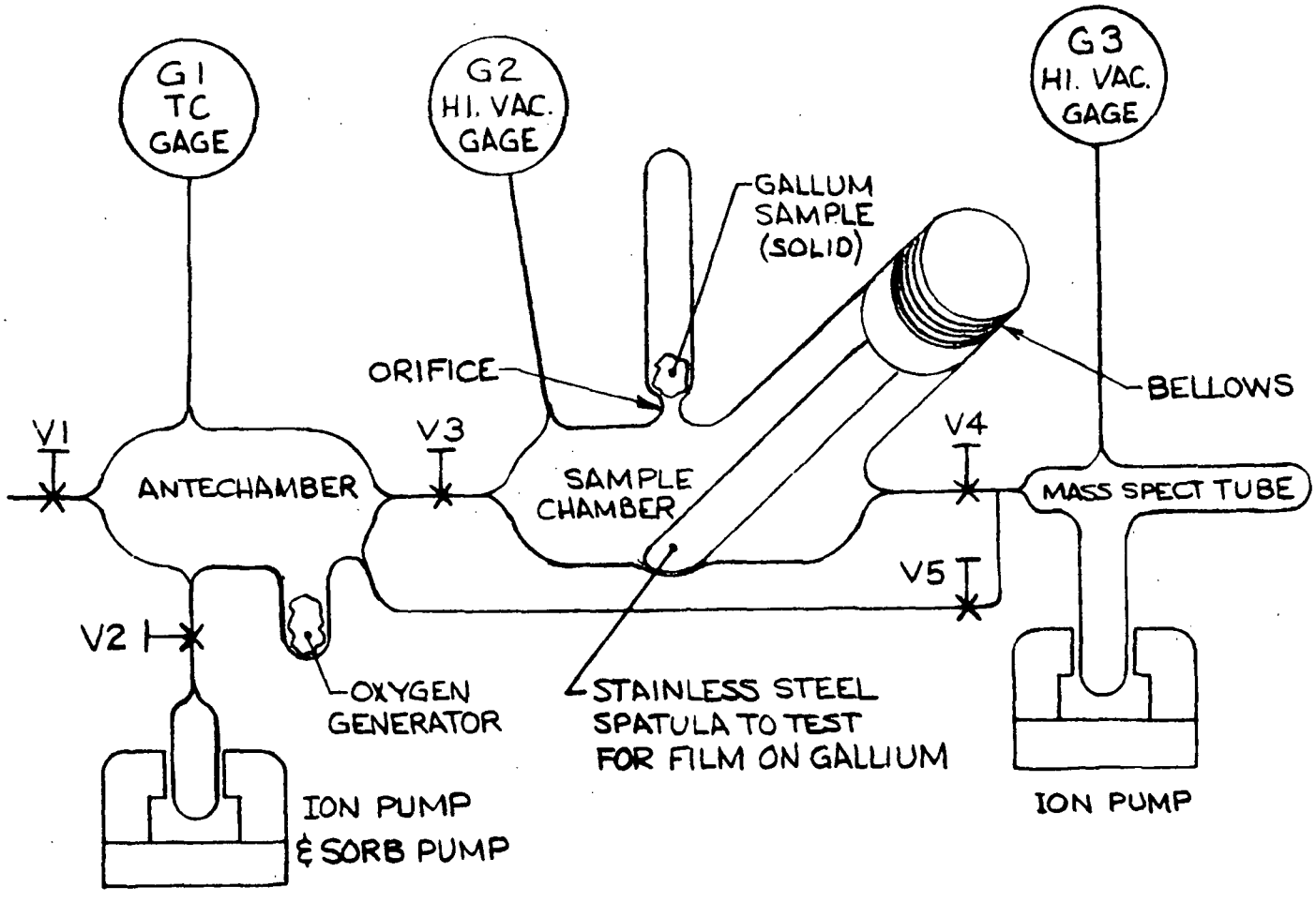

Antechamber and sample chamber to have approximately equal volumes.

Figure 75. Apparatus for Gallium Experiments

TABLE 17. MASS SPECTROGRAPH RESULTS, GALLIUM EXPOSED TO OXYGEN

Molecular Weight	Background Gases in M.S. chart mm	%	$\times 10^{-8}$ torr	Gases over Ga Sample, Hard Vac. chart mm	%	$\times 10^{-6}$ torr	After 5μ Oxygen chart mm	%	Possible Gases
2	37	28	1.00	28	20	1.01	40	7	H_2
4							3	0.5	He
12	1	1	.03				17	3	C
14				6	4	.22	40	7	N
15	1	1	.03						N
16	6	5	.16	1	1	.04	13	2.3	O, CH_4
17	8	6	.22				1	0.2	O
18	24	18	.65	2	1	.07	2	0.3	H_2O, O
19	8	6	.22						F
20	1	1	.03	1	1	.04	5	0.9	Ar^{++}, Ne
26							1	0.2	Mg
28	27	20	.73	85	62	3.08	~370*	64	N_2, CO, Si
29							10	1.7	Si
30	1	1	.03				4	0.7	N_2, Si
32	4	3	.11				1	0.2	O_2, S
34									O_2, S
40	4	3	.11	14	10	.51	40	7	A, K, Ca
44	11	8	.30	1	1	.04	29	5	CO_2, Ca
TOTAL	133	101	3.6×10^{-8}	138	100	5×10^{-6}	575	100	

* approximate only, off scale

++ double charge

TABLE 18. MASS SPECTROGRAPH RESULTS,
FURTHER EXPOSURE TO OXYGEN

Molecular Weight	2:52 PM		3:00 PM		3:40 PM		5:50 PM	
	chart mm	microns	chart mm	microns	chart mm	microns	chart mm	microns
2	20.5	.63	2.7	.47	1.1	.25	8.7	.23
4	1.8	.05	.4	.07	.4	.09	3.6	.10
12	18.9	.58	3.6	.62	.2	.05	2.4	.06
14	12.0	.37	1.6	.28	2.3	.54	21.7	.57
15	3	.09	.7	.12	.4	.09	1.9	.05
16	55	1.70	9.9	1.71	.9	.21	7.7	.20
17	2.4	.07	.5	.09	.8	.19	8.0	.21
18	6.2	.19	1.5	.26	2.0	.47	21.8	.58
19	1	.03	.4	.07	.1	.02	1.6	.04
20	3.9	.12	.8	.14	.6	.14	5.4	.14
26	1.4	.04	.4	.07	.2	.05	1.2	.03
28	340*	10.5	64.0	11.0	25.0	5.8	245*	6.46
29	7	.22	1.0	.17	.4	.09	4	.11
30	5.2	.16	1.4	.24	.8	.19	7.8	.21
32	280*	8.6	40	6.90	1.7	.40	18.9	.50
34	2.1	.06	.2	.03	.2	.05	0.6	.02
40**	29.5	.91	5.3	.91	3.9	.91	34.5	.91
44	37.5	1.16	10.1	1.76	1.1	.26	8.6	.24
Total		25.48	144.5	25***		9.80		10.66

* Approximate only, off scale

** Micron columns based on no change in partial pressure of Argon compared to 3:00 p.m. reading

*** Observed pressure of gases over gallium sample as measured with thermocouple gage

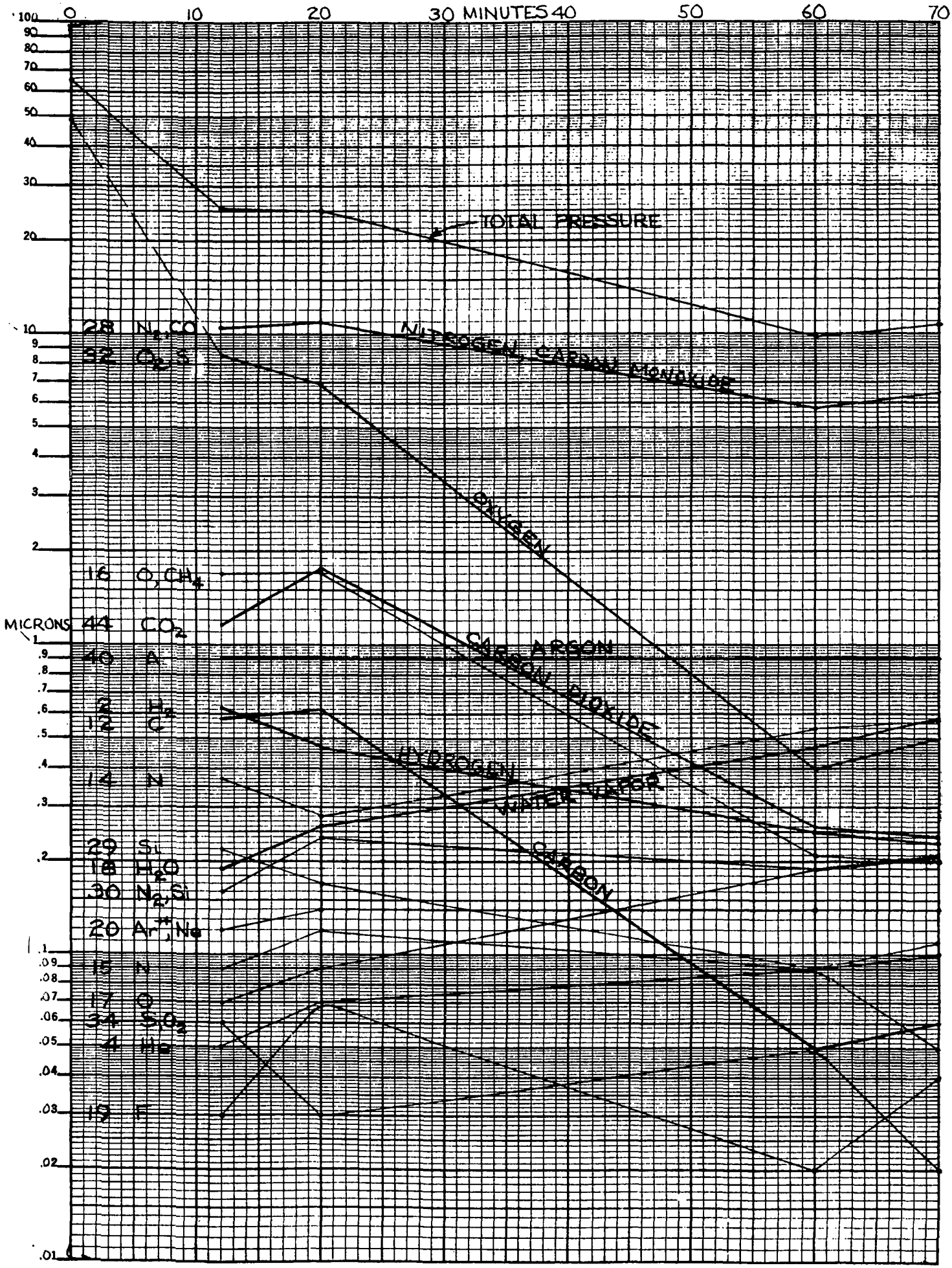

Figure 76. Mass Spectrograph Results, Gas Mixture Exposed to Gallium

Note in Table 17 that the possible gases include naturally occurring isotopes determined from Table VI of Reference 3.

A larger dose of aviators oxygen was then admitted quickly. The object was to provide a total dose of 100 ppm. The peak reading on the thermocouple gage was 65 microns. The results of mass spectrographs taken over a period of 70 minutes following this dose are shown in Table 18 and Figure 76. The final mass spectrograph is Figure 77. Note the two scales, one line being 10 times the gain of the other.

The data was normalized by assuming that the amount of argon (atomic weight 40) in the chamber did not change. Potassium and calcium also have naturally occurring isotopes with atomic weight of40 but the gas from such materials is probably small.

Again the oxygen was quickly used by the gallium. The amount of molecular weight 32 remaining after one hour is probably an isotope of sulfur remaining in the test setup due to previous experiments with sulfur hexafluoride.

Carbon, carbon monoxide and carbon dioxide significantly reduced during the 40 minutes separating two of the readings. The formation of gallium carbonate may be indicated. Water vapor showed a monotonic rise in concentration, while hydrogen decreased. Most other gases stayed constant within the accuracy of the experiment. The thermocouple gage read less than one micron at the end of the experiment, despite the calculation that more than 10 microns remained based on constant argon. The 10 microns were probably used in the leak to the mass spectrometer.

The surface film on the gallium was probed several times during the 70 minute time period. The film was quite pronounced, similar to that in an air atmosphere. Large drops could be separated and large protrusions caused on the main sample. Some wetting of the glass occurred. The gas absorption was probably influenced by this probing. The sample was about one centimeter in diameter and lenticular in shape, the bottom surface being formed by the glass cup. The chamber volume was about 400 cm^3. The sample supercooled to room temperature with the heat off.

The need for more careful control of the input gases led to revised experimental procedures and apparatus. The major change in apparatus was the addition of an antechamber so that gases could be carefully analyzed before being admitted to the gallium. The next sequence of testing was to determine how much oxygen is absorbed by frozen gallium.

A four gram sample of solid gallium was placed above the orifice, the tube was sealed, and the chamber evacuated. The gallium was then melted and ran down into the sample chamber where it was tested with the spatula and found to be free of film and to not wet the glass. The gallium was then frozen by flowing cold gas around the sample chamber.

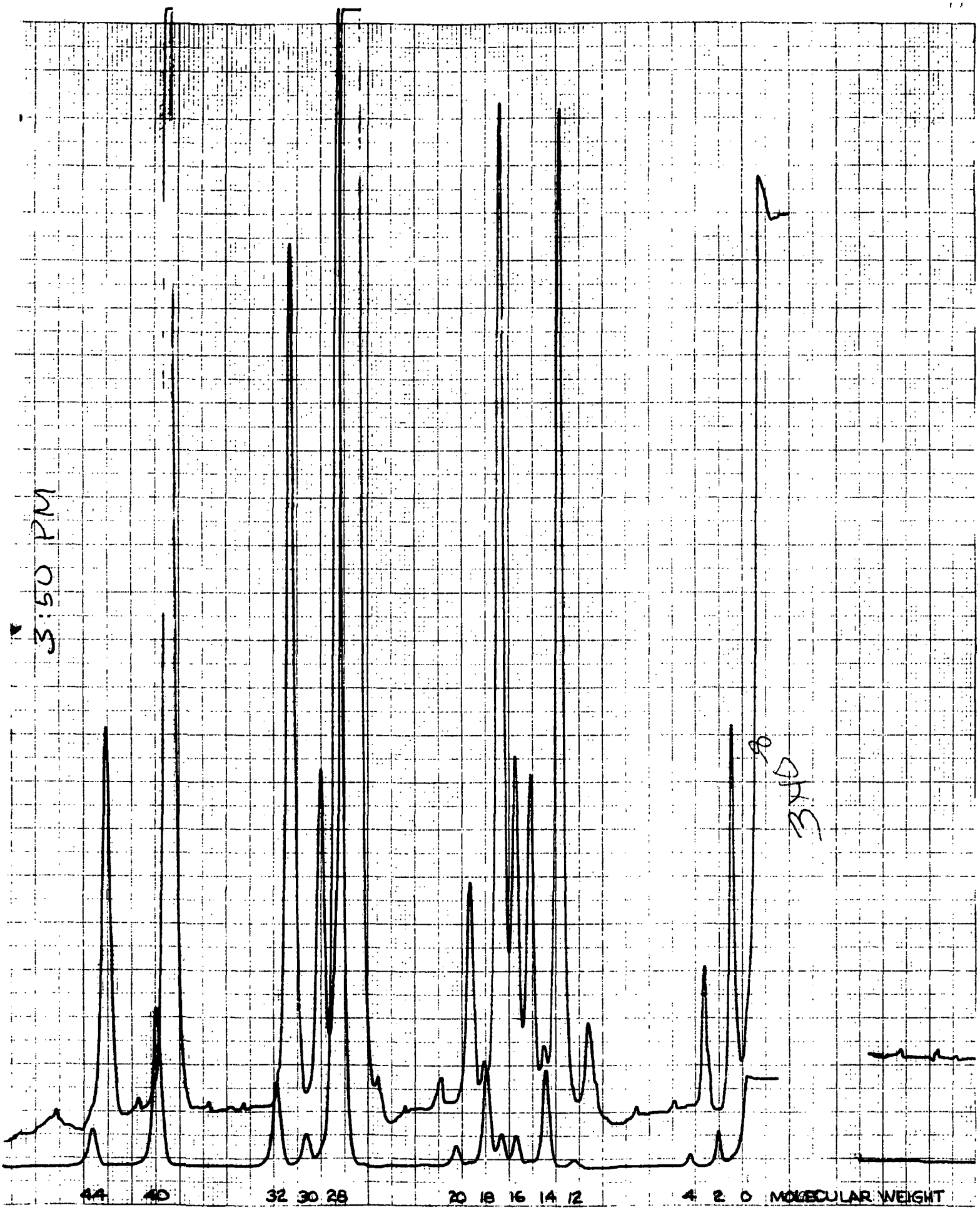

Figure 77. Typical Mass Spectrograph, Residual Gases over Gallium

Oxygen was generated in the antechamber by heating potassium permanganate to 225° C. The gas mixture was analyzed with the mass spectrometer then introduced to the sample chamber. The pressure, primarily due to oxygen, was 32 microns. The pressure and the composition of gases did not change appreciably during the one hour exposure to the frozen gallium. The gas was then evacuated and the gallium melted. The gallium remained free of film and did not wet the glass.

The sequence in the above paragraph was repeated with 210 microns of oxygen gas and with air. The results were the same: the frozen gallium did not absorb a significant amount of oxygen and the gallium remained film free and did not wet glass when remelted in a vacuum.

The data from this experiment is given in Table 19. The mass spectrograph was found to be inaccurate for obtaining quantitative values for the gases present but it was clear that oxygen was not being adsorbed by the frozen gallium, in sharp contrast to the previous experiment with the gallium liquid.

TABLE 19. FROZEN GALLIUM EXPOSED TO OXYGEN AND AIR

Event		Gas in Ante-Chamber	Gas Over Gallium			Gas in Ante-Chamber	Gas Over Gallium				Air in Ante-Chamber	Air Over Gallium	
Exposure Time		-	0	15 min.	60 min.	-	0	20 min.	40 min.	65 min.	-	10 min.	60 min.
Pressure[1]		40μ	32μ	32μ	32μ	260μ	220μ	210μ	210μ	200μ	760 Torr		
Md. Wt., Gas		%											
1	H	1.1	0.8	1.3	1.0	1.1	1.0	1.0	0.9	1.0	0.4	0.8	0.8
2	H_2	7.0	6.1	6.9	7.2	6.8	6.0	6.6	6.0	6.4	3.0	4.2	4.1
4	He	0.2	0.2	0.3	0.4	0.3	0.3	0.3	0.3	0.4	0.5	1.4	0.9
12	C	1.2	1.1	1.3	1.0	1.1	0.9	1.0	1.0	1.0	0.1	0.2	0.2
14	N	0.1	0.4	0.8	1.3	0.2	0.2	0.3	0.3	0.4	4.9	5.1	7.1
15	N	0.6	0.6	0.8	0.7	0.7	0.6	0.7	0.6	0.7	0.3	0.4	0.4
16	O, CH_4	7.4	6.4	7.7	6.9	7.7	6.4	7.7	7.4	7.4	1.1	1.2	1.2
17	O	1.3	1.7	1.8	1.6	1.8	1.9	1.8	1.9	1.7	0.2	0.3	0.2
18	H_2O, O	4.1	5.4	5.6	4.9	5.6	8.0	5.8	6.2	5.2	0.7	0.8	0.6
19	F	0.1	0.1	0.1	0	0.1	0.1	0.1	0.1	0.1	0	0.1	0.1
20	A^{++}, Ne	0.2	0.4	0.4	0.5	0.3	0.4	0.4	0.4	0.5	0.7	1.3	1.1
26	Mg	0.1	0.1	0.2	0.1	0.1	0.1	0.1	0.1	0.1	0.1	0.1	0.2
28	N_2, CO, Si	18.8	22.8	24.5	29.0	17.9	18.5	19.1	20.7	19.9	75.9	68.6	68.0
29	Si	0.4	0.4	0.4	0.5	0.4	0.4	0.4	0.4	0.3	0.7	0.7	0.8
30	N_2, Si	0.2	0.2	0.2	0.2	0.2	0.3	0.3	0.2	0.2	0	0.2	0.1
32	O_2, S	44.6	40.7	37.1	33.0	45.4	44.7	44.4	42.5	43.9	4.4	4.8	5.2
34	O_2, S	0.1	0.1	0.1	0.1	0.2	0.1	0.1	0.1	0.1	0	0.1	0.1
40	Ar, K, Co	2.1	2.7	2.3	3.1	2.9	3.0	3.2	3.3	3.5	6.2	9.0	8.1
44	CO_2, Co	10.5	9.8	8.1	8.6	7.1	7.1	6.7	7.4	7.2	0.6	0.7	0.7

(1) μ means microns of Hg.

DISCUSSION OF RESULTS

Preliminary Design Study

General Arrangements

The design approaches employed during the Preliminary Design Study were based on meeting all of the specified requirements to the maximum extent possible. The requirement for a through-shaft to provide for the transfer of torques and forces from the solar array to the housing assembly could only be satisfied by a large diameter shaft. The decisions to employ a conservative design approach for the high voltage rings and to utilize concentric slip rings to reduce the shaft length resulted in liquid metal slip rings with mean diameters ranging from 3.25 inches to 7.875 inches. A nominal operating clearance of .015 inch was adopted to accommodate tolerances and shaft displacements under load. This combination of large characteristic lengths meant that it was impossible to retain the gallium in the slip ring in a one-gravity field unless the gallium was frozen or the shaft axis was nearly vertical. A requirement to withstand continuous acceleration of 1.5 g's on all axes in the prelaunch test environment could not be met. A shock test requirement of 10-g peak, 10 ms half-sine with the gallium liquid probably could not be met.

It was decided to retain the configuration and accept the restrictions on testing and handling of the LMSR/SAOM. The alternate was to greatly miniaturize the slip rings, abandon the structural through-shaft, and accept much greater electrical stresses. The availability of this alternate at that time was questionable.

The results of evaluation testing have made the alternate seem much more attractive. The retention of the gallium is of such far-reaching importance that all efforts must be expended to ensure it. Thus attention was given in the latter part of the project to develop design parameters for a miniature slip ring assembly. The concept of large diameter concentric liquid metal slip rings mounted in platters may be suitable for earth-fixed installations with slowly-rotating vertical shafts but is now considered to impose too many limitations for practical use on spacecraft.

The concept that the stator platters of VHV rings should be on the ends of the assembly is considered to have worked out quite well. With this design it is not necessary to route the VHV leads through the shaft and the bearings. Attachments of VHV leads are therefore simplified, the reliance on solid insulation is greatly reduced and electrical stresses are minimized. This concept may prove useful for earth-fixed slip ring installations requiring operation at very high voltages.

High Voltage Considerations

The adoption of a maximum electrical stress of 100 volts per mil determined the sizing of the very high voltage (VHV) rings. At 15 kV the minimum spacing between centers of parallel cylindrical conductors becomes 0.367 inch and the cylinder diameter is 0.132 inch. A larger or smaller cylinder diameter with the same spacing increases the stress. For spheres the minimum center-to-center distance increases to 0.540 inch and the optimum diameter is 0.270 inch. A radial or axial space of three inches is thus required for the seven VHV rings at each end of the shaft.

The concentric arrangement of rings was adopted and with a 2.6 inch diameter shaft the housing inside diameter became 8.6 inches. This determined the basic diameter of the LMSR/SAOM, well within the specification.

Open construction was employed so that the vacuum became the most highly stressed dielectric. This resulted in a complex and expensive mechanism. The complexity and bulk are considered well justified by the need for reliable operation over long periods at the projected voltages. The probability of catastrophic failure by breakdown through the solid insulation or across the surface of the insulation was reduced to a negligible factor if gallium had not escaped and contaminated the insulation.

Liquid Metal Slip Ring Design

Two basic categories of liquid metal slip rings were studied. In one category the rotor and stator members are continuous rings operating in close proximity and with liquid metal bridging the gap between them around the whole perimeter. When ring pairs in this category are rotated with respect to each other the liquid metal surface must shear on both sides all the way around, a total distance approximately twice the perimeter.

The other category requires a continuous ring as only one member. The other member is a probe or brush which makes electrical contact with the ring by way of a liquid metal bridge at a restricted area of the ring. This small area of contact must be free to move around the ring. The length of liquid metal surface that is being sheared at a given instant is only the periphery of the probe or brush. Note that the shearing is much more complex, going from zero at the leading edge to zero again at the trailing edge. Testing must be relied upon to make the determination of which category of slip ring produces the least debris.

The brush type was seen to have a potential for greatly increased acceleration tolerance if the liquid metal would concentrate at the brush and leave the ring as dry as possible. The probe type, on the other hand, needs a trough wide enough for the probe plus clearance on either side to prevent rubbing. This trough full of gallium is wider than the gap in a radial or cup gap type ring for a given clearance. Thus it has less acceleration tolerance at the same diameter. The narrow probe also has a limited current-carrying

capacity (although parallel probes will probably be used in any application). Technical direction required that the probe type slip ring not be pursued in the preliminary design study. The probe type has a potential for limited operation in air. This would permit operation during spacecraft testing without requiring an inert atmosphere.

Design Evaluation Testing

Fabrication of the Evaluation Test Unit

The materials for the slip rings in the ETU are AISI type 304 CRES and 99.5 percent pure nickel. Both of these materials are very difficult to machine. The large diameter rings held to tight dimensional tolerances proved very expensive.

Attachment of ring supports and current taps to the rings using electron beam welding was generally successful. Warpage was minimal but must be accounted for in design. The best design used studs held in the rings by two small welds each. Continuous welds were subject to blowouts and heat distortion. Adequate penetration had not been achieved on the one weld that failed. Multiple current taps would be desirable for reliability. The electrical resistance of a welded joint could be used to determine if it has adequate fused area to handle the electrical load. The measurement would need to have a resolution of 10^{-7} ohms.

The rings and the epoxy-glass ring supports as assembled did not meet the design goals for runout. Special tooling could help in this regard. The critical surfaces of the rings might be final machined as mounted if the rings could be rigidly enough supported. Liquid metals with melting points around 400K might be useful to grip the rings as part of such tooling.

Metal parts that were not to be in contact with gallium were machined from AISI type 303 stainless. A great saving in fabrication cost could be realized if this material were found to be compatible with gallium. The addition of sulfur or selenium makes it much more machinable than 304 but sulfur and selenium are known to form compounds with gallium.

Wetting of Electrodes with Gallium

Wetting of the nickel with gallium was readily accomplished in air by abrasion with a nylon knit cloth impregnated with gallium. The initial wetting did not guarantee adhesion of the liquid gallium. After the liquid gallium has drained or has been wiped from a wetted surface the exposed surface becomes resistant to rewetting by simple contact after a few hours exposure to air. Surfaces once wetted must be maintained with a heavy film of gallium to prevent "drying out".

Wetting of the 304 stainless with gallium requires extremely clean surfaces and severe abrasion with a hardened tool to remove the oxide surface. This wetting is likely to be spotty and still escape detection where tested by wiping with a nylon knit cloth because the gallium may bridge from

spot to spot by virtue of its high surface tension. A better non-destructive test for the quality of wetting is needed.

Another difficulty in wetting is to obtain a smooth edge on the wetted area. Tape was used to mask the areas not to be wetted. The black desposits appeared to be associated with wrinkles in the gallium surface which were due to unevenness of the wetted edge. Machining of this edge with the gallium frozen is one likely solution.

Improved reliability of wetting might be obtained by acid etching and/or abrasive blasting of the area to be wetted to remove all traces of oil and grease. Cleaning with solvents does not appear to be adequate. Machining the electrode surface under a pool of liquid gallium is quite effective but the problem remains of removing the chips.

Electrical Resistance of Slip Rings

This is an area in which liquid metal slip rings excel. The measured resistance of the nickel cup-gap rings was on the order of one milliohm. Much of this resistance is due to the circumferential current flow. The measured resistance of the largest nickel ring varied sinusoidally from 0.50 milliohm to 1.12 milliohm as a function of rotation angle. Improved welding design for the current taps on the rotor would reduce this resistance.

Resistances of the stainless steel brush type rings were on the order of 25 milliohms due primarily to the high resistivity of the stainless steel.

In both cases the calculated resistance through the gallium is a very small part of the measured resistance. The lower limit of resistance between rotor and stator is primarily determined by the resistivity and cross-section of the electrodes.

There was never a danger of loss of electrical contact in the VHV or cup-gap rings despite the loss of some gallium. More than 80 percent of the gallium would have to be lost before loss of contact would be a serious concern with these designs.

Very High Voltage Capability

The conservative design approach for the very high voltage insulation was quite successful. If the gallium debris had not contaminated the insulation there is little doubt that each VHV ring would have reached 30 kV with no significant corona, as did ring 1. Rings 3 and 5 went to 28 kV before corona breakdown across the contaminated insulators became a crippling intensity. The only catastrophic breakdown of insulation was due to the shorting of ring 7 to the case by gallium.

Slip Ring Design versus Retention of Gallium

The most significant finding of the project was the poor retention of the gallium by the large diameter slip rings. The most likely mode of escape for the gallium was sloshing. Sloshing is a physical resonance of the gallium in the circumferential gap wherein the gallium is a distributed moving mass reacting against the compliance of the retention mechanism. A large diameter ring will have a low sloshing frequency. Damping is provided by the viscosity of the liquid metal and by the quazi-plastic surface film, but the viscosity of gallium is low. Radial accelerations well below the static acceleration capability of the rings can result in a spill if they are recurrent at a frequency approaching the sloshing resonance.

It will be noted that the trough of the cup-gap type rings gives little protection from sloshing when the diameter becomes large with respect to the depth. Extreme care had to be used in moving the filled stator rings of the cup-gap style before the rotor was put in place. The rotors and stators of the VHV rings were also critical. When the rotors and stators were joined the much reduced gap reduced the compliance of the surface film and increased the frequency, but spills still occurred.

It is likely that some of the debris came from twirlies. The lower surface of the gallium in the VHV rings may have been convex in places, particularly since the axis was far from vertical as set up in the vacuum chamber. When rotation was initiated in the vacuum, wrinkles in the residual quazi-plastic film would form the convex surface into a series of globules which would roll around in the lower reservoir and possibly escape.

In the case of the cup-gap rings the reservoirs were not configured in an optimum shape. Compare Figure 22 with Figure 7. This was done to reduce fabrication cost. A bulge in the gallium surface due to previous sloshing might persist due to the quazi-plastic surface film. Rotation might wrinkle the surface and then separate the bulge into globules of gallium which would rub on the top of the reservoir if they were large enough. Evidence of this was seen in cup-gap ring 6. Dome-shaped reservoirs may have been more tolerant of debris.

It had been postulated that the concave gallium surfaces, reservoirs and baffles as shown in Figure 6 would inhibit the formation and escape of gallium debris. These measures proved inadequate for use with the very large diameter rings in this program.

The reservoirs and baffles were successful in inhibiting the escape of the finely divided black residue. The black residue was seen in the reservoirs of most rings but was not noted outside of the rings.

The black residue was identified as small globules of gallium in Reference 1. It is not believed to be gallium that has evaporated and recondensed because it was not found in the gallium evaporation experiment. It behaves more as if the tiny globules have some velocity but are acted upon

by gravity. They apparently are ejected from the surface film where it is being folded and collect on adjacent surfaces.

It has been postulated that gas entrained in the gallium forms small bubbles that burst as they come to the surface. The bubbles would be circulated by the shearing in the operating gap and would tend to come to the surface at low pressure regions where the surface film is sharply folded such as the leading and trailing edges of wetted areas. This corresponds to the observed areas of black deposits.

The formation of conductive films on insulation due to the condensation of evaporated gallium at 10^{-7} torr and 350K was demonstrated to be insignificant. Measures to prevent the escape of gallium vapor are not required.

Brush Type Rings

Two factors are apparently responsible for the failure of the signal rings; too much axial runout of the rings and too little gallium. The brushes had been tested as being capable of being lifted more than 0.030 inch from the rings before losing contact when full. The outer rings rubbed the brushes on one side but had been set for .015 inch gap so they probably lifted more than .030 inch on the other side. It was also noted that the brushes drained their gallium onto the rings as they moved along. This "painting" left the gallium in the brushes at much lower pressure than that on the rings. It had been postulated that a pressure balance would retain the gallium in the brushes.

The signal rings could have been made to work despite the runout if an excess of gallium had been left on the rings. The rings would then have been subject to sloshing.

It is possible that the brush concept could be made to work by segmenting the rings. Each small segment could resemble a brush. The space between segments would be larger than a brush so that the brush would break with one segment before making with the next. Another brush would make contact during the break of the first. The brush contour would be lenticular to avoid having surface tension pull a sheet of gallium from brush to brush. Each segment would then share its gallium with the brush and the brush would not be drained.

The prospects for debris, unreliability and high cost of this approach make it unattractive despite the high acceleration capability that could be attained because the maximum gallium "head" would be quite short, a brush length plus a segment length.

Freedom from Sludge

The simple expedient of not permitting the slip rings to be rotated in air prevented the entrainment of the gelatinous surface film into the

gallium to form sludge. This is considered a very significant result from two standpoints:

1. The very low friction of the liquid metal slip rings would soon be degraded by sludge formation if unrestricted rotation in air were allowed.

2. Assembly of the slip rings in air is practical as long as rotation in air is not permitted.

Inert Atmosphere

The technology and equipment exist for building film-free liquid metal slip rings with gallium. Glove boxes using argon gas and controlling oxygen, nitrogen and water vapor to less than one part per million are available and inhibit film formation to an acceptable level. Liquid metal slip rings assembled in argon gas and with a suitably sealed shroud could be tested as part of a completed spacecraft without need for limitations on the number of rotations.

A noticeable quazi-plastic surface film forms on liquid gallium with oxygen concentration as low as 10 parts per million but film-free gallium can be exposed to air if frozen and will not have a noticeable surface film when remelted in vacuum. Thus a slip ring assembly that had been built and tested in an inert atmosphere or vacuum could be chilled to freeze the gallium and need not be kept in an inert atmosphere for storage, shipping or even through launch if the temperature can be maintained well below 300°K (85°F).

Design Recommendations

Gallium spillage or the ejection of gallium debris from slip rings can cause catastrophic electrical failures. Satisfactory retention of gallium in large diameter rings is extremely difficult to achieve. It is thus recommended that the through-shaft requirement be removed and the liquid metal slip rings be designed around the smallest diameter through which the electrical leads can be removed. The shaft for the liquid metal slip rings should have no other structural requirements than to support the slip ring rotor electrodes.

The bearings for the solar array would then be required to cantilever the panels from the sides of the spacecraft. Some flexibility would be required in the cables from the slip ring rotor assembly to the solar panels.

These measures would permit the use of slip rings with diameters of 5 cm or less and radial and axial clearances in the order of 0.1 mm or less. Acceleration capability then becomes almost 10 g and there is little likelihood of spillage during handling and test. The gallium would still need to be frozen for launch.

SUMMARY OF RESULTS

The design of a liquid metal slip ring/solar array orientation mechanism was undertaken to advance the new technology of liquid metal slip rings by designing to projected requirements for a high power satellite. The work was based on the results of previous experimental projects and included test evaluation of preliminary designs. Design requirements include 116 slip rings, the use of the liquid metal gallium, and a single axis driven by dual brushless torquers.

Three significantly different slip ring designs were evaluated for an arrangement having a through shaft to support large solar panels on either side of the spacecraft. Fabrication tolerances and sloshing of the gallium in the large (to 20 cm diameter) rings proved unduly difficult to control. It is concluded that a requirement to carry structural loads through the slip ring shaft should be eliminated. This permits miniaturization of the slip rings so that the liquid metal can be reliably retained during testing and handling. The miniature rings can be tested in any attitude.

The design requirements include 14 slip rings to operate at potentials to 15 kilovolts. A slip ring assembly design using space as the most highly stressed dielectric was operated in a vacuum at 30 kilovolts with no corona.

Liquid metal slip rings designed for currents to 30A had measured resistances of approximately one milliohm. The only electrical noise associated with these rings was a once per revolution sinusoidally varying resistance component of a few tenths of a milliohm due to the changing relative positions of the current taps on the rotor and stator.

Gallium is subject to a surface film which forms in air. The quasi-plastic film may mix with the gallium to form a sludge when the slip rings are rotated in air. In the present test 20 rings were rotated more than 1000 revolutions each (the equivalent of 3 years in synchronous orbit) in a vacuum and found to be free of sludge. The rings were assembled in air but not allowed to rotate except in a vacuum.

Experiments with gallium answered several questions. It was shown that gallium evaporation does not result in the deposition of a conductive film on insulation at the temperatures and pressures expected in a spacecraft.

Oxygen was definitely identified as the major cause of the quasi-plastic surface film. A noticeable surface film was found to form on liquid gallium at oxygen concentrations less than ten parts per million but frozen gallium does not absorb oxygen and remains film free after exposure to air.

Gallium can be kept film free in vacuum or in a suitably purified argon atmosphere. The slip rings can thus be rotated as part of spacecraft testing if suitable controls are exercised.

Electrical slip rings using liquid metal have extremely low friction and excellent electrical characteristics. The present work has answered many questions about their suitability for use in space. A fully suitable design was not demonstrated but the necessary design parameters and handling requirements were explored and no overwhelming obstacles were encountered. Successful application of liquid metal slip rings in spacecraft can now be confidently predicted. The very low friction compared to conventional slip rings is expected to permit improved attitude stabilization.

REFERENCES

1. Clark, R. B.: Experimental Liquid Metal Slip Ring Project, NASA CR-72780, 1970.

2. Bouwers, A. and Cath, P. G., "The Maximum Electrical Field Strength for Several Simple Electrode Geometries," Philips Technical Review, Vol. 6, No. A, September 1941.

3. Latimer and Hildebrand, "Reference Book of Inorganic Chemistry," Third Edition, The Macmillan Company, New York, 1951.

APPENDIX

NEW TECHNOLOGY

The following reports of new technology were submitted based on work performed under Contract NAS 3-13731:

PD-72412 NT	BRUSH TYPE LIQUID METAL SLIP RINGS by R. W. Grant and R. B. Clark. The brush type liquid metal slip ring is initially described on pages 25 and 41 with additional references throughout the report.
PD-72413 NT	LIQUID METAL SLIP RINGS FOR VERY HIGH VOLTAGE by R. B. Clark. The liquid metal slip ring design for very high voltage is initially described on pages 55 and 56 with additional references throughout the report.

DISTRIBUTION LIST

National Aeronautics & Space Administration
Headquarters
Washington, D. C. 20546

Attention:	ED/L. Jaffee	1 copy
	ECC/A. M. G. Andrus	10 copies
	EC/R. B. Marsten	1 copy
	RP/W. H. Woodward	1 copy

NASA-Lewis Research Center
21000 Brookpark Road
Cleveland, Ohio 44135

Attention:	J. H. Childs (M. S. 3-3)	1 copy
	H. W. Plohr (M. S. 54-1)	1 copy
	W. H. Robbins (M. S. 501-1)	1 copy
	H. O. Slone (M. S. 501-6)	2 copies
	Technology Utilization Officer (M. S. 3-19)	1 copy
	Library (M. S. 60-3)	2 copies
	Report Control Office (M. S. 5-5)	1 copy
	N. T. Musial (M. S. 500-311)	1 copy
	R. R. Lovell (M. S. 54-3)	50 copies
	Contract Section B (M. S. 500-313)	1 copy
	A. F. Forestieri (M. S. 302-1)	1 copy

NASA-George C. Marshall Space Flight Center
Huntsville, Alabama 35812

Attention:	Library	1 copy

NASA-Goddard Space Flight Center
Greenbelt, Maryland 20771

Attention:	Library	1 copy

NASA-Ames Research Center
Moffett Field, California 94035

Attention:	Library	1 copy

NASA-Langley Research Center
Langley Station
Hampton, Virginia 23365

Attention:	Library (M. S. 185)	1 copy

NASA-Manned Spacecraft Center
Houston, Texas 77001

Attention:	Library	1 copy
	F. E. Eastman (EB8)	3 copies
	C. Robinson (EP52)	1 copy

Jet Propulsion Laboratory
4800 Oak Grove Drive
Pasadena, California 91103

Attention:	Library	1 copy
	W. Hasbach	1 copy

NASA Scientific and Technical Information Facility
Box 7500
Bethesda, Maryland 20740

Attention:	NASA Representative	3 copies

General Dynamics, Convair Division
P. O. Box 1128
San Diego, California 92112

Attention:	F. J. Dore/Advanced Programs Laboratory	1 copy

Air Force - Aero Propulsion Laboratory
Wright-Patterson Air Force Base
Ohio 45433

Attention:	L. D. Massie (APIP-2)	1 copy

Philco-Ford Corporation
Western Development Laboratories Division
3939 Fabian Way
Palo Alto, California 94303

Attention:	R. G. Wales	1 copy
	D. L. Elder	1 copy

TRW Incorporated
TRW Systems
One Space Park
Redondo Beach, California 90270

Attention:	H. Low	1 copy
	W. Wellens	1 copy

Federal Communications Commission
521 12th Street
Washington, D. C. 20554

Attention:	M. Fine	1 copy

Ball Brothers Research Corporation
Box 1062
Industrial Park
Boulder, Colorado 80302

Attention:	R. M. Ringeon	1 copy
	C. L. Anderson	1 copy
	V. Frubel	1 copy

Lockheed Missiles and Space Company, Incorporated
P. O. Box 504
Sunnyvale, California 94088

Attention:	J. W. Plummer	1 copy
	E. E. Crowther	1 copy

Communications Research Centre
Shirley Bay, P. O. Box 490
Station "A"
Ottawa, Ontario Canada
K1N8T5

Attention:	C. A. Franklin	1 copy
	W. F. Payne	1 copy

U. S. Information Agency
25 M Street, S. W.
Washington, D. C. 20547

Attention:	IBS/EF/G. Jacobs	1 copy

Naval Electronic Systems Command
PME 116
Washington, D. C. 20350

Attention:	Lt. Commander L. Wardel	1 copy

McDonnell Douglas Corporation
5301 Bolsa
Huntington Beach, California 92647

Attention:	J. Chester (A-3-BBDO-830)	2 copies

Poly Scientific Division
Litton Industries
1213 N. Main Street
Blacksburg, Virginia 24060

Attention: E. Glossbrenner — 2 copies

Spar Aerospace Products
925 Caladonia Road
Toronto, Ontario 315
Canada

Attention: S. Ahmed — 1 copy
T. Ussher — 2 copies

COMSAT Laboratories
Box 115
Clarksburg, Maryland 20734

Attention: W. L. Pritchard — 2 copies

Hughes Aircraft Company
Technology Division
Box 92919 Airport Station
Los Angeles, California 90009

Attention: R. B. Clark — 3 copies

General Electric Company
Space Systems
Valley Forge Space Center
P.O. Box 8555
Philadelphia, Pennsylvania 19101

Attention: S. Weinberger — 1 copy